NOTE TO USERS

This reproduction is the best copy available.

SEISMIC RESPONSE OF A SIX STORY INSTRUMENTED BUILDING

by

Antonios Koniakos

A Thesis Presented to the
FACULTY OF THE GRADUATE SCHOOL
UNIVERSITY OF SOUTHERN CALIFORNIA
In Partial Fulfillment of the
Requirements for the Degree
MASTER OF SCIENCE
(CIVIL ENGINEERING)

May 2005

DEDICATION

To my parents

Triantafyllos & Reggina

For their continuous love and support

ACKNOWLEDGEMENTS

I wish to express my gratitude to my advisor, Professor James C. Anderson, for his guidance, consideration and valuable comments throughout the preparation of this report.

Furthermore, I am grateful to my close friends Ricardo, Karthik and Mario, for the valuable things they taught me during the last year, for their support and help whenever needed despite their heavy schedule.

TABLE OF CONTENTS

CHAPTER 6

CONCLUSIONS

LIST OF TABLES

LIST OF FIGURES

ABSTRACT

In 1993, California Department of Geological Survey (CDGS) instrumented one of the buildings on the University of Southern California campus under the Strong Motion Instrumentation Program (SMIP). The name of the building is HEDCO Neurosciences Building (HNB), located at the University Park Campus and is referred as SMIP Station No. 24652.

This report presents processed strong motion data recorded during the 1994 Northridge Earthquake in order to conduct a detailed comparison of the response of the HNB recorded by SMIP during the earthquake and the response predicted by an analytical model created for ETABS V7.10 computer program. The design criteria were based on the Uniform Building Code 97 (UBC 97). During the analysis of the data, Fourier Transforms and Transfer Functions were obtained in order to identify the frequencies of the vibration modes of the building.

Critical comparisons were made between the recorded data and the calculated response.

A detailed model of the structure was created and was subjected to 3-D Dynamic Analysis. Base Shear analysis indicated that the building behaved adequately under the UBC 97.

This report includes also a detailed description of the building and its soil characteristics.

CHAPTER 1

INTRODUCTION

1.1 General

In 17th of January 1994 an earthquake of magnitude 6.7 occurred in the Los Angeles region of southern California giving a rude awaking to more than ten million people. Although moderate in size, the earthquake had immense impact on people and structures because it was centered directly beneath a heavily populated and built-up urban region.

California Geological Survey (CGS) has instrumented several buildings in the Southern California region during the past years. Since the beginning of the Strong Motion Instrumentation Program (SMIP) CGS has collected structural response records from several earthquakes that have occurred. Significant records were obtained from the 1994 Northridge Earthquake for the steel frame building that is analyzed in this report, Hedco Neurosciences Building, located on the University Park Campus of the University of Southern California in Los Angeles, California. The response data collected by SMIP provided the author with the opportunity to study this building's dynamic behavior at force and deflection levels directly relevant to earthquake engineering.

Generally the analyses of full scale building responses is a major section of structural engineering research and can lead to improved analysis and design methods.

1.2 1994 Northridge Earthquake

The 1994 Northridge Earthquake occurred on January 17, 1994 at 4:30:55 am Pacific Standard Time in the city of Los Angeles, California. The earthquake was characterized as moderate with a moment magnitude of 6.7, but was one of the most monetarily costly earthquakes in the history of the United States.

The epicenter was in the San Fernando Valley, originally believed to be in the community of Northridge (later shown to actually have occurred within the neighboring community of Reseda), about 32 km (20 miles) northwest of downtown Los Angeles. The National Geophysical Data Center places the epicenter's geographical coordinates at 34.213 N and 118.537 W, which is the end of Elkwood St., just east of Baird Av.

Damage occurred up to 77 km (52 mi) away, with the most damage in the west San Fernando Valley and the city of Santa Monica. Fifty seven people were killed and over 1500 were seriously injured. Major freeway damage occurred up to 32 km (20 miles) from the epicenter. Portions of Interstate 10 (the Santa Monica Freeway) and the California State Highway 14 (the Antelope Valley Freeway) collapsed and had to be rebuilt. Figure 1.1 shows a picture of a collapsed freeway.[1]

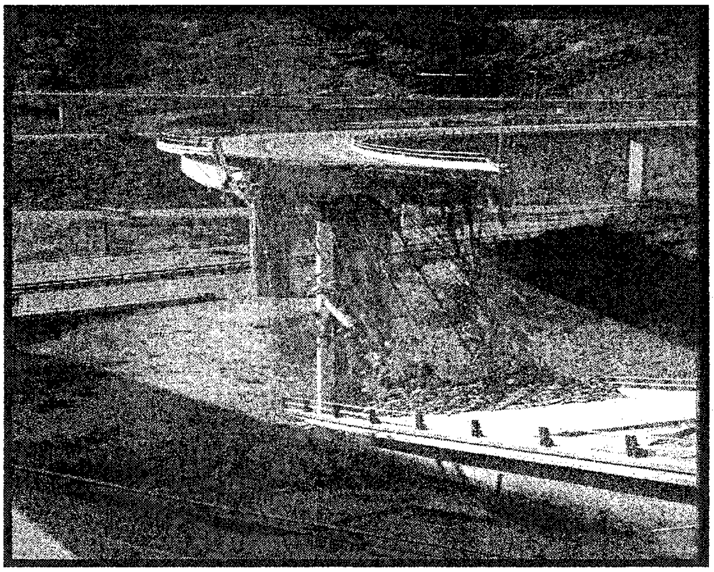

Figure 1.1 Collapsed Part of the Route 14/Interstate 5 (9. USGS)

---

[1] 9. U.S. Geological Survey for the Federal Emergency Management Agency (FEMA), 'USGS Response to an Urban Earthquake: Northridge '94', Open-File Report 96-263, <URL:http://pubs.usgs.gov/of/1996/ofr-96-0263/>,(Last Modified: Fri Jun 15 13:57 EST 2001) (Accessed: 30 March 2005)

Figure 1.2 shows a perspective aerial view of the Los Angeles region from the south, it illustrates how the earth ruptured beneath the San Fernando Valley and shows some of the effects the resulting earthquake had on the land above.[2]

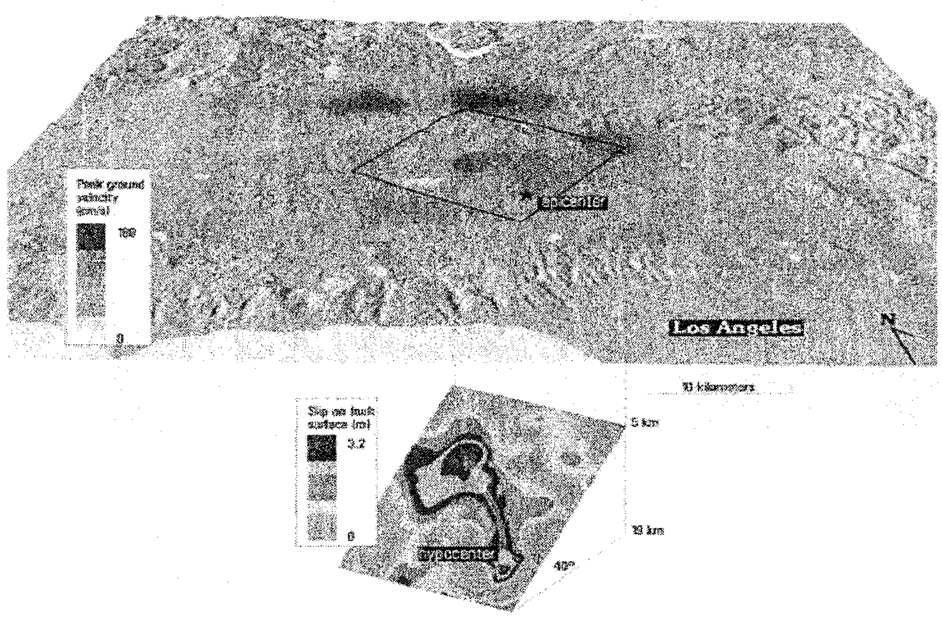

Figure 1.2 Aerial View of the Los Angeles Area showing the effects of the earthquake on the land (9. USGS)

This earthquake was unusual because the epicenter was within a major metropolitan area. Although several commercial buildings collapsed, loss of life was minimized because of the early

---

[2] 9. U.S. Geological Survey for the Federal Emergency Management Agency (FEMA)

morning hour of the earthquake and because it occurred on a federal holiday, the birth date of Martin Luther King, Jr. Through investigation of damaged buildings, it was discovered that structural steel did not perform as well as expected. Nobody anticipated that steel would fail at the rate it did, buildings that were not expected to have major damage were red-tagged many months after the earthquake, when the inspectors finally got to look at them. This new information on the nature of earthquake damage resulted in even more stringent building codes.

The earthquake produced unusually strong thrust, with accelerations in the range of 1.0 g over a large area. While most of the damage was caused by shaking, some damage was also caused by fire and by ground deformation. In some areas the ground surface was permanently uplifted by up to 50 cm (20 in). This was the third very destructive earthquake to occur in California in 23 years. The first was the Mw 6.6 San Fernando (Sylmar) Earthquake, affecting the same area in 1971; the second was the Mw 6.9 (Richter magnitude 7.1), 1989 Loma Prieta earthquake south of San Francisco. The 1994 event is the most damaging earthquake to strike the United States since the San Francisco earthquake of 1906. In terms of financial loss, the earthquake is also one of the worst natural disasters in U.S. history, comparable to Hurricane Andrew in 1992.

Several key hospitals suffered severe structural damage and were rendered unusable after the earthquake. Not only were they unable to serve their local neighborhoods, they had to transfer out their inpatient populations, which further increased the burden on nearby hospitals that were still operational. As a result, the state legislature passed a law requiring all California hospitals to ensure that their acute care units and emergency rooms are in earthquake-proof structures by January 1, 2005 (Data obtained by the USGS website). Table 1.1 lists the main facts of the 1994 Northridge Earthquake at a glance:

Time:	January 17, 1994 4:31 PST
Location:	34° 12.80'N 118° 32.22'W 20 miles WNW of Los Angeles 1 mile SSW of Northridge
Depth:	18.4 km
Magnitude:	M_w6.7
Fault:	Northridge Thrust (also known as Pico Thrust)
Rupture Area:	300 km^2
Economic Loss:	$20-$40 billion
Deaths:	57 people
Displaced from homes:	20,000+ people

Table1.1 Facts of 1994 Northridge Earthquake at a glance

1.3 California Strong Motion Instrumentation Program (CSMIP)

The California Strong Motion Instrumentation Program (CSMIP) was established in 1972 by California Legislation to obtain vital earthquake data for the engineering and scientific communities through a statewide network of strong motion instruments.

CSMIP installs state-of-the-art earthquake monitoring devices called "accelerographs" at various representative geologic formations consisting of different soil materials throughout California to measure the ground shaking. When activated by earthquake shaking, the devices produce a record from which important characteristics of ground motion (acceleration, velocity, displacement, and duration) can be calculated.

Data from monitoring devices are retrieved by modem and computers or by physically recovering the records at the station. Modern equipment is designed to automatically call CSMIP headquarters when it senses ground shaking.

In 1989, CSMIP established a project for data interpretation and utilization. The primary objective of this project is to increase the understanding of earthquake ground shaking and its effects on structures through interpretation and analysis studies of CSMIP data (Strong Motion Instrumentation Program).[3]

1.4 Objective

The objectives of this report are:

1. Analyze and interpret the recorded response of the HEDCO Neurosciences Building due to the 1994 Northridge Earthquake in order to identify important engineering parameters such as mode shapes, period and damping.
2. Create a model of the structure with a computer program that is commercially available around the world, ETABS V7.10, based on structural drawings obtained for the building.
3. Perform a comparative analysis of the measured data and the program's computed results.
4. Analyze and explain the results obtained from the above steps with current code procedures in order to evaluate current design and analysis methods.

---

[3] 6. Strong Motion Instrumentation Program (SMIP), <URL: http://www.consrv.ca.gov/CGS/smip/index.htm>, last edited on 30 March 2005.

1.5 Organization of Report

Chapter 2 of this report will give a thorough description of the HEDCO Neuroscience Building. Chapter 3 will describe the strong motion data recorded in the building for the 1994 Northridge Earthquake. Chapter 4 will describe the engineering analysis of the recorded response from the Northridge Earthquake. Chapter 5 will present a description of the model and the dynamic analysis was performed. Finally, Chapter 6 will present the conclusions of this report.

CHAPTER 2

BUILDING DESCRIPTION

2.1 General Configuration

HEDCO Neuroscience Building (HNB) is located on USC University Park Campus, Los Angeles, California, at 3641 Watt Way Street. Figure 2.1 shows a map of the University Park Campus (UPC) highlighting the instrumented building. A north, south, east and west facade of the building can be shown in the photos in Figures 2.2, 2.3, 2.4, and 2.5.

HNB was designed in 1988 and the construction started in 1989. Figures 2.6 show a typical framing plan and Figure 2.7 shows an elevation view. In elevation the building consists from a basement of 15'-6" height and 5 stories of 14' height each above grade.

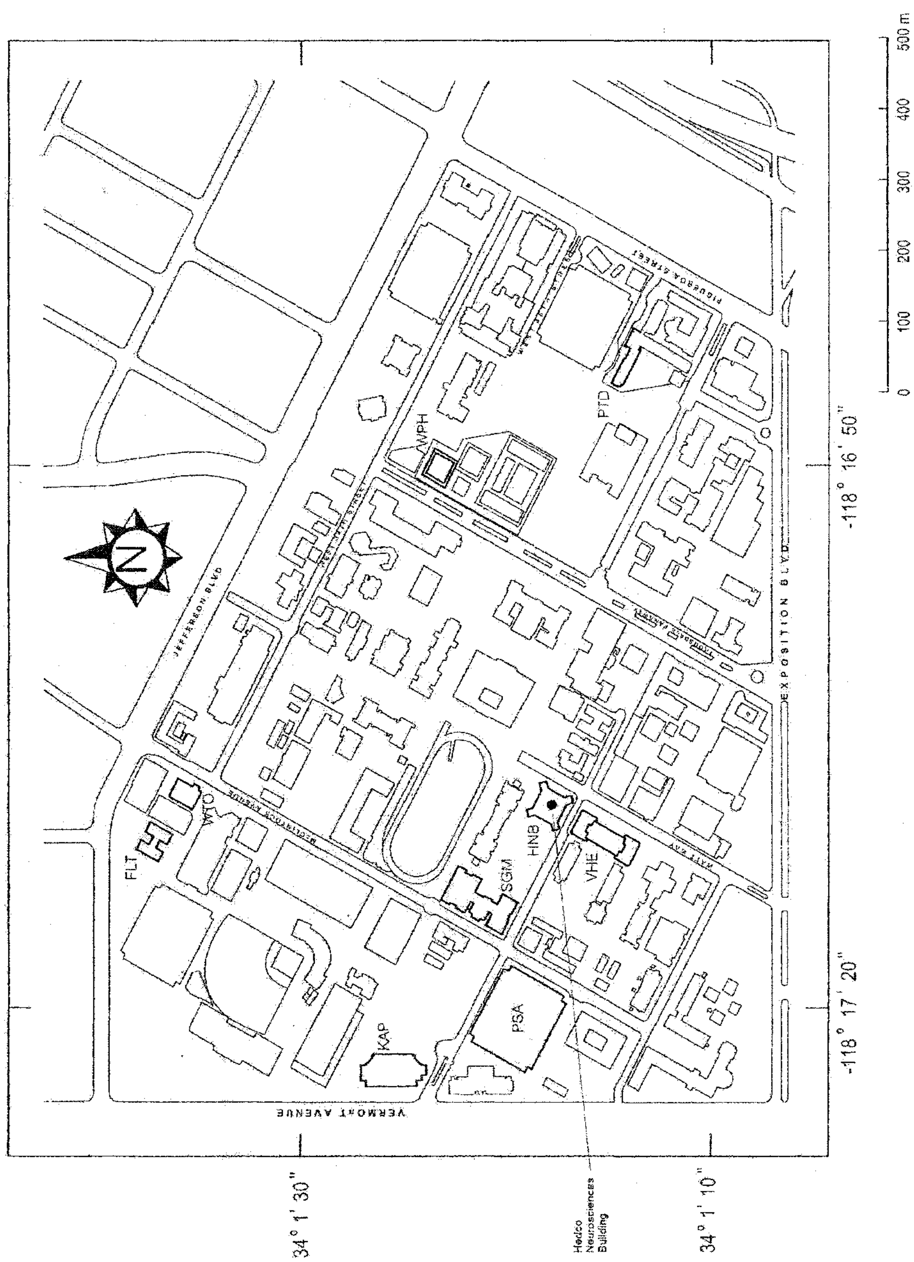

Figure 2.1 Map of the USC University Park Campus with the location of HNB highlighted

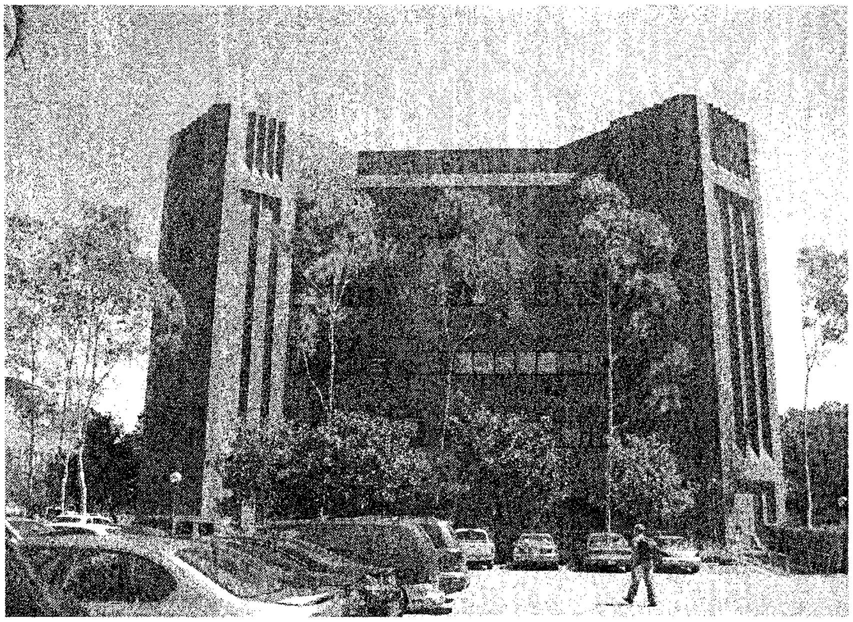

Figure 2.2 West Facade of HNB Building

Figure 2.3 South Facade of the HNB Building

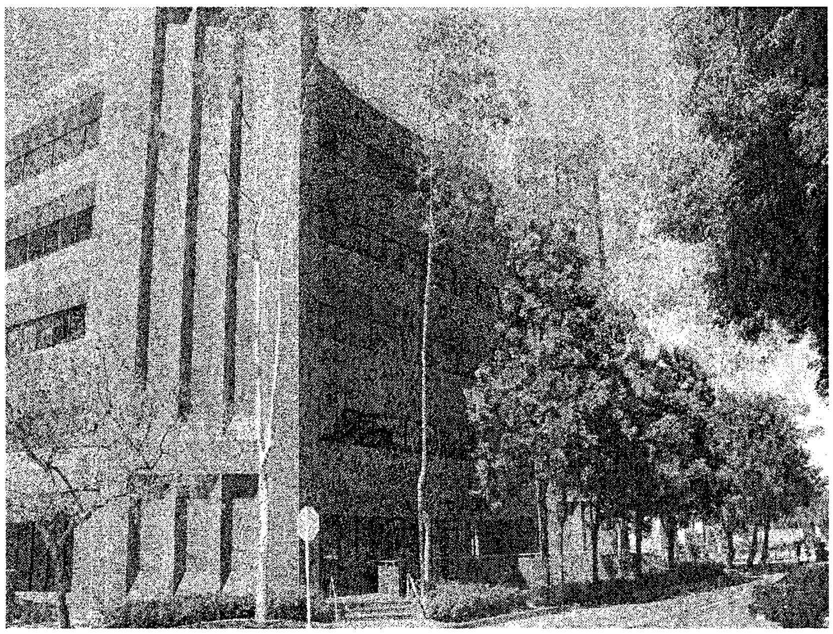

Figure 2.4 East Facade of the HNB Building

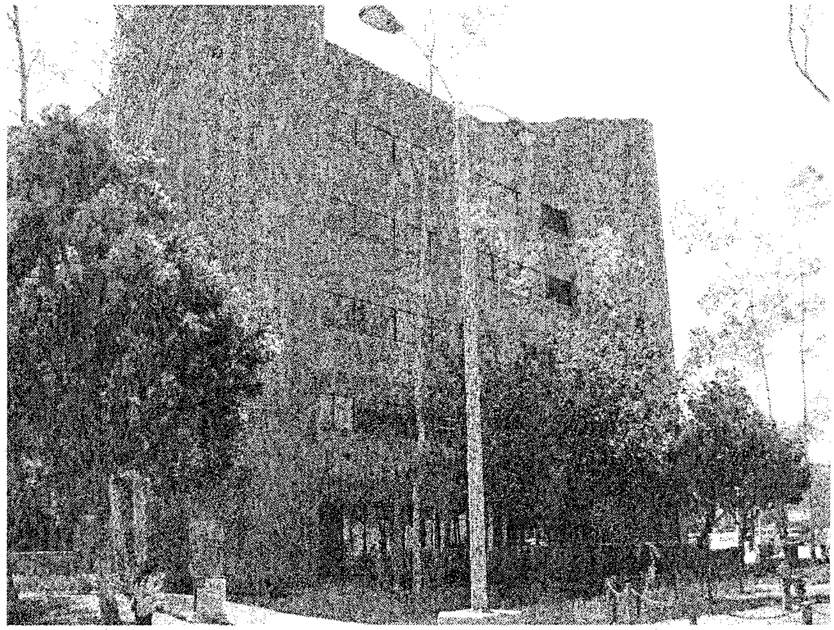

Figure 2.5 North Facade of the Building

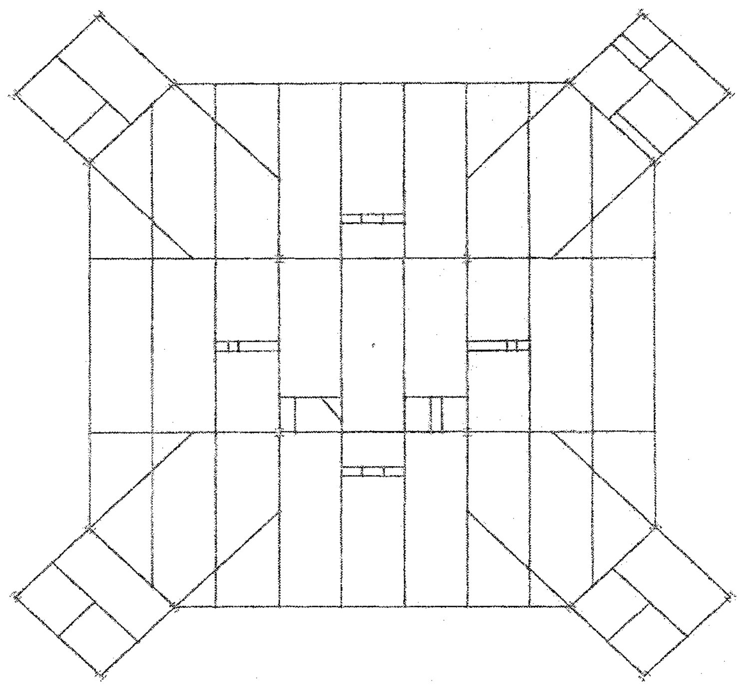

Figure 2.6 Typical Framing Plan

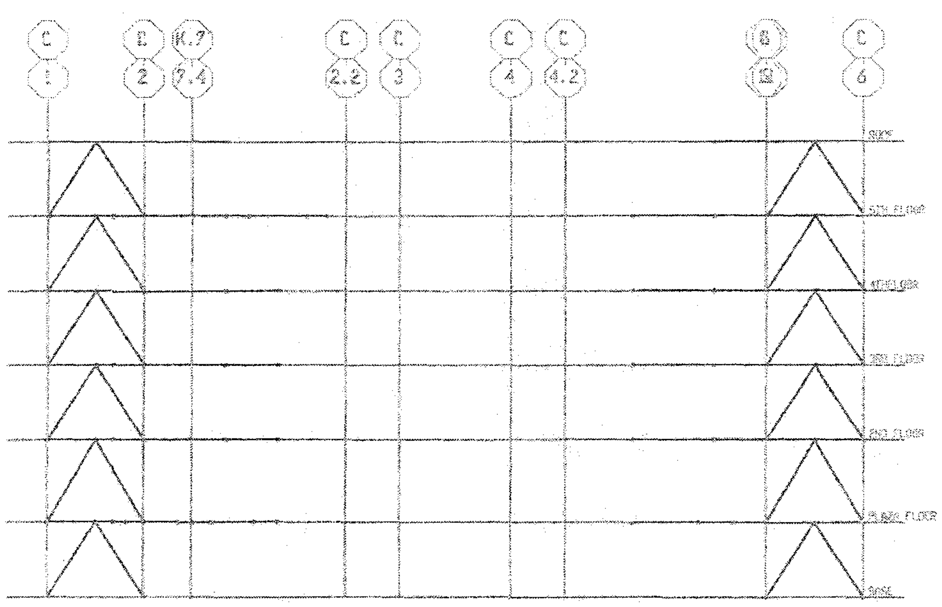

Figure 2.7 Elevation View

The structure is supported vertically by wide flange, hot rolled structural steel columns. The columns are supported by the base plates on the foundation beams which in turn are supported on concrete piles. The type of foundation is mat foundations for the four towers and spread footings anywhere else. A typical column footing detail is shown on Figure 2.8.

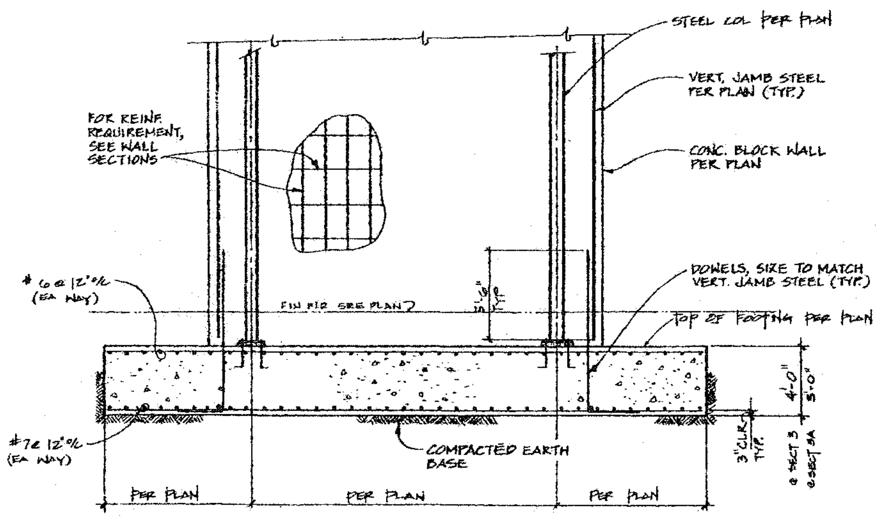

Figure 2.8 Typical Column Footing Detail

The buildings columns are unspliced from the basement until one foot above the second floor, and then spliced again one foot above the fourth floor from where they continue until the roof. Reduced column sections were used after each splicing. Figure 2.8 shows the typical column splice.

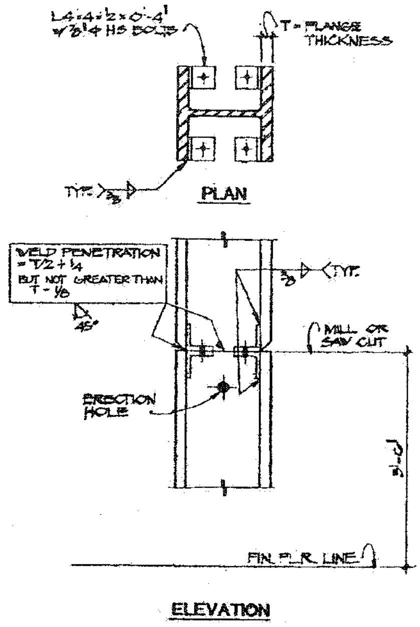

Figure 2.9 Typical Column Splice

Wide flange beams in the East – West direction and wide flange girders in the north – south direction are forming the floor framing system. The beams and girders are connected to the columns with two types of beam to column connections, moment and shear connections. In the analysis that was done moment connections were considered to be rigid joints and shear connections to be pins, that means they could transfer shear but no moment (rotational stiffness).

2.2 Lateral Force Resisting System

The building's Lateral Force Resisting System is formed by four, 17 by 20 feet, towers that are located in the corners of the square, 93.5 ft by 93.5 ft, main part of the building and are symmetric about the center of the building plan in terms of the arrangements of the columns. Two of these towers have Chevron type steel braced frames in the NW-SE direction for lateral resistance and moment resisting steel frames in the SW-NE direction for torsional resistance and the other two have exactly the opposite, Chevron type steel braced frames in the SW-NE direction for lateral resistance and moment resisting steel frames in the NW-SE direction for torsional resistance.

2.3 Vertical Load Carrying System

For the Vertical Load Carrying System light weight concrete was used (120 pcf) over 2.5 psf metal deck supported by steel frames.

2.4 Floor Diagram

The floor diagram consists of a 3.25 inch thick light weight concrete slab over a 3 inchx20 metal decking. Figure 2.10 presents the detail of the floor diagram together with the beam to which the slab is connected.

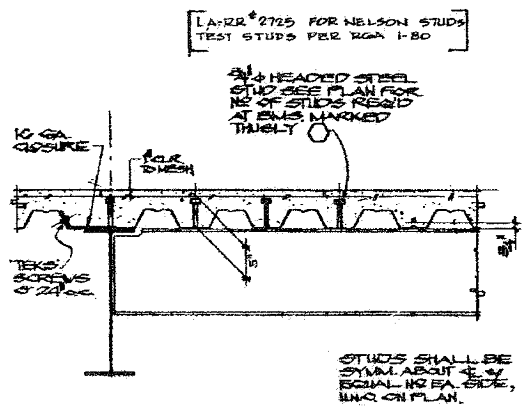

Figure 2.10 Floor diagram detail along with the beam where the slab is connected

2.5 Connections

The connections that were used between the structural elements were mainly moment and shear connections. In terms of modeling the moment connections can be described as rigid and the shear connections can be described as pin (simple). Figure 2.11 illustrates a moment connection used within the four towers on the corners of the building, which are considered as rigid connections. Figure 2.12 illustrates a shear connection which is used mainly in the rest of the building, having the ability to rotate under bending action.

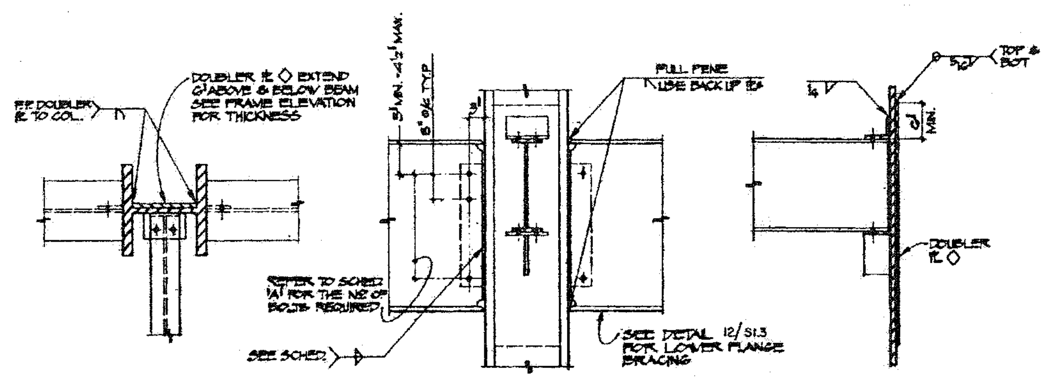

Figure 2.11 Typical Rigid Frame Connection

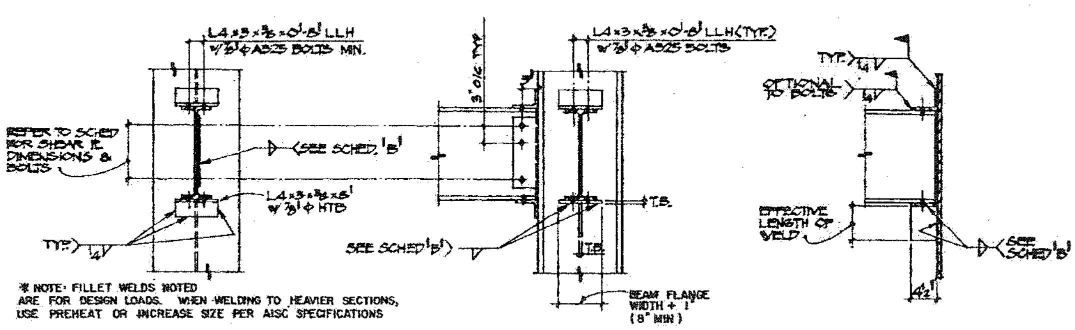

Figure 2.12 Typical Non Rigid Column Shear Connection

2.6 Material Properties

The following material properties were established by using information from the structural drawings of the building.

- Reinforcing Steel

All reinforcing steel was deformed bars conforming to ASTM A-615. Reinforcing bars were spliced with a lap as follows with 1′ 6″ minimum lap unless:

In Masonry:	40 bar diameters
In Concrete:	
At indicated locations on drawings:	24 bar diameters
At locations not included:	
#6 bars and smaller:	40 bar diameters
#6 bars and smaller when spaced 6″ and more or alternate laps staggered 40D:	32 bar diameters
#6 bars and smaller when spaced 6″ and more and bar laps staggered 40D:	32 bar diameters
#7 bars and larger were welded or lapped as required by the Structural Engineer	
Splice of top bars in beams or joists was lapped 50% longer than noted above.	

Reinforcing steel had the following minimum cover:

Formed surfaces in contact with earth – 2″

Walls, Interior Face – 1″

Slabs – ¾″

All reinforcing was supported with conformance with "The manual of Standing Practice for Reinforced Concrete Construction" – Latest edition at the time of construction.

- Structural Steel

Structural steel used in the girders and beams was conformed to ASTM, A-36. Rigid frame columns conformed to ASTM A-572, 50 Grade. Tube columns conformed to ASTM A-500, Grade B. Pipe columns conformed to ASTM A-53, Grade B. All fabrication and construction materials were in accordance with the latest AISC specifications of that time, as approved by the Building Department.

- Concrete

Concrete had a minimum compressive strength at 28 days as noted in Table 2.1.

DATA	CONCRETE	REINF. GRADE			CONT. INSP	
ITEM	STRENGTH	A-615 GR.40	A-615 GR. 60	A-185 MESH	YES	NO
Footings	3000 psi H.R		•◊		•	
Grade Beams	3000 psi H.R		•◊		•	
Slab on Grade	2500 psi H.R		•◊	•		•
Concrete Topping over Deck	3000 psi LT.WT		•◊	•	•	
◊: Denotes #3 or #4 bars						

Table 2.1 Concrete and Reinforcing Schedule

- Masonry

Reinforced block walls were of material and the construction was defined in Chapter 24 of the Building Code. Blocks were light weight units conforming to ASTM C-90 Grade M-1, except those noted as sand gravel blocks.

Mortar was type S, one part cement, ¼ to ½ part hydrated lime or lime putty, 2-1/4 to 3 parts sand. SIKA chemical red label was used. Mortar had a minimum strength of 2000 psi at 28 days.

Grout had a minimum strength of 2000 psi at 28 days with one part cement, two to three parts sand, 1-1/2 PEA gravel. SIKA chemical grout Aid GA Type I or Type II was used.

- Bolts

Bolts were specified as ASTM A-307 unless noted otherwise. High strength bolts conformed to ASTM A-325 Friction Type. Installation of high strength conformed to the "Specifications for Structural Joints using ASTM A-325 or A-490 Bolts".

2.7 Soil information

The soil conditions have been investigated at the site by LeRoy Crandall Association (LCA) in 1986, by drilling three boreholes at locations shown in Figure 2.13. The logs for these boreholes are presented in Figures 2.14, 2.15 and 2.16. The natural soils consist of moderately firm silty sand and very firm and dense underlying gravelly sand. Water was not encountered within the 30-foot depth explored. The building is founded on concrete mats and spread footings, which are placed at least one foot into the dense gravelly sand. The soil conditions have been investigated at the nearby Exposition Park by Duke and Leeds in 1962 (Hao, 2004)[4]. The generalized soil profile is summarized in Figure 2.17 (Stewart and Stewart, 1997)[5].

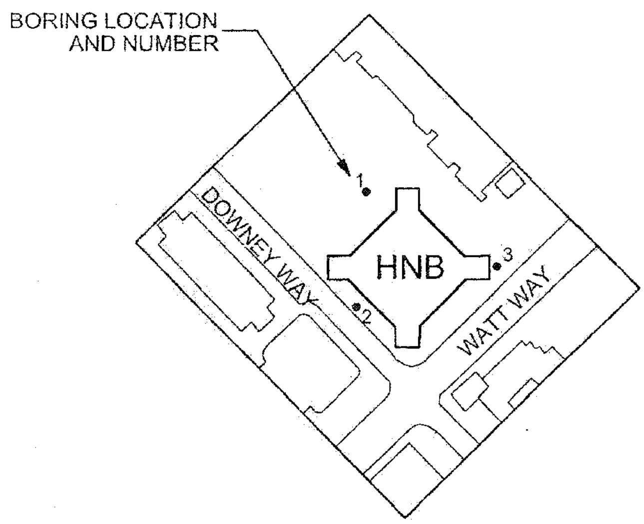

Figure 2.13 Boring Location and Number (3. Hao, A9.1.2)

[4] 3. Hao, T-Y., Trifunac, M.D., Todorovska M.I. (April 1994), "Instrumented Buildings of University of Southern California-Strong Motion Data, Metadata and Soil-Structure System Frequencies, Report CE 04-01, University of Southern California, Los Angeles, California

[5] 5. Stewart, J.P. and Stewart, A.F. (1997), "Analysis of Soil-Structure Interaction Effects on Building Response from Earthquake Strong Motion Recordings at 58 Sites, Report No. UCB/EERC-97/01, Earthquake Engineering Research Center, University of California, Berkeley, California.

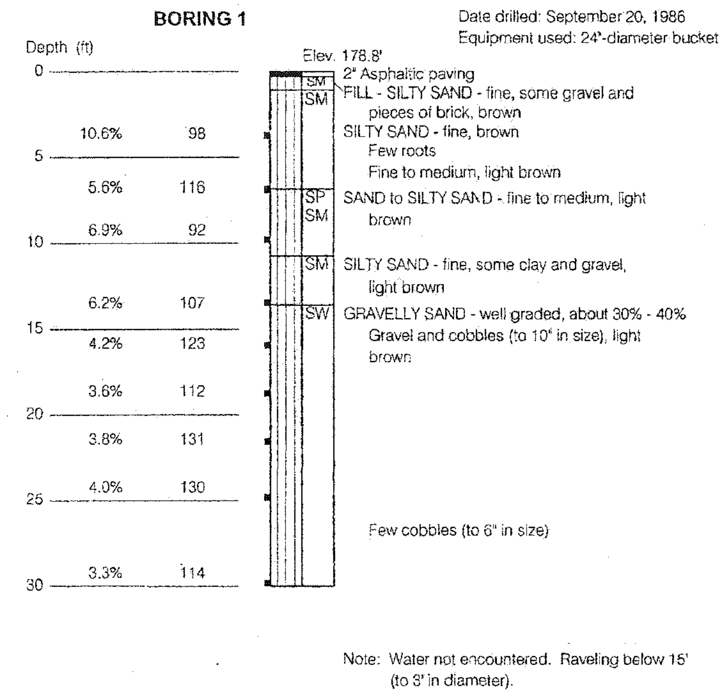

Figure 2.14 Boring Log 1(3. Hao, A9.1.7)

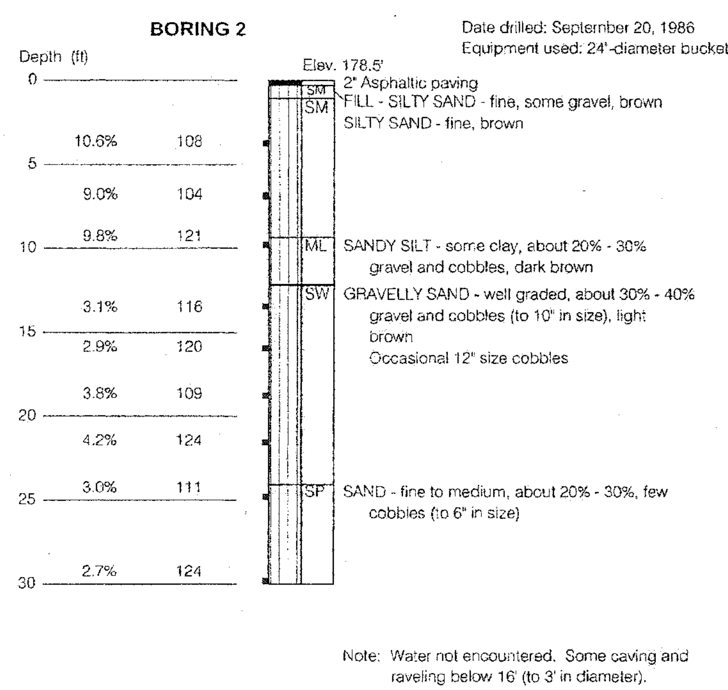

Figure 2.15 Boring Log 2 (3. Hao, A9.1.7)

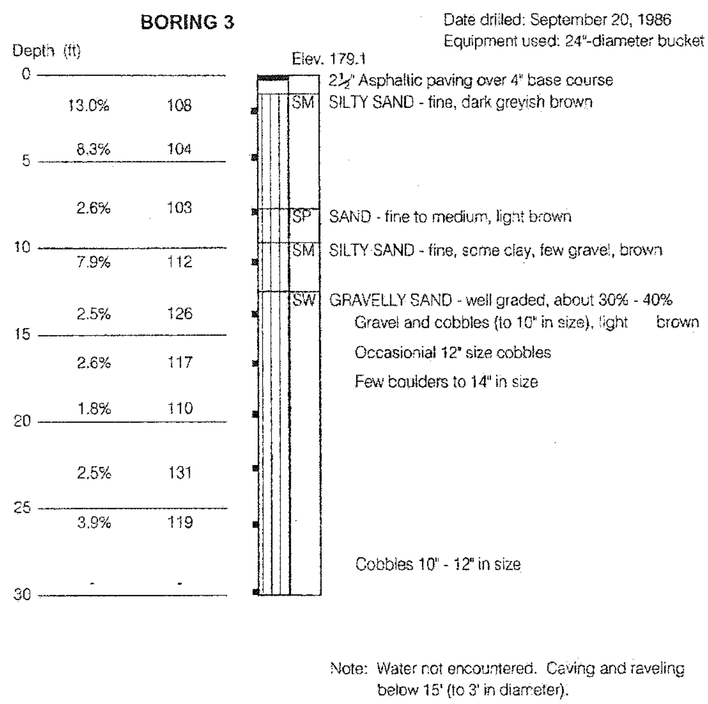

Figure 2.16 Boring Log 3 (3. Hao, A9.1.7)

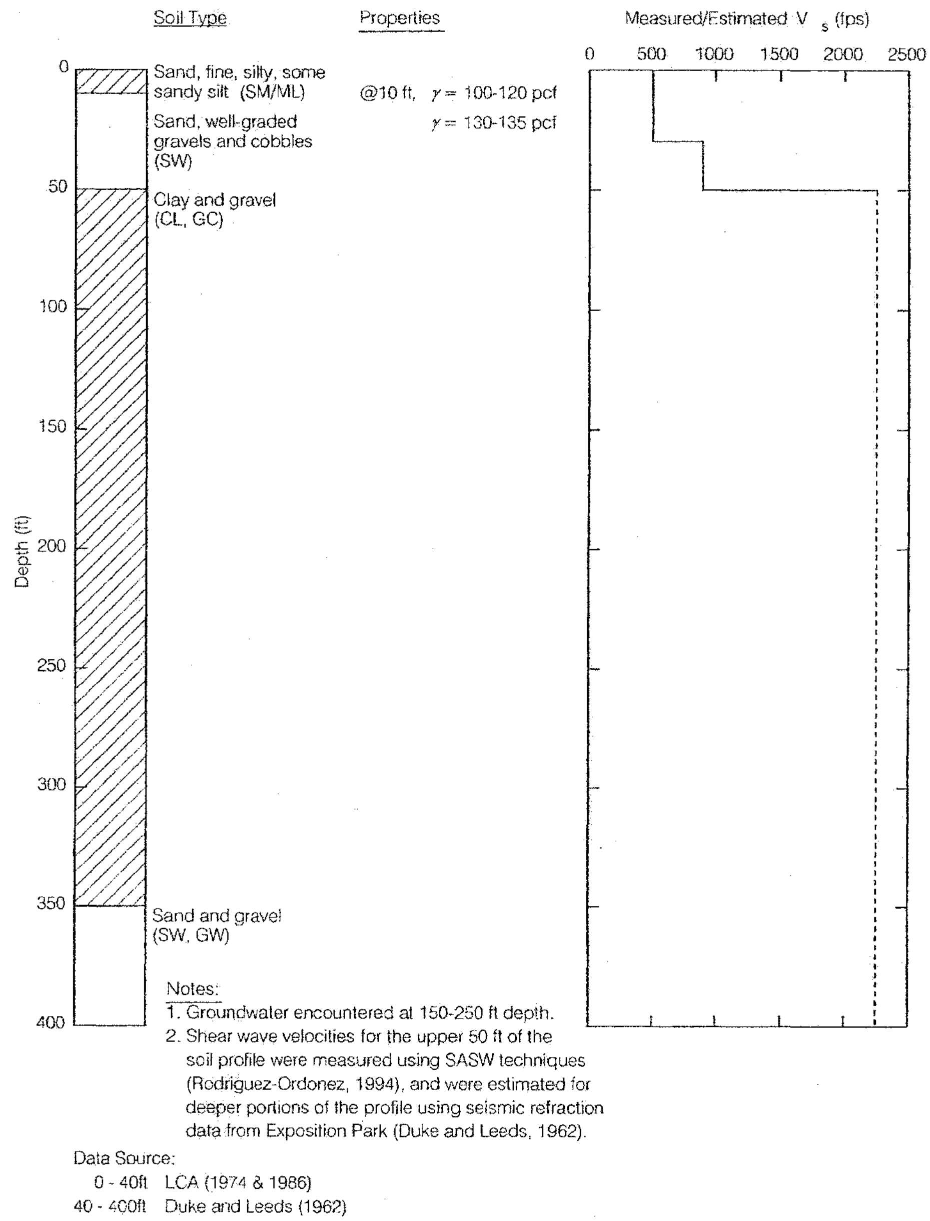

Figure 2.17 Generalized Soil Conditions
(Stewart and Stewart, 1997).

CHAPTER 3

DESCRIPTION OF STRONG-MOTION DATA PROCESSING

3.1 General

During the past years California Geologic Survey, through the Strong Motion Instrumentation Program (SMIP) instrumented several modern steel structures at various places in the State of California. The SMIP obtained records for these instrumented buildings from a number of earthquakes that occurred during the last 20 years, including the 1994 Northridge Earthquake. The data obtained from this particular earthquake for the HEDCO Neurosciences Building are processed in this report.

During the 1994 Northridge Earthquake an array of 15 strong motion accelerometers produced records for the HNB Building located in University Park Campus at Los Angeles, California, 31.33 kilometers from the epicenter of the earthquake.

3.2 Instrumentation Scheme

HEDCO Neurosciences Building was instrumented for the Strong Motion Instrumentation Program (SMIP) by the California Geological Survey (CGS) in 1993. It is recognized as SMIP Station No. 24652. It was instrumented by SSA-2 digital accelerometers recording 15 channels of acceleration at 4 levels in the building (basement, first, fourth and roof levels). The sensor locations are shown in Figures 3.1 through 3.5 which include the following instruments:

a. Two vertical accelerometers in the basement, located at the west corner of the building.

b. Three horizontal accelerometers in the basement, two in N-S direction (one located in the west corner and the other one on the east corner) and one in E-W direction located in the west corner.

c. Three horizontal accelerometers on the first floor, two in N-S direction (one located in the west corner and the other one on the east corner) and one in E-W direction located in the west corner.

d. Three horizontal accelerometers on the third floor, two in N-S direction (one located in the west corner and the other one on the east corner) and one in E-W direction located in the west corner.

e. One vertical accelerometer on the third floor, located in the middle of the girder between the west and the south corner of the building.

f. Three horizontal accelerometers on the roof, two in N-S direction (one located in the west corner and the other one on the east corner) and one in E-W direction located in the west corner.

This instrumentation recorded the 1994 Northridge earthquake.

At the time performing the analysis presented in this report, the records for the channels No. 6,7,8,9 and 10 that were located on the first and third floor were not available from the CDMG web page. So all the analyses were done with the data that were available, and more important, from the rest of the channels, located on the basement and the roof.

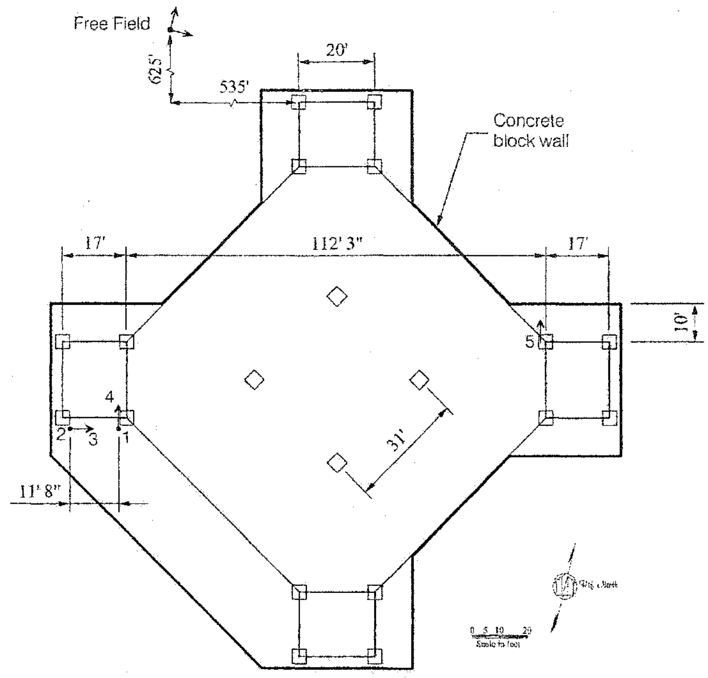

Figure 3.1 Sensor Locations (Channels 1, 2, 3, 4, 5) in the Basement (3. Hao, A9.1.2)

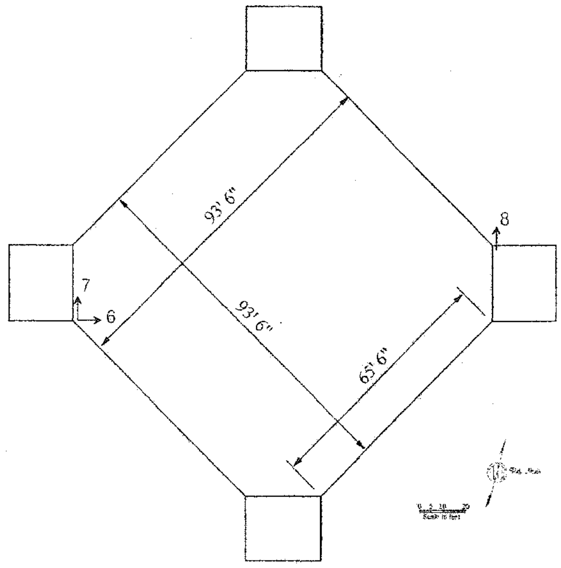

Figure 3.2 Sensor Locations (Channels 6, 7, 8) in the 1st Floor (3. Hao, A9.1.3)

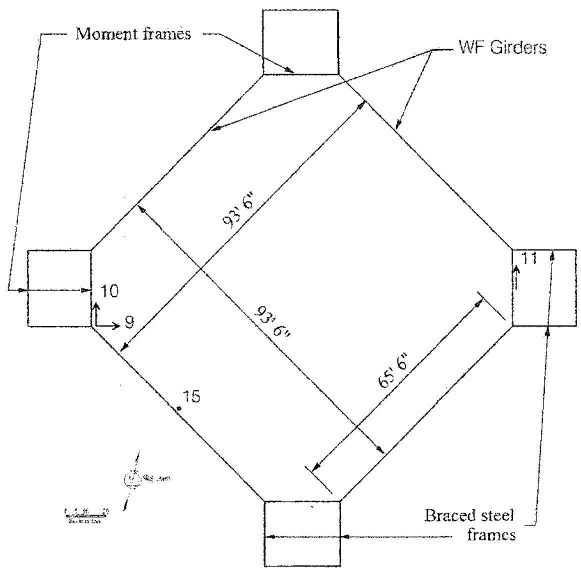

Figure 3.3 Sensor Locations (Channels 9, 10, 11, 15) in the 3rd Floor (3. Hao, A9.1.4)

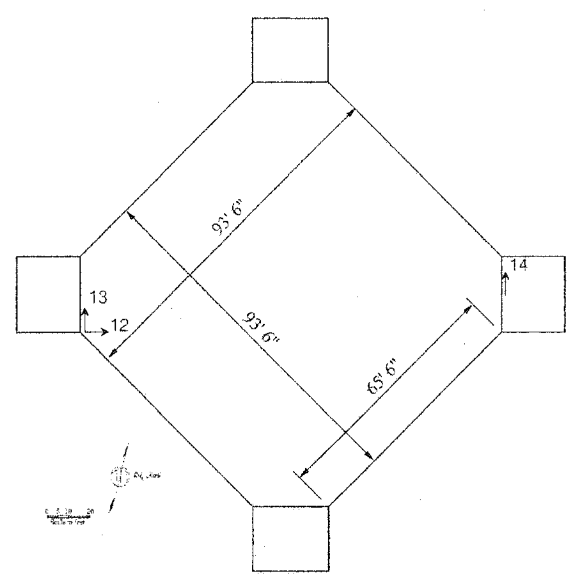

Figure 3.4 Sensor Locations (Channels 12, 13, 14) in Roof (3. Hao, A9.1.5)

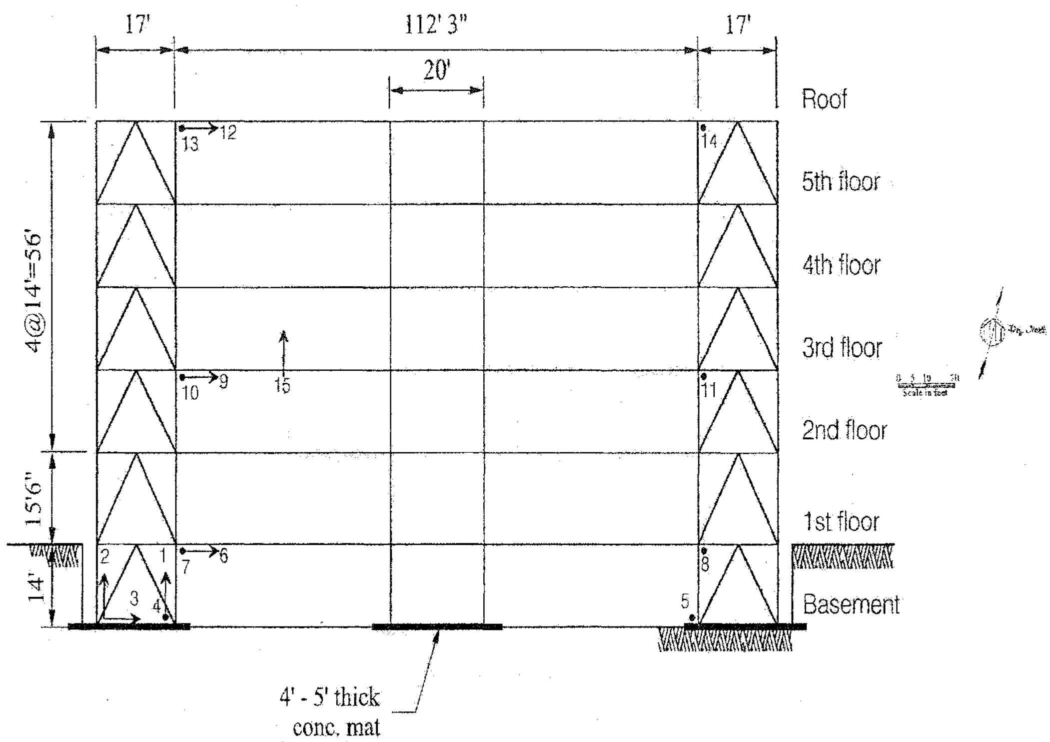

Figure 3.5 Elevation - Sensor Location (3. Hao, A9.1.6)

Peak accelerations, velocities and displacements are listed in Table 3.1. Plots of the recorded accelerations, velocities and displacements are shown on Figures 3.6 to 3.11

HEDCO Neurosciences Building (CSMIP Station No. 24652) Northridge Earthquake (Jan. 17, 1994, M=6.4, R=31.33 km)						
Channel (#)	Elevation	Location	Orientation	Accel (cm/sec^2)	Vel (cm/sec)	Displ (cm)
1	Basement	SE Corner of West Tower	UP	74.832	4.269	-1.448
2	Basement	SW Corner of West Tower	UP	74.243	4.429	-1.444
3	Basement	SW Corner of West Tower	E-W	-237.587	20.597	4.832
4	Basement	SE Corner of West Tower	N-S	-161.568	10.263	2.157
5	Basement	NW Corner of East Tower	N-S	-203.355	11.265	-2.218
6	1st Floor	SE Corner of West Tower	E-W	-	-	-
7	1st Floor	SE Corner of West Tower	N-S	-	-	-
8	1st Floor	NW Corner of East Tower	N-S	-	-	-
9	3rd Floor	SE Corner of West Tower	E-W	-	-	-
10	3rd Floor	SE Corner of West Tower	N-S	-	-	-
11	3rd Floor	NW Corner of East Tower	N-S	212.245	-19.053	-3.118
12	Roof	SE Corner of West Tower	E-W	472.248	-69.677	11.173
13	Roof	SE Corner of West Tower	N-S	288.121	-38.398	-6.246
14	Roof	NW Corner of East Tower	N-S	283.854	-37.137	-5.477
15	3rd Floor	SW Wall	UP	148.347	-6.741	-1.564

Table 3.1 Northridge Earthquake Records (Peak Accelerations, Velocities, Displacements, Orientation, location)

3.3 Data processing

The data used were obtained from the web site of the California Geologic Survey (CGS), Strong Motion instrumentation Program (SMIP).

The 15 accelerograms recorded at the building during the 1994 Northridge Earthquake had previously been processed and digitized by CGS on 21 October 1994. For the low frequency noise the data were bandpass filtered with ramps at 0.120 -0.240 and 46.00 – 50.00 cyc/sec. 12001 points of instrument – and baseline –corrected acceleration, velocity and displacement data were obtained at equally spaced intervals of 0.010 sec.

The data were obtained from CGS website in files having a .V2 extension. Each file contained general information about the earthquake, (time, location etc), information and location of the sensor used, the peak acceleration, velocity and displacement along with their time of occurrence. After that, the actual data followed, starting with 12001 acceleration data, continuing with 12001 velocity data, and ending with 12001 displacement data, one after the other.

In order to be able to do the accelerographs the data had to be separated in different files in order to be correctly read and processed. For that reason a macro in Microsoft Excel was used that could identify the acceleration, velocity and displacement data in the .V2 file and separate them in three different .txt files. The program was obtained from Mr. Ricardo Taborda.

Once the accelerographs were built up in column .txt files and were plotted in Excel, an additional problem rose. All signals at all channels presented a sort of noise-perturbation problem after 45 seconds. A typical sample of the problem —for the acceleration time-history of channel 4- is shown in Figure 3.6 for a time window between 60 to 70 sec in contrast with the whole signal and a clean-of-noise time window between 30 to 40 sec. Usage of this portion of the signal (i.e., from 45 to 120 sec) would have affected the frequency analysis. Therefore, all channels were cut off 45 sec after trigger. Since the intense phase of the motion took place approximately between 10 and 35 sec, it has been assumed that having truncated the signals does not affect the results here discussed.

In order to obtain the Fourier Transforms a Matlab program was created which is displayed in Appendix I.

The transfer functions were obtained after that, by dividing the Fourier Transforms of the Channels located in the roof of the buildings with the ones located in the basement.

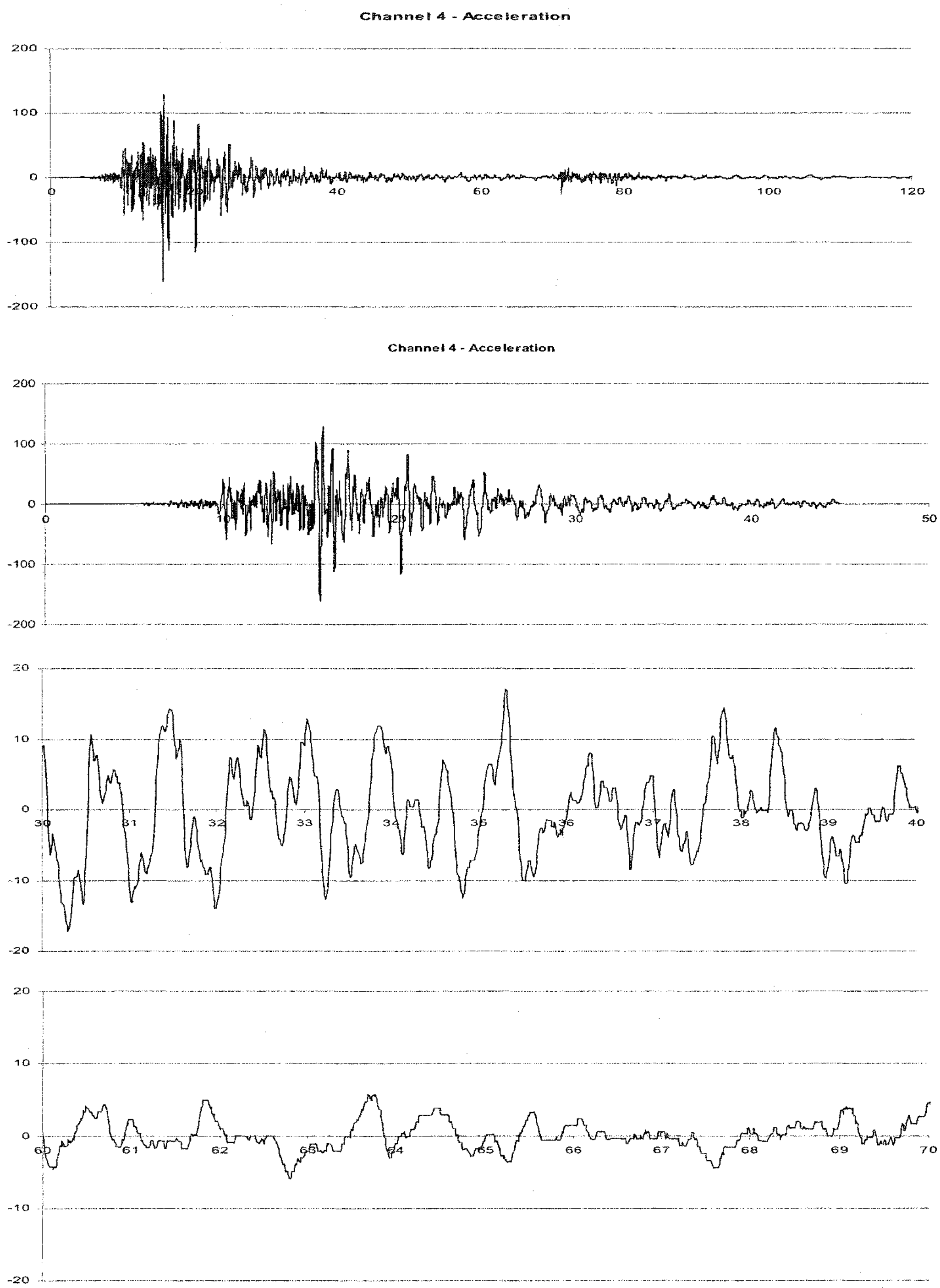

Figure 3.6 Example of an accelerograph time window (60-70 sec) in contrast with the whole signal and a clean-of-noise time window (30-40 sec).

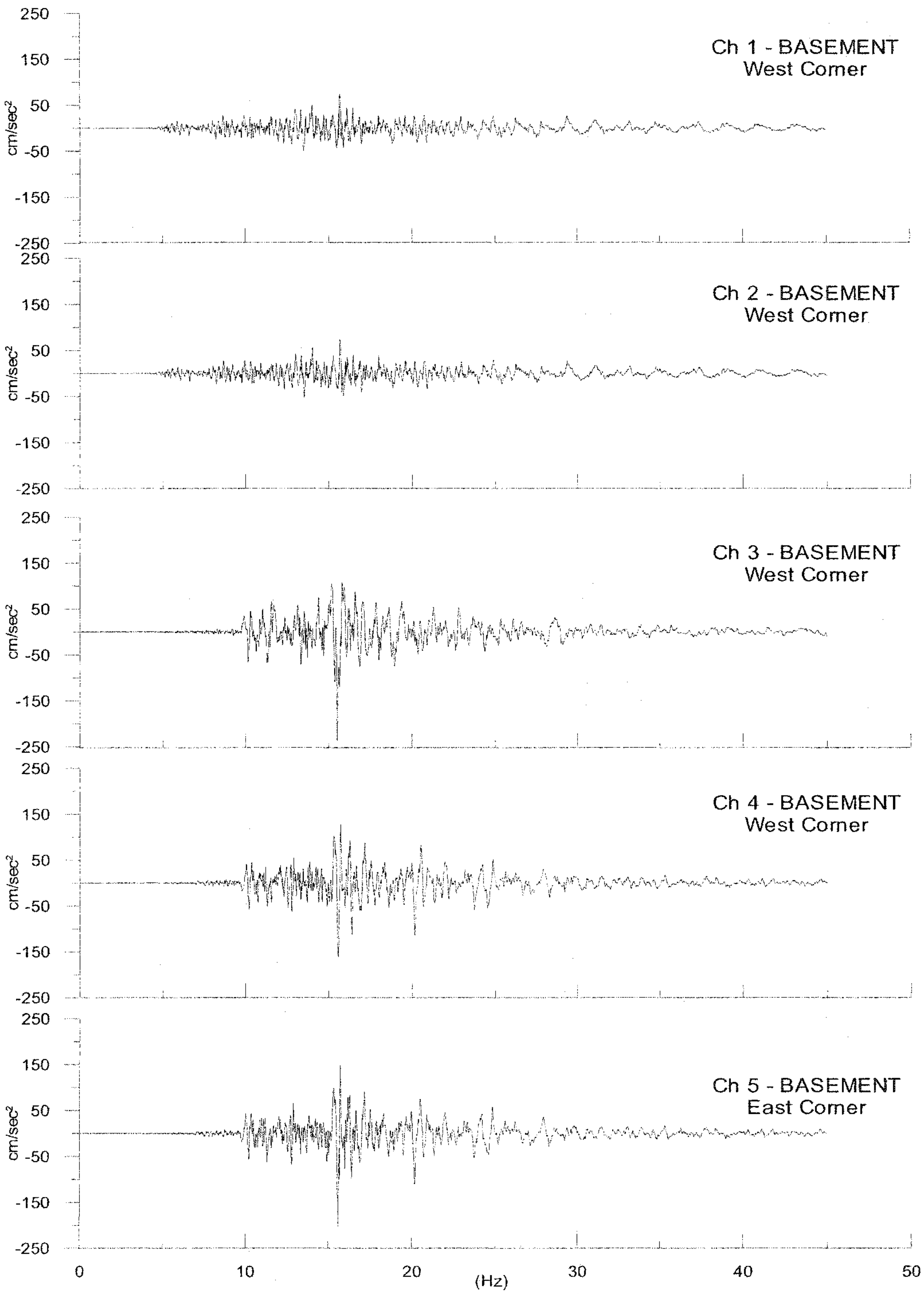

Fig.3.7 Hedco Neuroscience Building
Recorded Acceleration Time-Histories

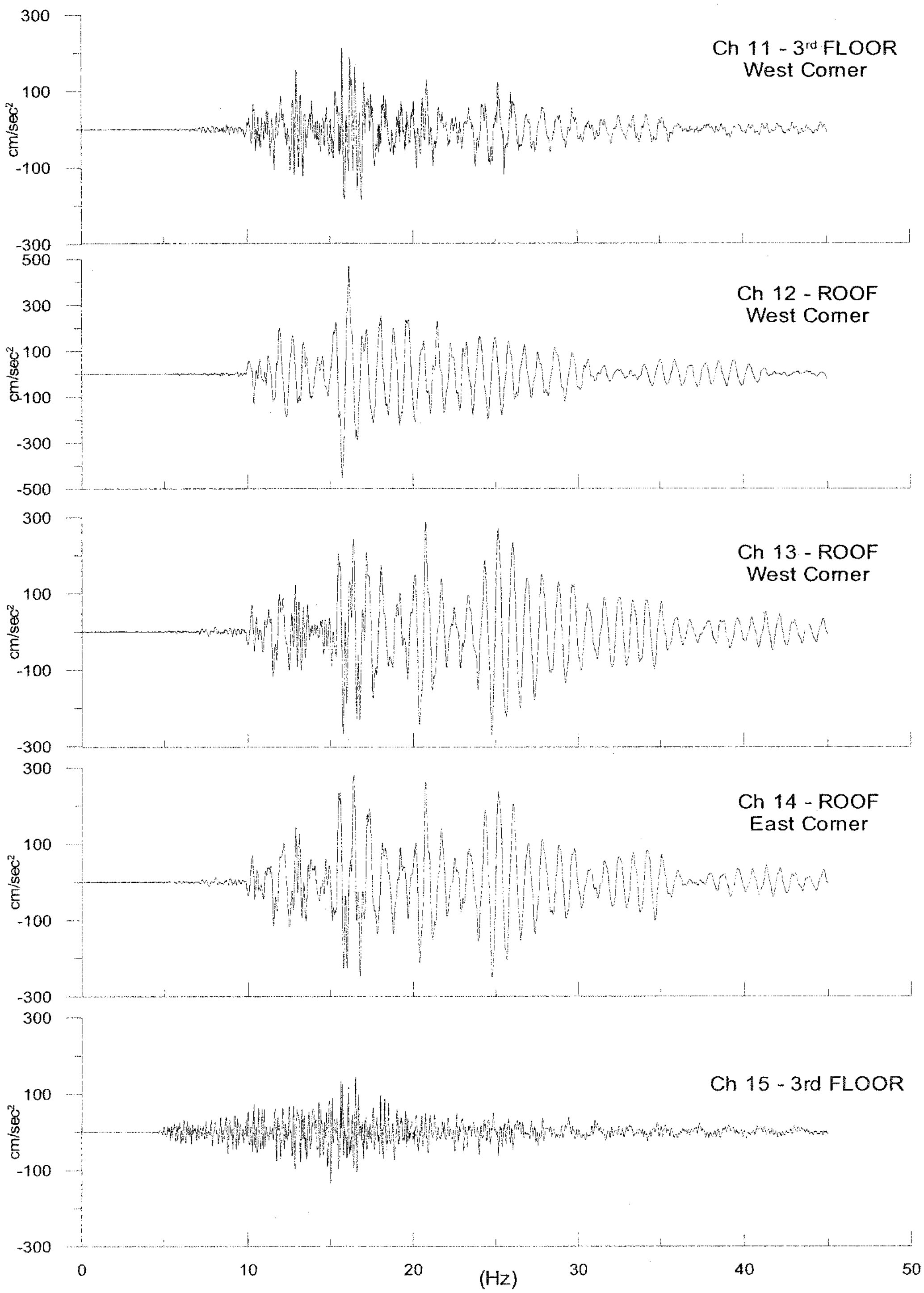

Fig.3.8 Hedco Neuroscience Building
Recorded Acceleration Time-Histories

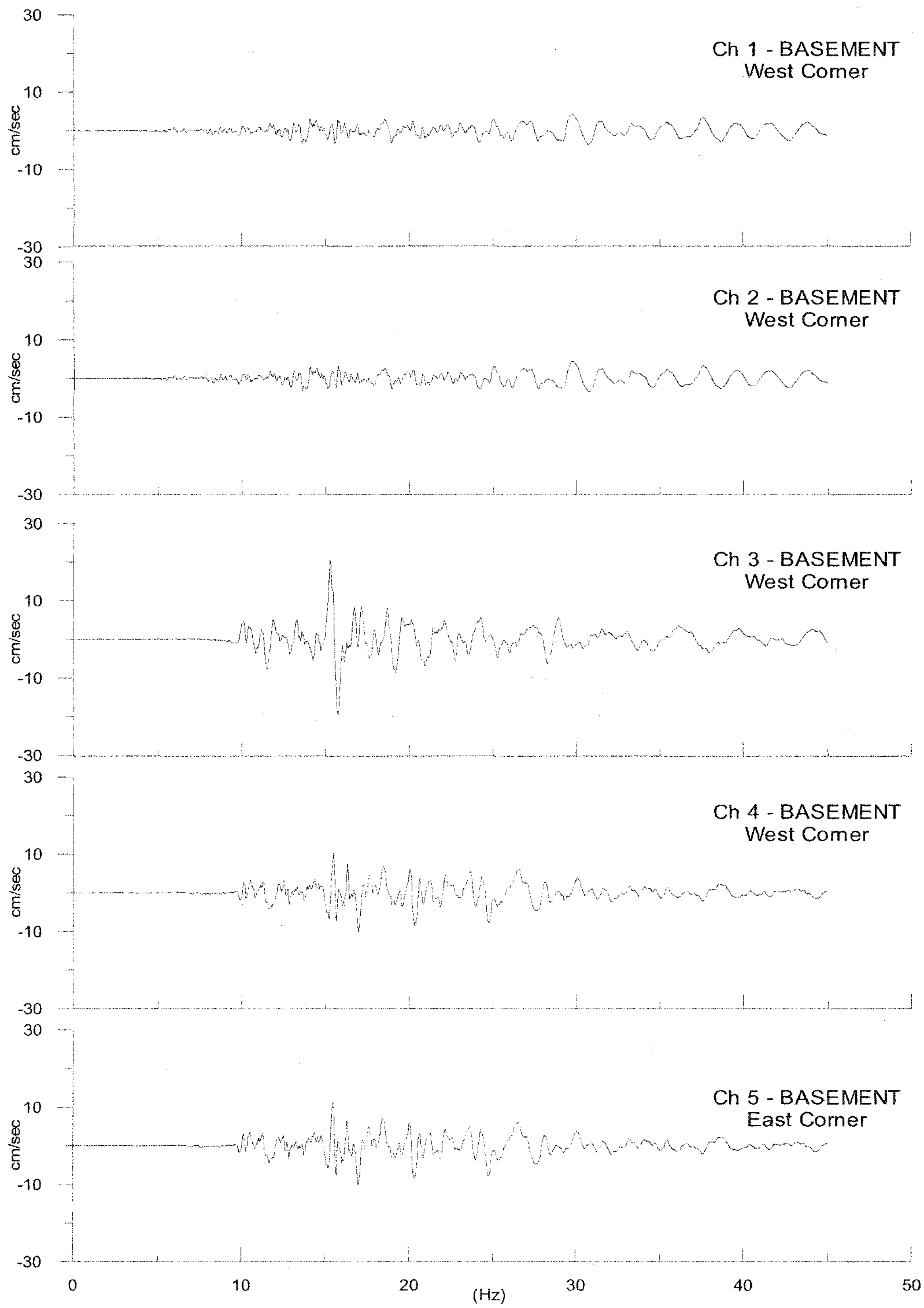

Fig.3.9 Hedco Neuroscience Building
Recorded Velocity Time-Histories

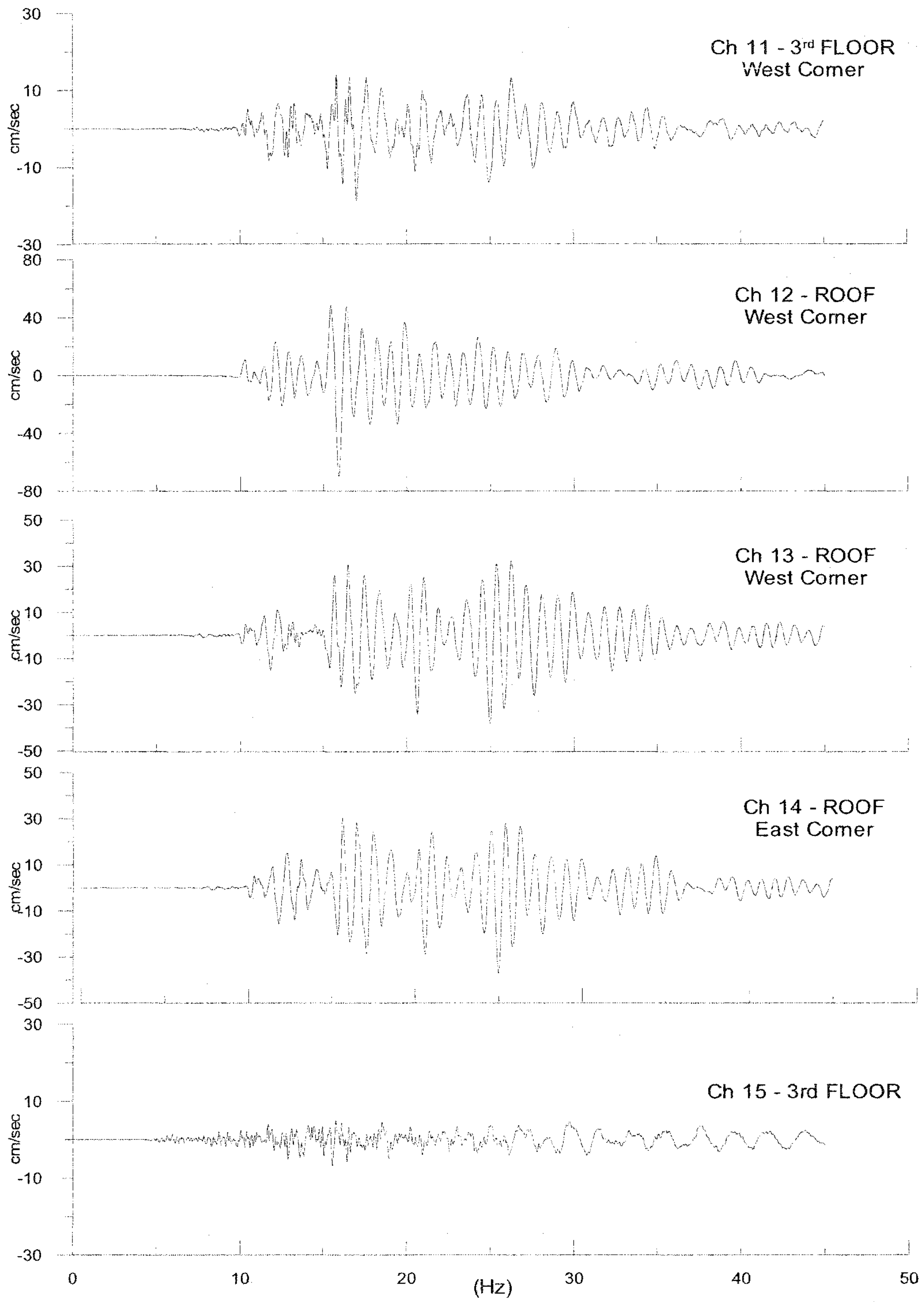

Fig.3.10 Hedco Neuroscience Building
Recorded Velocity Time-Histories

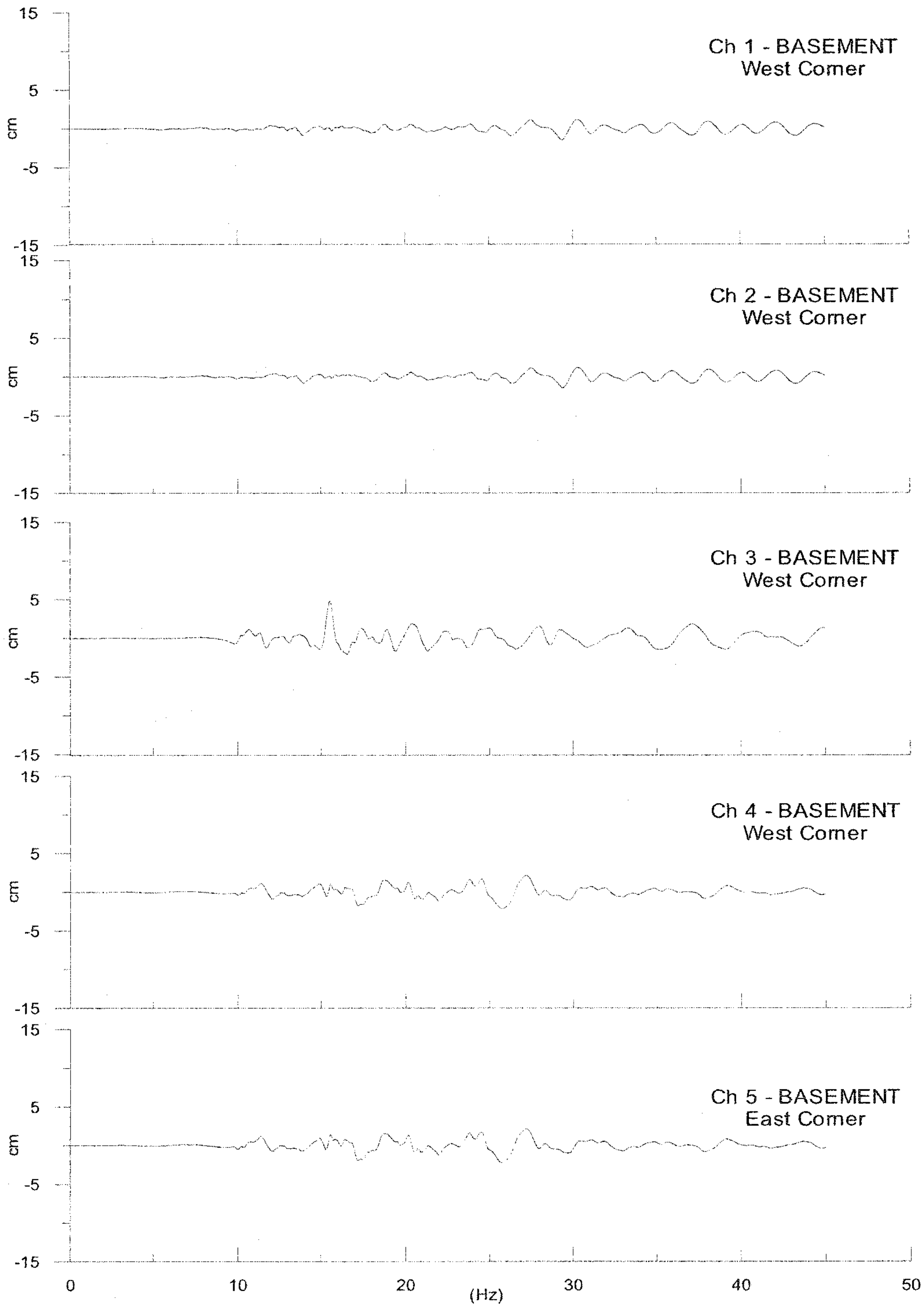

Fig.3.11 Hedco Neuroscience Building
Recorded Displacement Time-Histories

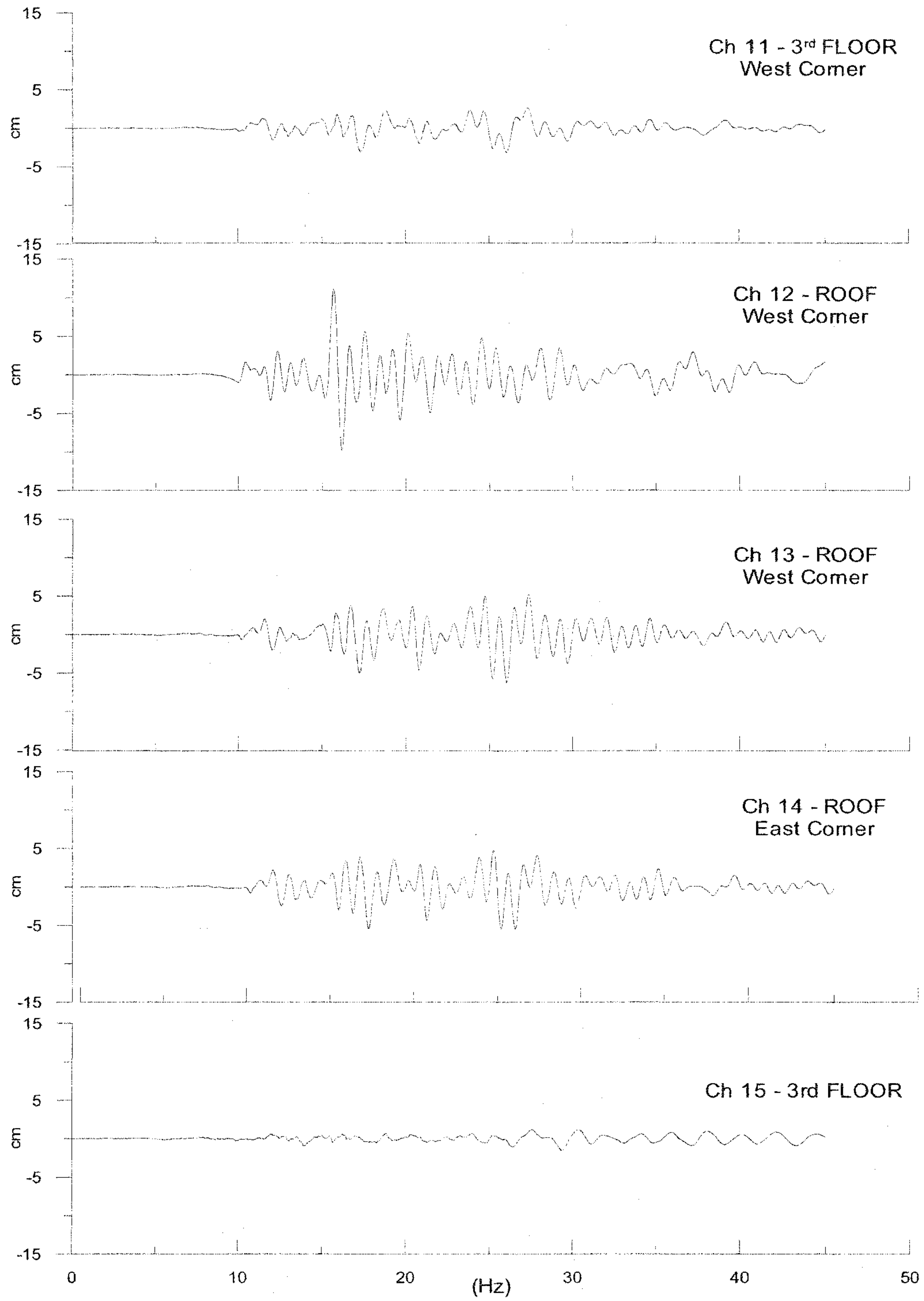

Fig.3.12 Hedco Neuroscience Building
Recorded Displacement Time-Histories

CHAPTER 4

ENGENEERING INTERPRETATION OF RESPONSE OF HEDCO NEUROSCIENCES BUILDING TO THE 1994 NORTHRIDGE EARTHQUAKE

4.1 General

This chapter talks about the engineering interpretation of the response of the HEDCO Neurosciences Building to the 1994 Northridge Earthquake. A detailed description of the building and of the ground motion processing was given in the previous chapters.

The recorded data from accelerograms with the refined filtering techniques used provide considerable information of engineering interest. Basic engineering parameters such as periods of vibration are identified and some significant response characteristics are discussed. The discussion is carried out in both the time and frequency domain.

4.2 Time Domain Analysis

4.2.1 Acceleration Records

Accelerograms, the recordings from strong-motion accelerographs, contain information about the large-amplitude seismic waves in the region close to large earthquakes. This information is used primarily by engineers to help establish seismic safety codes to protect buildings from future earthquakes. It is also used by seismologists to understand the details of the fault-rupture process and the complicated wave propagation effects that control the intensity of earthquake shaking.

4.2.1.1 Peak Values

The peak values of accelerations of the structure in the East-West (E-W) and North-South (N-S) directions were obtained from processed accelerograms and were summarized in Table 3.1. The peak amplification ratios of all records in the E-W and N-S directions, along with the maximum accelerations and their time of occurrence are shown in Table 4.1. The peak amplification ratio of the structure in one direction is defined as the ratio of the peak acceleration of the structure in that direction to the corresponding peak ground acceleration in the same direction. It is clear from Table 4.1 that the building is apparently symmetric about its center; the maximum acceleration for both directions happens in the roof, but with a substantial difference in the value. Maximum acceleration at the roof level, for the E-W direction was 472.248 cm/sec^2 occurring at 16.130 sec and for the N-S direction it was 288.121 cm/sec^2 at 20.730, slightly higher than half the value in the E-W direction.

In general, the earthquake ground shaking and the building response recorded in the E-W direction were stronger than the corresponding values recorded in the N-S direction. The peak values of vertical ground acceleration were about half of the horizontal ones and occurred approximately at the same time.

HEDCO Neurosciences Building (CSMIP Station No. 24652)						
Channel (#)	Elevation	Location	Orie/ tion	Peak Accel (cm/sec^2)	Amplification	Time of Occurrence
1	Basement	SE Corner of West Tower	UP	74.832	-	15.670
2	Basement	SW Corner of West Tower	UP	74.243	-	15.640
3	Basement	SW Corner of West Tower	E-W	-237.587	-	15.500
4	Basement	SE Corner of West Tower	N-S	-161.568	-	15.550
5	Basement	NW Corner of East Tower	N-S	-203.355	-	15.650
6	1st Floor	SE Corner of West Tower	E-W	-	-	-
7	1st Floor	SE Corner of West Tower	N-S	-	-	-
8	1st Floor	NW Corner of East Tower	N-S	-	-	-
9	3rd Floor	SE Corner of West Tower	E-W	-	-	-
10	3rd Floor	SE Corner of West Tower	N-S	-	-	-
11	3rd Floor	NW Corner of East Tower	N-S	212.245	1.0437	15.760
12	Roof	SE Corner of West Tower	E-W	472.248	1.9876	16.130
13	Roof	SE Corner of West Tower	N-S	288.121	1.7832	20.730
14	Roof	NW Corner of East Tower	N-S	283.854	1.3958	16.400
15	3rd Floor	SW Wall	UP	148.347	-	16.480
Northridge Earthquake (Jan. 17, 1994, M=6.4, R=31.33 km)						

Table 4.1 Peak Accelerations, Amplifications Ratios & Time of Occurrence

4.2.1.2 Characteristics

A study of the acceleration records in terms of frequency and amplitude patterns yielded the following characteristics:

a. In all the accelerograms of the horizontal sensors it can be identified that the first wave comes approximately 10 sec after the trigger time.
b. Peak acceleration values for all the channels took place between 15 and 16 sec except that of channel 13 where the peak acceleration occurred at 20 sec.
c. High frequency responses with very small amplitudes are identified for all the horizontal accelerations consistently between the 10 and 15 second of the ground motion. After that the pattern of the acceleration of the records remains the same in the two directions.
d. From the accelerograms of the vertical sensors located at the basement and 3rd floor, channels 1, 2 & 15, a high frequency and considerable amplitude can be

identified between the 5^{th} and 10^{th} sec of the earthquake.

e. In the E-W direction, it can be seen throughout the whole roof accelerogram that the building filtered the high frequency content of the input ground motion; nevertheless the peak values occurred at almost the same time.

f. In the N-S direction, it can be seen that from 10 to 15 sec the building didn't filter the high frequency content of the ground motion, nevertheless one of the peak values at the roof occurred at almost the same time as the one in the basement.

4.2.2 Displacements Responses

The following observations were made from Figures 3.14 and 3.15 and Table 4.2:

a. In general the displacements in the E-W direction were larger; more that double in the basement and almost double in the roof, than those in the N-S direction.

b. In all the displacement histories of the sensors it can be identified that there is hardly any movement for 10 sec after the trigger time.

c. The peak displacements happen in the E-W direction, both for the basement and for the roof, and occur almost the same time, at 15.5 sec.

d. The peak displacements in the N-S direction happen considerably later than that of the E-W direction, approximately 10 to 12 sec later, at the 27 sec.

e. From the displacements of the vertical sensors located at the basement and 3rd floor, channels 1,2 & 15, no significant movement can be identified compared with the horizontal displacements.

f. Story drifts (D/h_i) were less than 0.4% at the roof level as shown in Table 4.2

4.2.3 Translational Effects

In order to identify the translation frequency of the building without the effect of torsion present in Channels 4, 5, 13, 14, the average of Channels 4 and 5 at the basement and 13 and 14 at the roof was assessed to obtain the signals at the center of both levels. The resultant generated signals are shown in Figure 4.1.

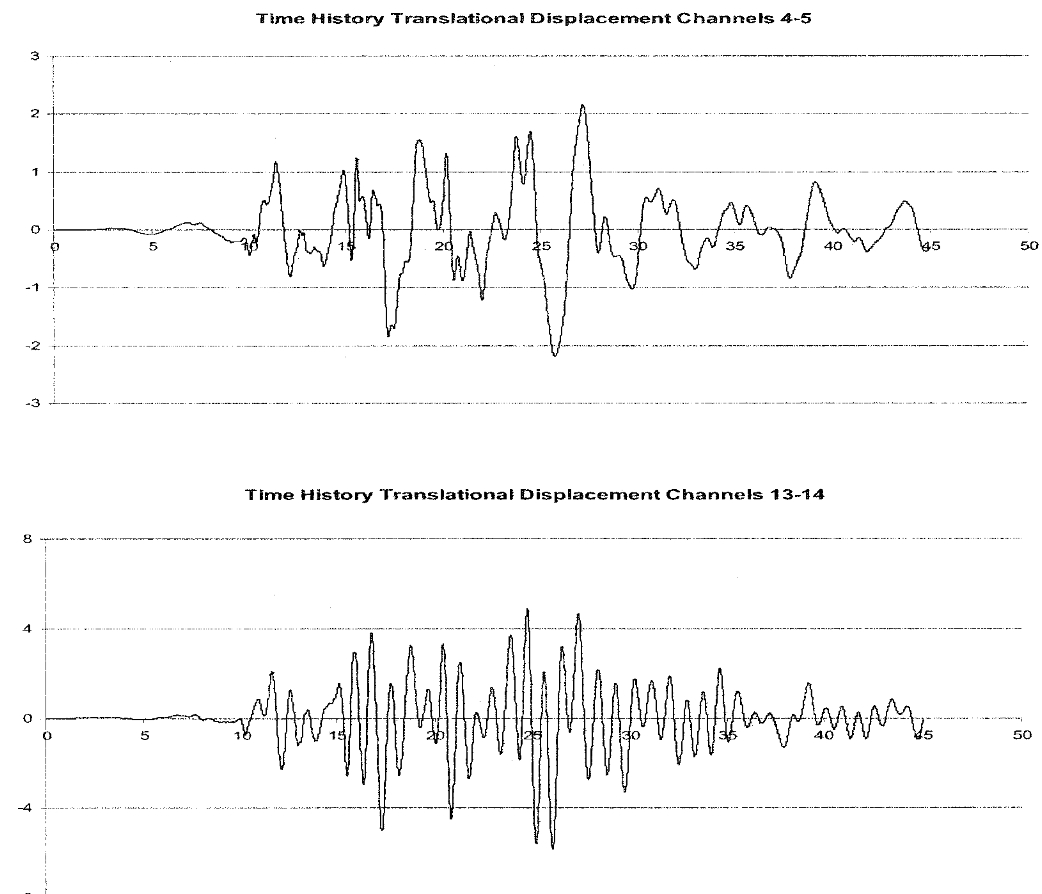

Figure 4.1 Time History Translational displacements of the resultant generated signal from the average of Channels 4&5 and 13&14 signals

4.2.4 Torsional Effects

In the case of the torsional effects, new signals were also generated by taking the difference between Channels 4 and 5, and

13 and 14, divided by the correspondent distance between them at both the roof and the basement.

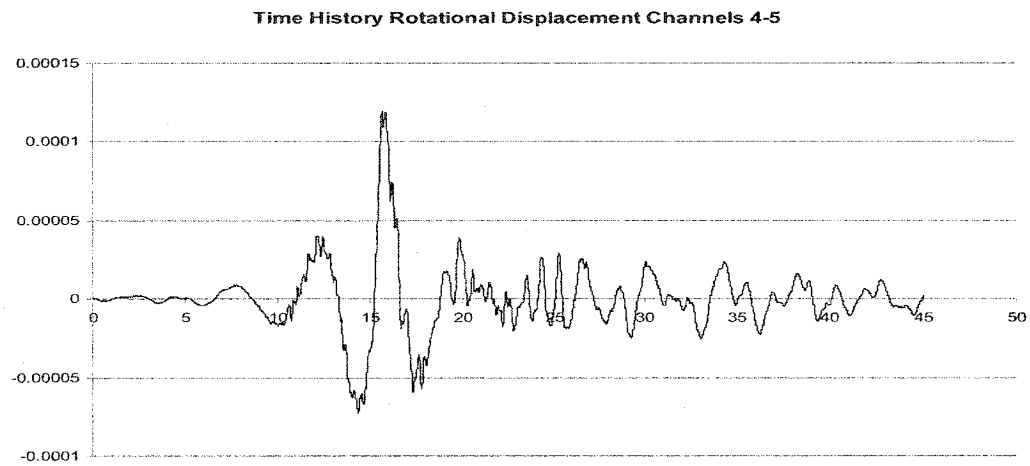

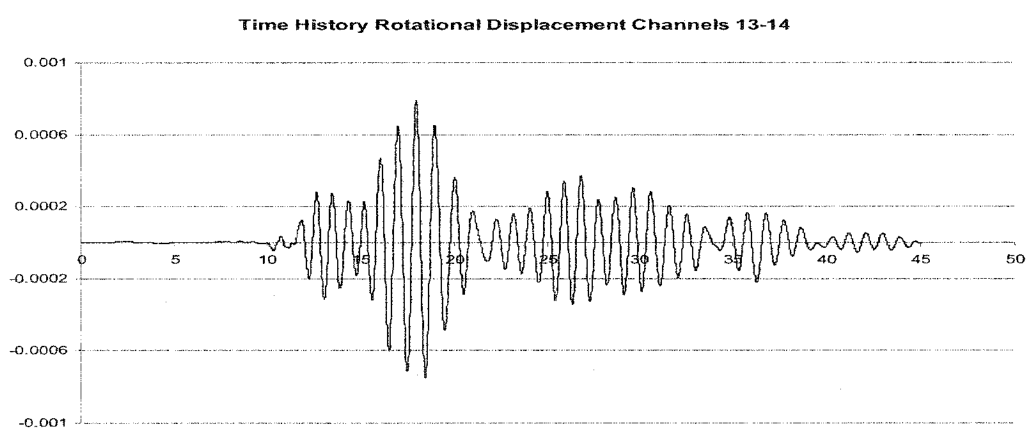

Figure 4.2 (a) Time History Rotational Displacements of the new generated signal (average of Channels 4&5 and 13&14 signals divided by their correspondent distance)

Figure 4.2 (a) shows the obtained signals for the case of displacements (amplitude values correspond to rotational displacement in radians). Figure 4.2 (b) shows a comparison between the two pairs of channels in the case of acceleration.

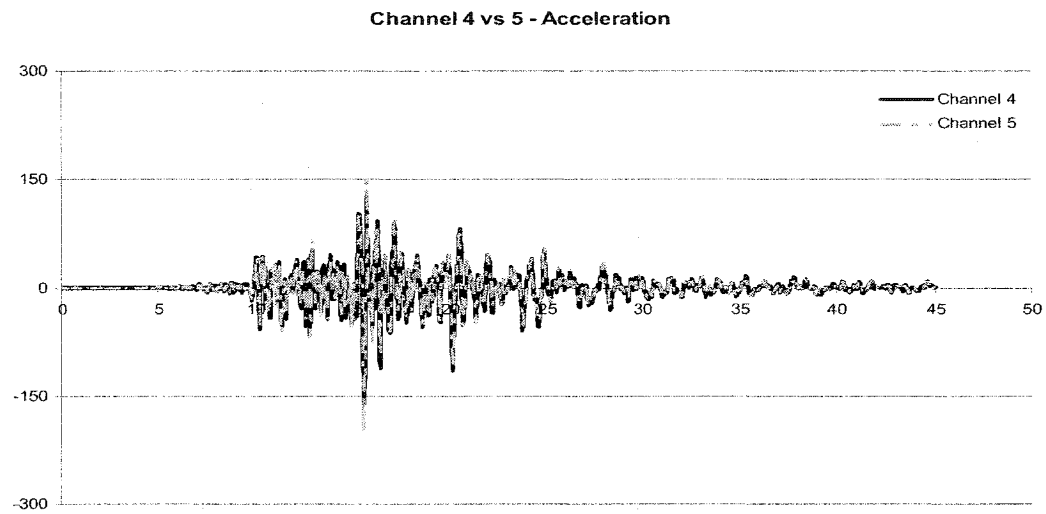

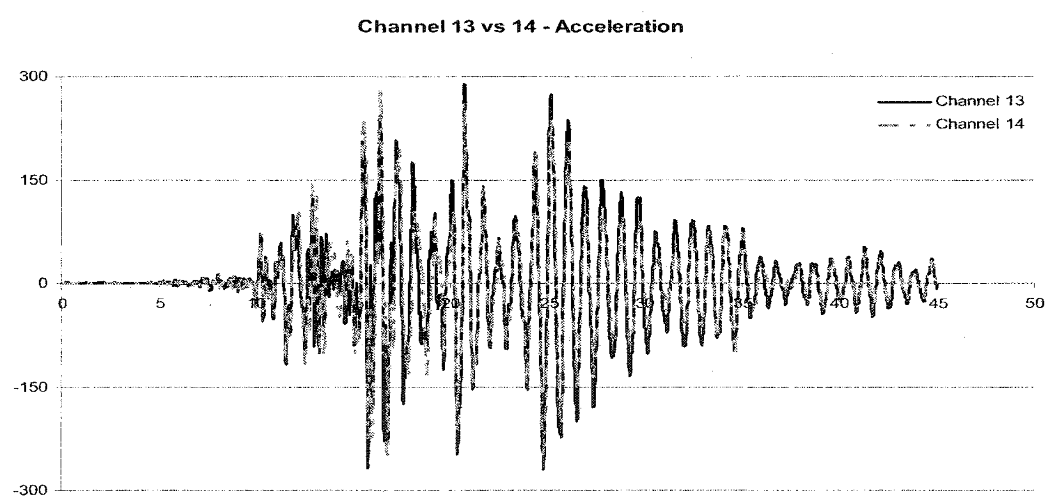

Figure 4.2 (b) Time History Acceleration Comparisons for Channels 4 vs. 5 and 13 vs. 14

HEDCO Neurosciences Building (CSMIP Station No. 24652)						
Channel (#)	Elevation	Location	Orientation	Displ (cm)	Displ. Coefficient (Max D/h_i)	Time of Occurrence (sec)
1	Basement	SE Corner of West Tower	UP	-1.448	0.000555	29.370
2	Basement	SW Corner of West Tower	UP	-1.444	0.000554	29.380
3	Basement	SW Corner of West Tower	E-W	4.832	0.001854	15.510
4	Basement	SE Corner of West Tower	N-S	2.157	0.000827	27.160
5	Basement	NW Corner of East Tower	N-S	-2.218	0.000851	25.740
6	1st Floor	SE Corner of West Tower	E-W	-	-	-
7	1st Floor	SE Corner of West Tower	N-S	-	-	-
8	1st Floor	NW Corner of East Tower	N-S	-	-	-
9	3rd Floor	SE Corner of West Tower	E-W	-	-	-
10	3rd Floor	SE Corner of West Tower	N-S	-	-	-
11	3rd Floor	NW Corner of East Tower	N-S	-3.118	0.001964	15.760
12	Roof	SE Corner of West Tower	E-W	11.173	0.004287	15.680
13	Roof	SE Corner of West Tower	N-S	-6.246	0.002396	26.010
14	Roof	NW Corner of East Tower	N-S	-5.477	0.00210	25.190
15	3rd Floor	SW Wall	UP	-1.564	0.00060	29.370
Northridge Earthquake (Jan. 17, 1994, M=6.4, R=31.33 km)						

Table 4.2 Maximum Displacements & Time of Occurrence

4.3 Frequency Domain Analysis

4.3.1 General

Frequency domain analysis is another way of studying the characteristics of the response. Important dynamic parameters can be identified with this method like modal damping, periods and mode shapes. In this particular case frequency domain analysis was just used to identify the frequencies of the building. The procedure followed was the subsequent:

a. Fourier amplitude spectra were obtained from recorded accelerations.

b. Transfer functions were computed by dividing the Fourier amplitude spectrum of acceleration recorded at the roof of the building by that recorded at the basement. In that way the motion of the soil-structure system was isolated from the input ground motion.

c. The frequencies of the system were identified by looking at the peak values of the transfer functions.

4.3.2 Determination of Response Characteristics

The Fourier amplitude spectra (transfer functions) of the acceleration and the amplification spectra are presented in Figures 4.3 to 4.8 respectively.

The amplification factor for the E-W direction of the roof, measured from channels 12&3, shows a predominant single peak at 1.123 Hz with one small overlapping adjacent peak at 1.074. The amplitude at 1.123 Hz is almost the same with the next strongest peak which occurs at 3.83 Hz. From this particular graph one may assume that the first peak at 1.123 is the first mode and the second peak at 3.83 is the second mode. No conclusions can be made about the third mode from the graph because there are no predominant peak that could be identified as third mode. Maybe if more sensors were placed in the building in this particular direction and if we had the data from the sensors located in the first and third floor, the 3^{rd} mode could be identified.

The amplification factor for the N-S direction of the roof in the west corner, measured from the channels 13&4 shows dominant single peak at 1.123 Hz, with two small overlapping adjacent peaks at 1.22 Hz and 1.29 Hz. The amplitude at 1.123 Hz is 5 times greater than that of the next strongest peak that occurs at 3.89 Hz. A third peak is identified at 8.39 Hz. Since the amplitudes of the second and third peak are so small comparing with the amplitude of the first peak, no safe conclusions can be made about the identification of the second and third mode.

The roof amplification spectrum in the N-S direction in the east corner, measured by channels 14 & 5, shows a predominant peak at 1.147 Hz, with two small overlapping peaks at 1.232 Hz and 1.293 Hz. The amplitude at 1.147 Hz is 6 times greater than that of the next strongest identifiable peak which occurs at 3.89 Hz. The second mode can be identified from this graph at 3.89 Hz. A third peak can also be identified at 6.87 Hz which probably represents the third mode.

Nevertheless more accurate conclusions about the identification of the modes in N-S direction can be made, when comparing the average signal from channels 4 and 5, located in the ground, and the average signal of channel 13 and 14, located in the roof.

The average roof amplification spectra were obtained by averaging the acceleration data from Channels 13 & 14 on the roof and the acceleration data from Channels 4 & 5 on the basement. The Fourier transforms were obtained and then they were divided between them to get the Transfer Function. Figure 4.6 shows a dominant rounded peak between 1.135 Hz and 1.147 Hz, with two adjacent overlapping peaks at 1.22 Hz and 1.29 Hz. The next strongest peak occurs at 3.9 Hz and represents the second mode. A third peak can also be identified for this direction from the only channel data was available, located in the third floor. Three predominant peaks are identified at 1.147 Hz, 3.89 Hz and 6.87 Hz respectively, representing the first three modes in the N-S direction.

Trying to identify the torsion frequency the Fourier transform from the difference of the acceleration data of Channels 4 and 5 divided by their distance (the length of the building) was taken for the basement, and the difference of the acceleration data of Channels 13 and 14 divided by their distance taken for the roof. Then the Fourier Transform of the roof was divided with the Fourier Transform of the basement in order to obtain the Transfer Function. A rounded peak was identified at 1.025 Hz representing the first mode, with two smaller adjacent peaks at 1.123 Hz and

1.239 Hz. The next dominant peak occurred at 3.06 Hz which may represent the second mode.

The following table gives a summary of the frequencies obtained from our ETABS model, which is described thoroughly in the next chapter and the frequencies obtained by identifying the peaks of the transfer functions of the recorded data.

Frequencies (Hz) obtained by recorded data from the 1994 Northridge Earthquake		Frequencies (Hz) obtained by ETABS V7.12 Model	
Mode 1		Mode 1	
Torsion	1.025	Torsion	0.9
N-S Direction (Average)	1.135-1.147	N-S Direction	1.25
E-W Direction (West Corner)	1.123	E-W Direction	1.27
Mode 2		Mode 2	
Torsion	3.06	Torsion	2.85
N-S Direction	3.9	N-S Direction	3.98
E-W Direction	3.83	E-W Direction	4.08
Mode 3		Mode 3	
Torsion	-	Torsion	5.47
N-S Direction	6.87	N-S Direction	7.19
E-W Direction	-	E-W Direction	7.27

Table 4.3 Frequencies obtained by recorded data and model

Mode 1 from the model was identified as 1st Torsion. Mode 2 as 1st N-S direction and Mode 3 was identified as 1st E-W direction. Mode 4 was identified as 2nd torsion, Mode 5 as 2nd N-S direction, and Mode 6 as 2nd E-W direction. Mode 7 was identified as 3rd Torsion, Mode 8 as 3rd N-S direction and Mode 9 as 3rd E-W direction.

By looking at the frequencies on Table 4.3 the following conclusions can be obtained:

For the 1st mode, the smallest frequency obtained from both the recorded data and from the model belongs to torsion. From the recorded data the value obtained for the 1st mode was 1.025 Hz and from the model was 0.9 Hz. For the 2nd mode, the value obtained from the recorded data was 3.06 Hz and from the model was 2.85 Hz.

Both frequencies obtained from the data for the E-W and N-S direction are smaller than the ones obtained from the model. Values for N-S and E-W direction from the recorded data are 1.123 Hz and 1.135-1.147 Hz, and from the model the frequencies obtained are 1.25 Hz and 1.27 Hz respectively.

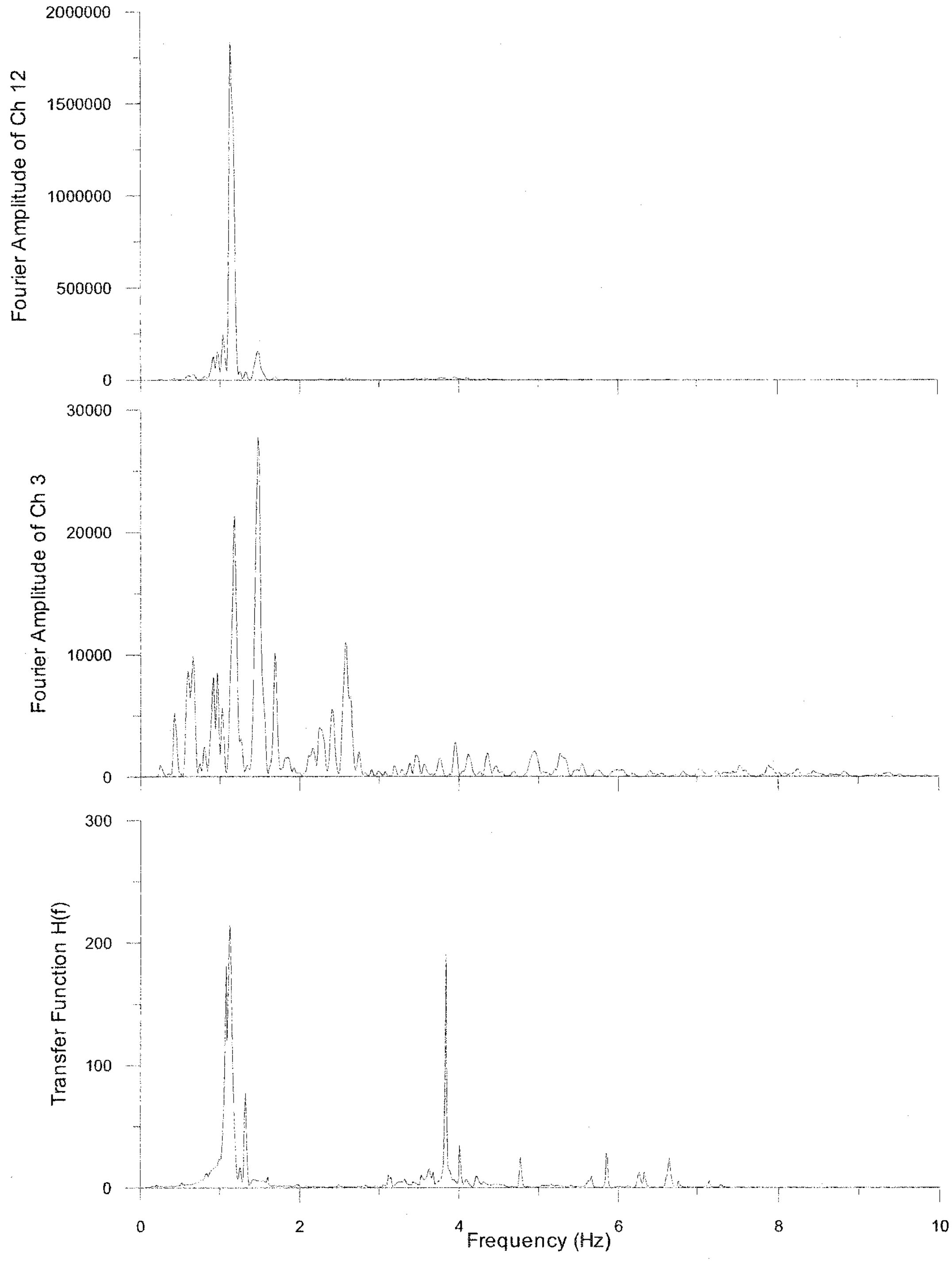

Fig. 4.3 HNB - Fourier Ampitudes of Ch 3 (Bottom Level) & Ch 12 (Top Level) accelerations, and the corresponding transfer function of the soil-structure system during the 1994 Northridge Earthquake

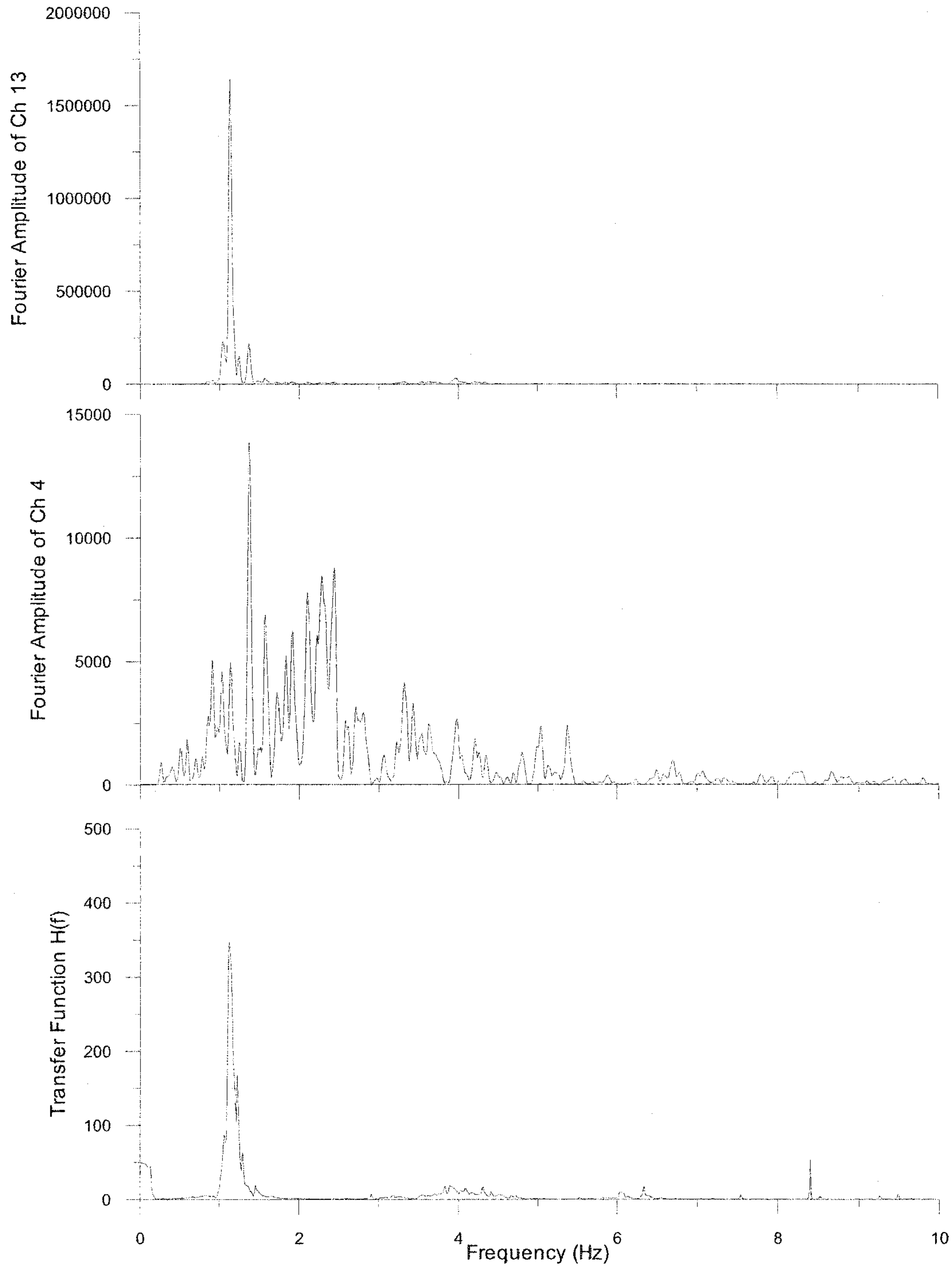

Fig. 4.4 HNB - Fourier Ampitudes of Ch 4 (Bottom Level) & Ch 13 (Top Level) from accelerations, and their corresponding transfer function of the soil-structure system during the 1994 Northridge Earthquake

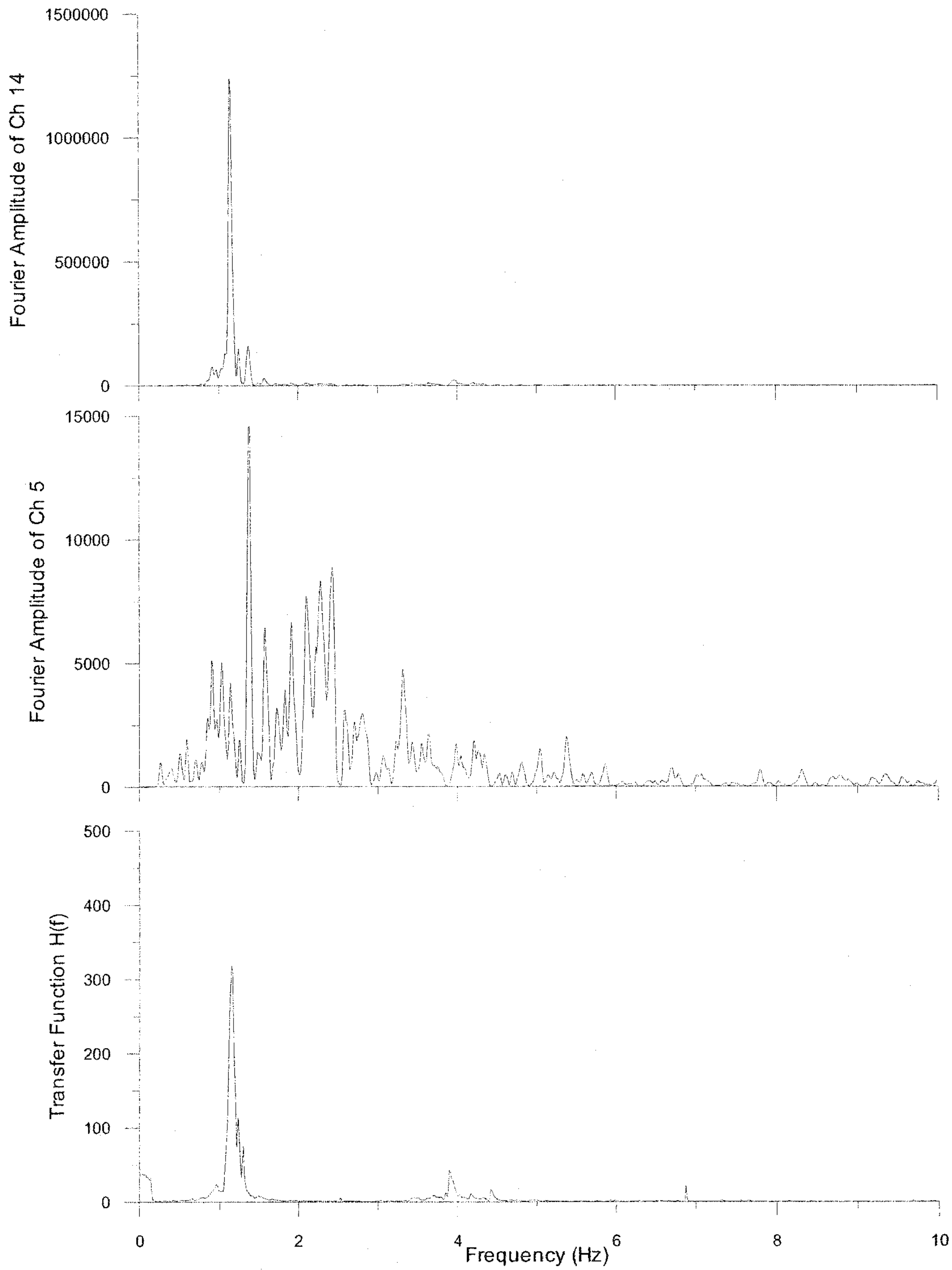

Fig. 4.5 HNB - Fourier Ampitudes of Ch 5 (Bottom Level) & Ch 14 (Top Level) accelerations, and the corresponding transfer function of the soil-structure system during the 1994 Northridge Earthquake

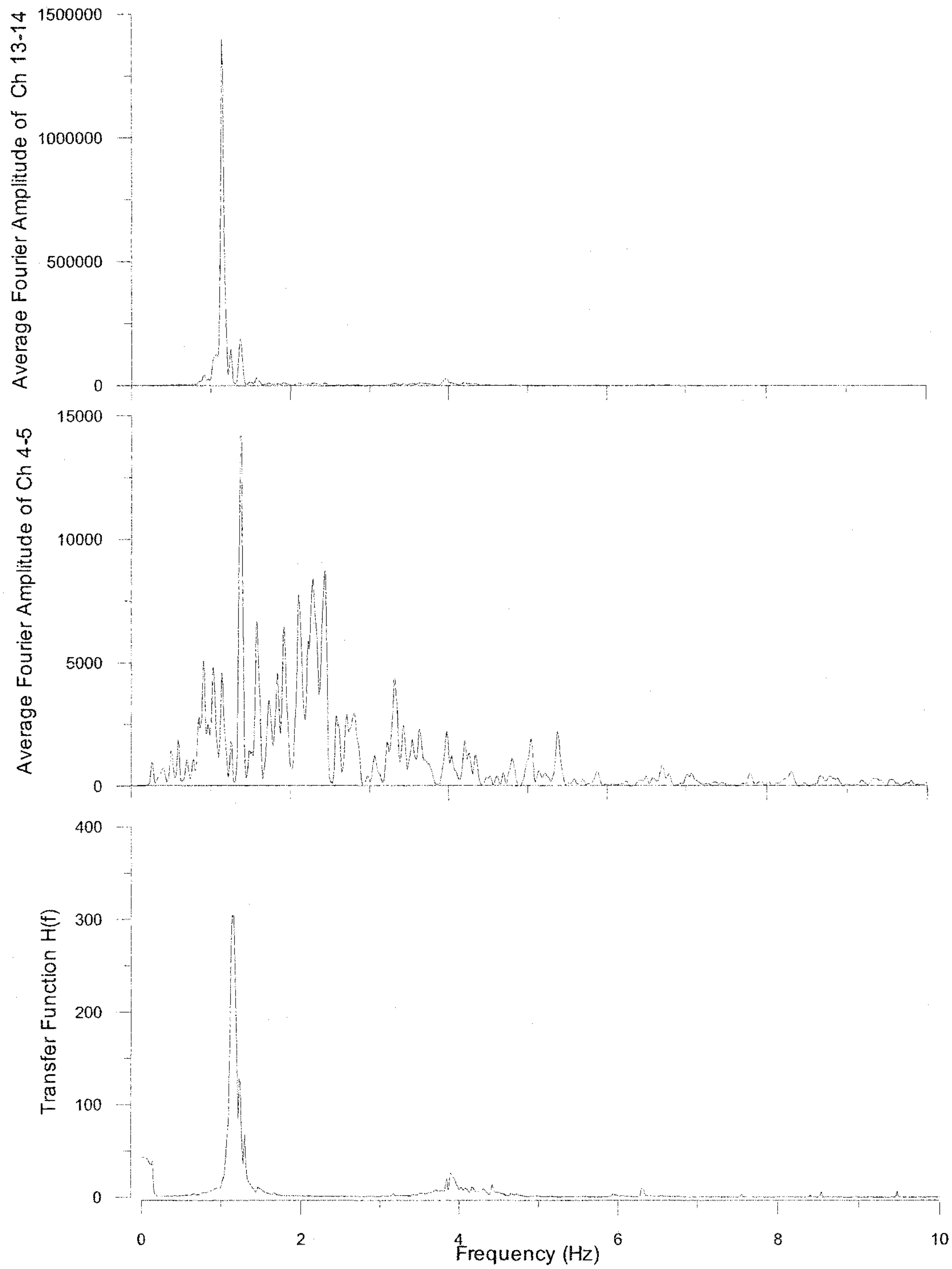

Fig. 4.6 HNB - Average Fourier Ampitudes of Ch 4-5 (Bottom Level) & Ch 13-14 (Top Level) accelerations, and the corresponding transfer function of the soil-structure system during the 1994 Northridge Earthquake

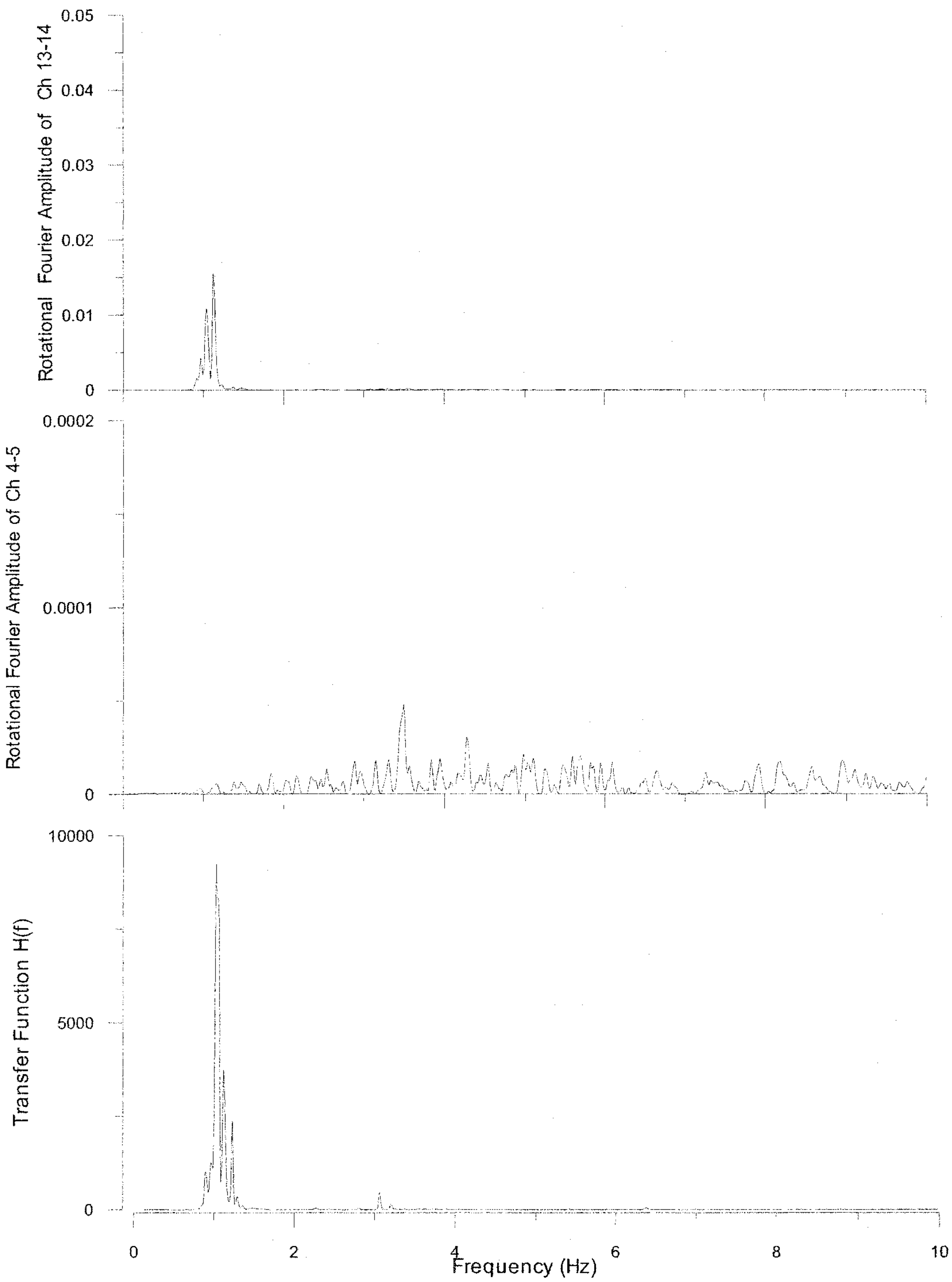

Fig. 4.7 HNB - Rotational Fourier Ampitudes of Ch 4-5 (Bottom Level) & Ch 13-14 (Top Level) accelerations, and the corresponding transfer function of the soil-structure system during the 1994 Northridge Earthquake

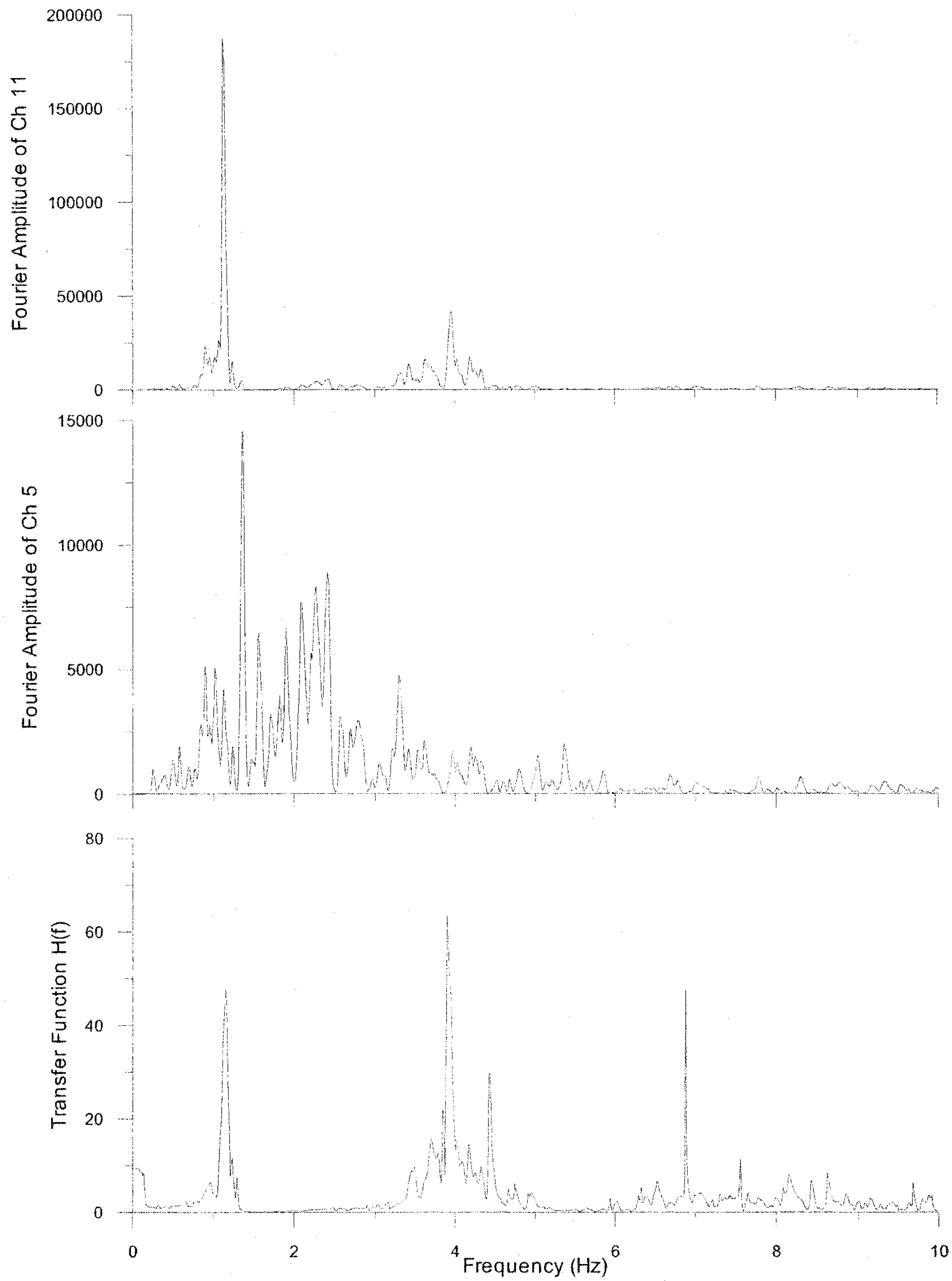

Fig. 4.8 HNB - Fourier Ampitudes of Ch 5 (Bottom Level) & Ch 11 (3rd floor) accelerations, and the corresponding transfer function of the soil-structure system during the 1994 Northridge Earthquake

CHAPTER 5

DYNAMIC ANALYSIS OF HEDCO NEUROSCIENCES BUILDING

5.1 General

This chapter describes the way the model of the building was created. Furthermore a comparative analysis of the acceleration and displacement data obtained by the 1994 Northridge Earthquake and the model is given. Base Shear calculations are made in order to verify current design procedures and analytical techniques, and understand the behavior of the building.

5.2 HEDCO Neurosciences Building Analytic Model Development

The first thing, and most difficult, that was done in ETABS, was the creation of the two grids; a global grid and an inverted one by 45 degrees, from the structural drawings. The grids helped significantly in the identification of the points were the columns had to be placed. After that the story data were defined by assigning heights, elevation and labels. Then the assigning of columns took place, following by the assigning of beams and girders in each floor. Lastly all the connections were checked, making changes were it was indicated by the drawings.

In the ETABS program there is the option of considering the floor diaphragm as rigid in its own plane. That was the way the perimeter columns and the core was chosen to be connected by the floor diaphragm.

Load Assigning was performed next. For the mass of the building the following loads were used:

Perimeter Wall	
Glass:	10 lb/ft^2 of wall
Red Brick Veneer :	40 lb/ft^2 of wall
Floor	
Floor Deck	
Metal Deck:	2.5 lb/ft^2
Lightweight Concrete Fill:	120 pcf
Equipment:	5 lb/ft^2
Partition:	20 lb/ft^2
Hung Ceiling:	8 lb/ft^2
Floor Finish:	1 lb/ft^2
Roof	
Hung Ceiling:	8 lb/ft^2
Roofing:	6 lb/ft^2
Mech Equip/Penthouse	46 lb/ft^2

In order to convert from ft^2 of wall are to ft^2 of floor area the following equation was used:

$$\frac{\text{Perimeter(ft)xHeight(ft)xLoading}(lb / ft^2)}{\text{FloorArea}}$$

The calculations were done in the following way:

The perimeter of the building was divided in two sections, the perimeter from the four towers and the main core. That was because the towers don't have windows and the hall height of the floor had to be considered as weight in the conversion of the skin, from area of wall to area of floor. For the core of the building half of the height of each floor was considered as glass, and half was considered as red brick veneer. The dead load of the brick veneer was taken 40 lb/ft^2 of wall, glass was taken as 10 lb/ft^2. The perimeter of the towers was 219.04 ft and that of the main core was 260.92 ft. The area of each floor was calculated from ETABS to be 9735 ft^2.

Calculation of the skin for a 14 ft height floor:

Towers: $$\frac{219.04x14x40}{9735} = 12.6lb/ft^2$$

Main Building:

Brick Veneer: $$\frac{260.92x7x40}{9735} = 7.5lb/ft^2$$

Glass: $$\frac{260.92x7x10}{9735} = 1.876lb/ft^2$$

Adding all these together the skin in ft^2 of floor area for a 14 ft story is 21.976lb/ft^2.

Calculation of the skin for a 15.5 ft height floor:

Towers: $$\frac{219.04x15.5x40}{9735} = 13.95lb / ft^2$$

Main Building:

Brick Veneer: $$\frac{260.92x7.75x40}{9735} = 8.3lb / ft^2$$

Glass: $$\frac{260.92x7.75x10}{9735} = 2.07lb / ft^2$$

Adding all these together resulted that the skin in ft^2 of floor area for a 15.5 ft story is 24.32lb/ ft^2.

During the creation of the model more grids were defined that helped in the identification of sections that were not on in any of the grids defined by the structural drawings.

The dynamic analysis that was done was a full 3-D Dynamic Eigenvector analysis with 30 modes. The eigenvectors parameters were zero frequency shift, cutoff frequency and relative tolerance.

The time history analysis was made with the ground motion data obtained by SMIP from channels 3,4 and 5 located in the basement. Acceleration in the E-W direction was obtained from channel 3 and acceleration for N-S direction was obtained by averaging the acceleration data of Channel 4 and 5. Acceleration data for both the E-W and N-S direction were entered at the same time. Comparative analysis of the channel points located in the roof with the equivalent joints of the model located in the same place is made moreover to this chapter.

The output file of the program is presented in Appendix II. The first nine modes of the building obtained from the ETABS model are displayed in Appendix III.

5.3 Base Shear Calculations

According to Uniform Building Code 97 (UBC 97) the Base Shear V_s is:

$$V_{base} \text{ is } \begin{bmatrix} = \left(\dfrac{C_v I}{RT}\right) W \\ \le \left(\dfrac{2.5 C_a I}{R}\right) W \\ \ge \left(0.11 C_a I\right) W \end{bmatrix} \text{ where:}$$

C_a = Seismic Coefficient (acceleration)

C_v = Seismic Coefficient (velocity)

T = Period

W = Building Seismic Dead Load

I = Seismic Importance Factor (1.0 to 1.25)

R = Force Reduction Coefficient

N_a = Near Source Factor (acceleration)

N_v = Near Source Factor (velocity)

Z = Seismic Zone Factor (0.075 – 0.4)

S = Soil Profile Type

In order to identify the soil profile type from Table 16-J of UBC 97, the shear wave velocity had to be identified first by Figure 2.16-Generalised Soil Conditions, indicating a value of 500 ft/sec. The value was less than 600 ft/sec so the soil profile type was characterized as type S_E. From Figure 16-2 of UBC 97-Seismic Zone Map, Los Angeles area was determined as zone 4 with Z=0.4. The Seismic Importance Factor was identified as 1, determined from Table 16-K of the UBC 97 under Occupancy Category 3 – Special Occupancy Structures. The Force Reduction Coefficient was calculated from Table 16-N of the UBC 97 as R=4.2, under the Dual Systems category - Ordinary braces with Ordinary Moment Resisting Frames. Seismic Coefficient C_a was calculated as $0.36N_a$ from Table 16-Q of the UBC 97 and Near Source Coefficient N_a was calculated as 1 from Table 16-S of the UBC 97.

Calculations for the E-W direction with Period T = 0.796 resulted at:

$$V_b = \left(\frac{C_v I}{RT}\right) w = \left(\frac{0.96x1}{4.2x0.796}\right) x6487.680 = 1862.937$$
$$V_b \le \left(\frac{2.5 C_a I}{R}\right) w = \left(\frac{2.5x0.36x1}{4.2}\right) x6487.680 = 1390.217$$
$$V_b \ge (0.11 C_a I) w (0.11x0.36x1) x6487.680 = 256.912$$

So the Shear Base in E-W direction was taken as V_b=1390.217

Calculations for the N-S direction with Period T = 0.786 resulted:

$$V_b = \left(\frac{C_v I}{RT}\right) w = \left(\frac{0.96x1}{4.2x0.786}\right) x6487.680 = 1886.639$$
$$V_b \le \left(\frac{2.5 C_a I}{R}\right) w = \left(\frac{2.5x0.36x1}{4.2}\right) x6487.680 = 1390.217$$
$$V_b \ge (0.11 C_a I) w (0.11x0.36x1) x6487.680 = 256.912$$

So the Shear Base in N-S direction was also taken as V_b=1390.217.

The Base Shear Accelerations from the recorded data were obtained by ETABS V7.12 software are displayed in the following figures, in order to identify whether there were any points that exceeded the above values. This would verify if any significant damage to the building could have happened.

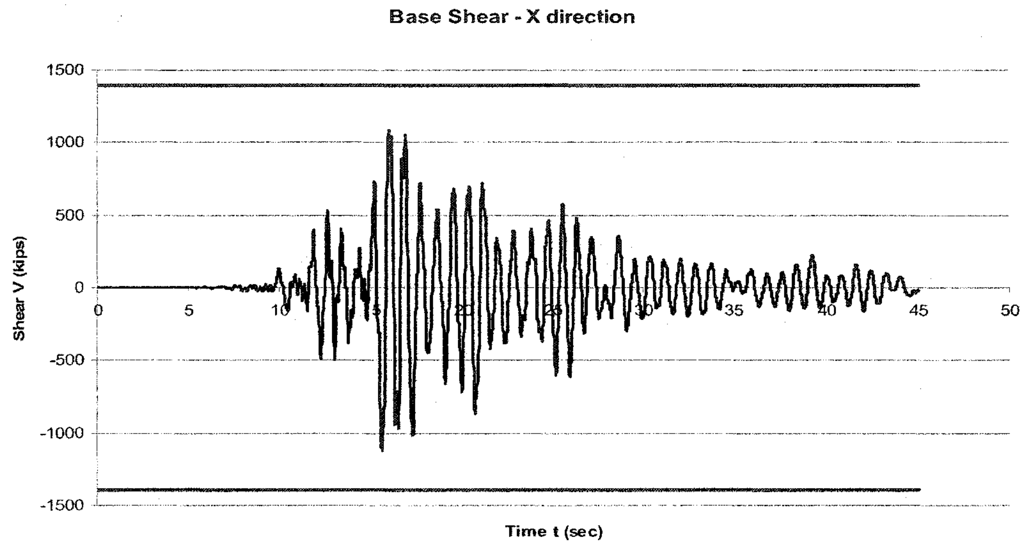

Figure 5.1 Base Shear Acceleration in E-W direction with UBC 97 Maximum Allowable Shear Value

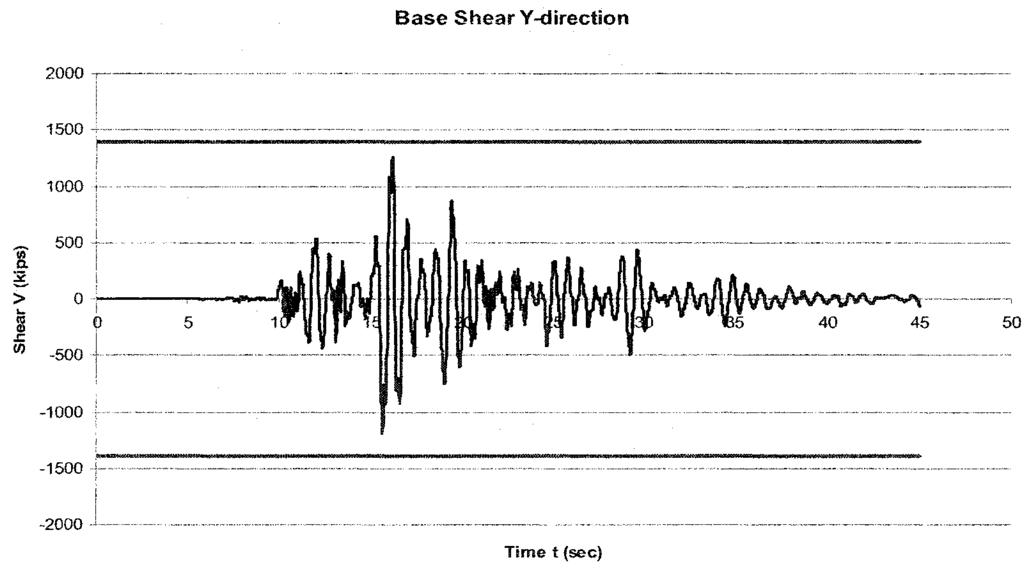

Figure 5.2 Base Shear Acceleration in N-S direction with UBC 97 Maximum Allowable Shear Value

Figures 5.1 and 5.2 designate that the building responded in a linear elastic manner to the earthquake's recorded data, at no point it exceeded the ultimate calculated Base Shear Value of UBC 97, even though UBC 97 regulations are stricter than the ones it was designed with, UBC 88. This was expected because the epicenter of the earthquake was quite far from the building, approximately 31.33 km.

5.4 Comparative Analysis of the Acceleration and Displacement Data Obtained by the 1994 Northridge Earthquake and the Model Created in ETABS V7.10

The locations of the sensors are shown previously in Chapter 3, on Figures 3.1 to 3.4. Since data were available only for points located in the basement and the roof, calculations were made only for the three sensors in the roof. Channels 12 and 13 are located in the same place in the roof, on the east tower, facing E-W and N-S direction respectively. These two channels are identified at the model as point C7 located at the roof. Channel 14 is located at the roof as well, on west tower, and is identified at the model as point C34.

The data obtained from the model were compared with the recorded data. The comparison was done both for the acceleration and displacement data.

The graphs for the acceleration and displacement comparisons of the recorded and model data are displayed in Figures 5.3 to 5.8. In the figures, the black color represents the data obtained from the ground motion and the grey color represents the data obtained from the model.

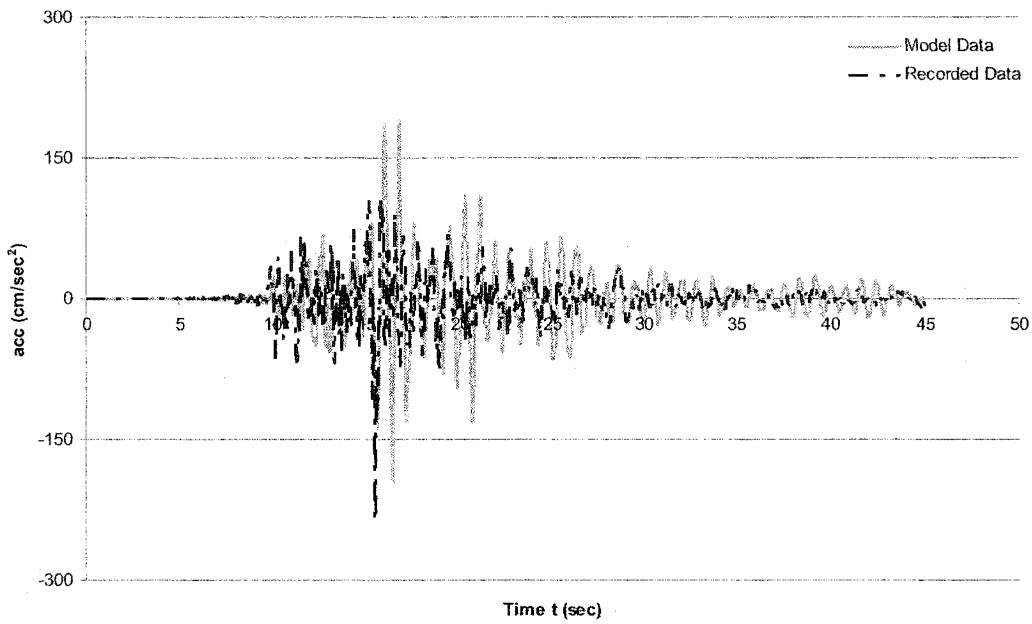

Figure 5.3 Acceleration Comparison in E-W Direction at Point C7

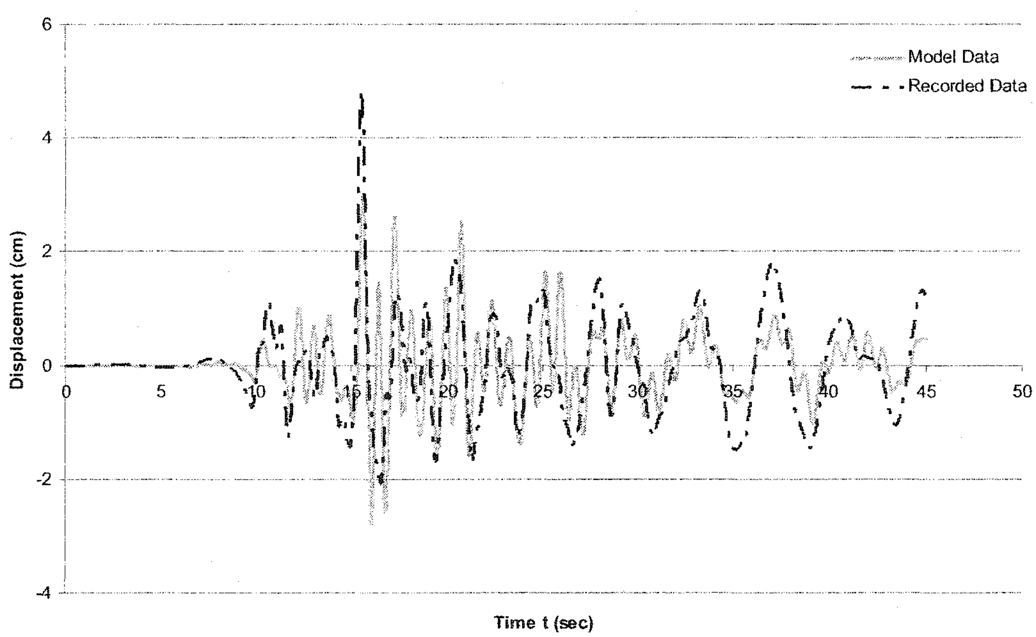

Figure 5.4 Displacement Comparison in E-W Direction at Point C7

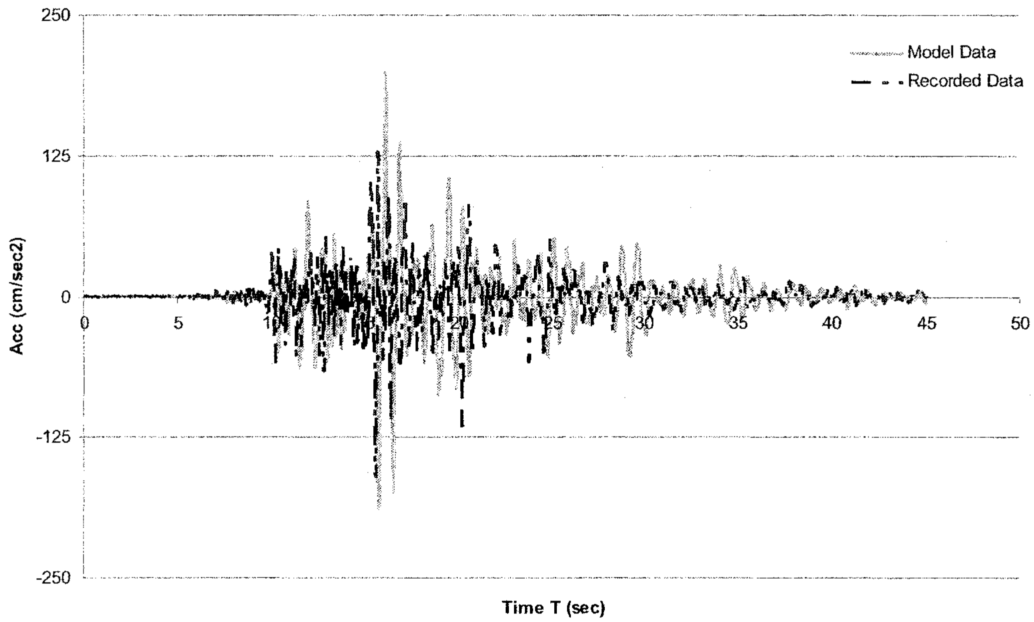

Figure 5.5 Acceleration Comparison in N-S Direction at Point C7

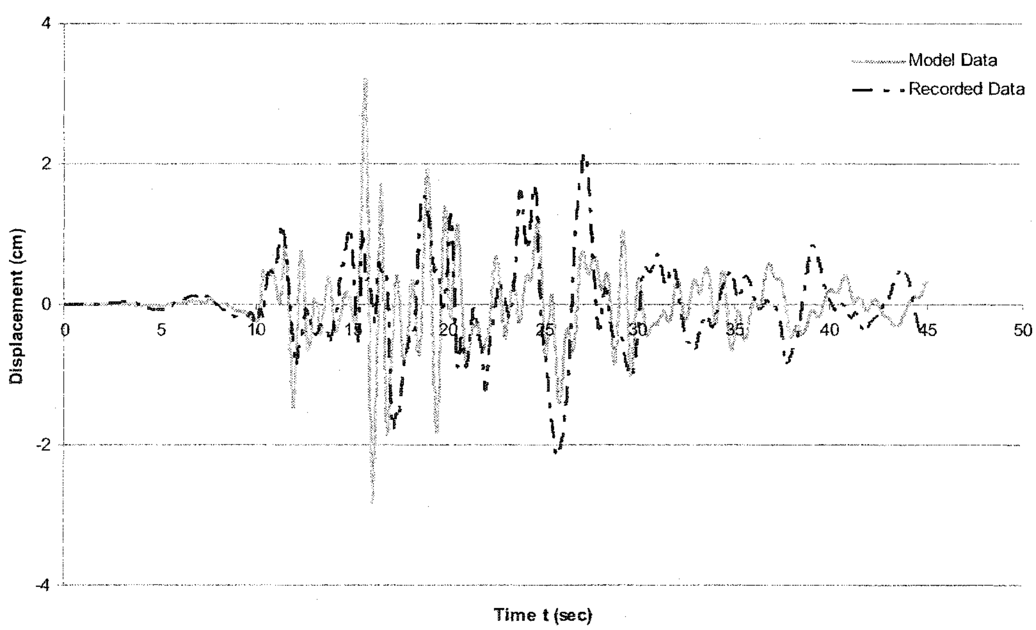

Figure 5.6 Displacement Comparison in N-S Direction at Point C7

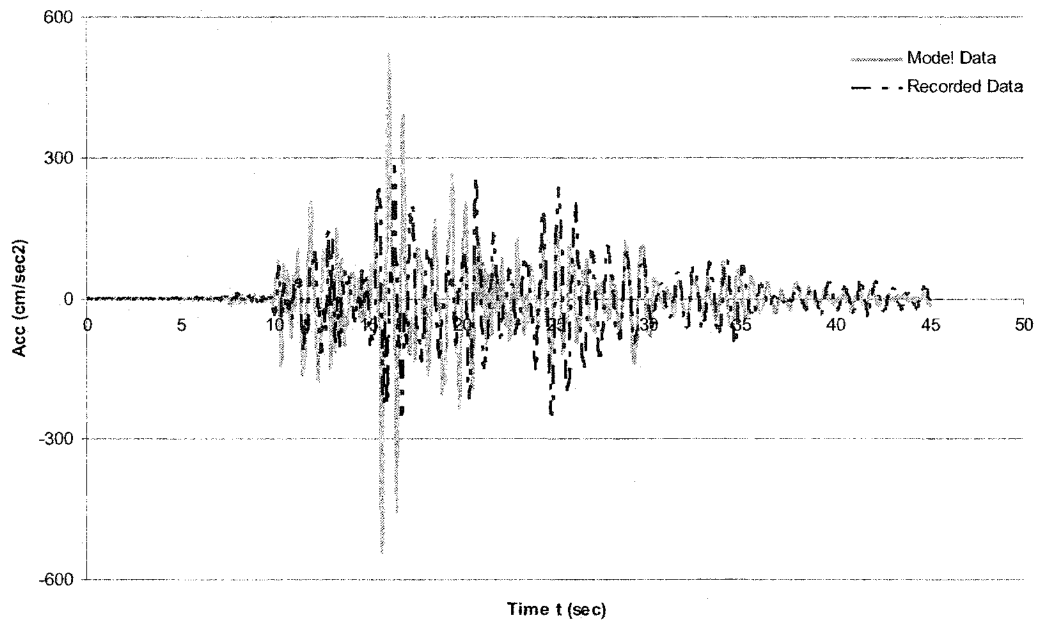

Figure 5.7 Acceleration Comparison in N-S Direction at Point C34

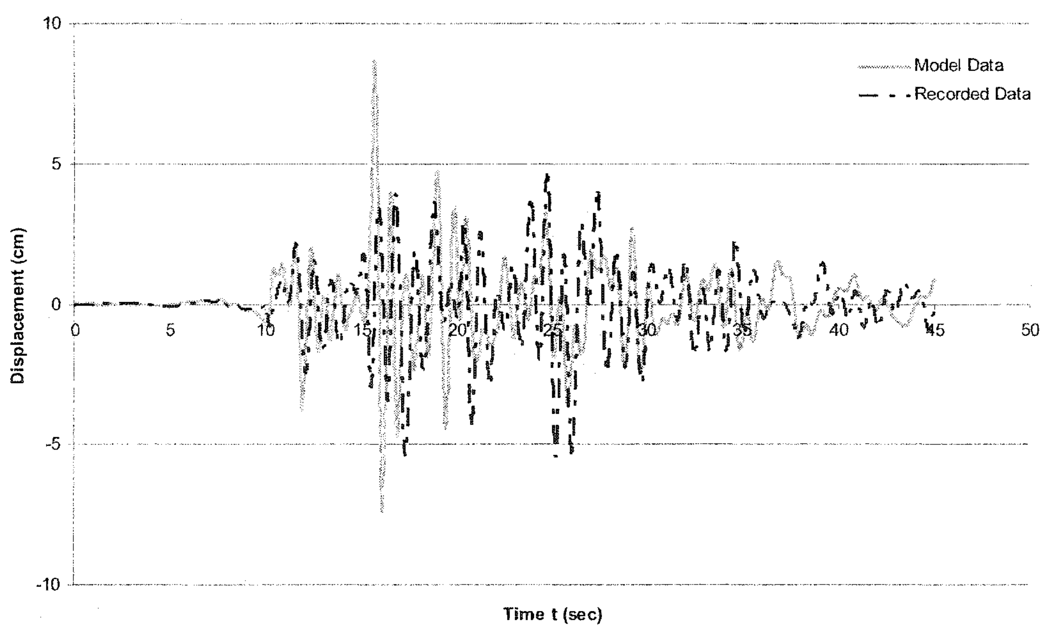

Figure 5.8 Displacement Comparison in N-S Direction at Point C34

At Point C7, in the E-W Direction, the maximum acceleration obtained from the recorded data was 237.587 cm/sec^2 and the one obtained from the model was 194.795 cm/sec^2. In the N-S Direction the maximum value from the recorded data was 161.568 cm/sec^2 while the one recorded from the model data was 199.451 cm/sec^2.

The maximum displacement obtained from the model in the E-W Direction was 2.952 cm, while the maximum recorded displacement was 4.832 cm. In the N-S Direction the maximum displacement obtained from the model was 3.22 cm while the one obtained from the recorded data was 2.157 cm.

At point C34, only data for the N-S Direction were available. The maximum acceleration obtained from the model was 541.5677 cm/sec^2, and acceleration obtained from the recorded data was 283.854 cm/sec^2. The displacement obtained from the model was 8.699 cm, while the displacement obtained from the recorded data was 5.477 cm.

From the above results it can be observed that the values obtained in the N-S Direction for acceleration and displacement from the model where bigger than the recorded data. From the other hand, in the E-W Direction, the accelerations and displacements obtained by the recorded data where bigger than the one predicted by the model. It would be expected that the values obtained from the model be more conservative than the ones actually recorded, but this is not the case in E-W Direction.

CHAPTER 6

CONCLUSIONS

In the following paragraphs the conclusions take place from the thorough interpretation of data and results obtained in the previous chapters.

The ground motion excitation produced displacements of about 11 cm. The frequencies and the first two mode shapes of the building in each direction were clearly identified in the Fourier Spectra as shown in Table 4.3. The frequency ratios were consistent with the building's configuration. Therefore, it seems the estimates of frequency and mode shapes are realistic.

Realistic periods and dynamic response were obtained by the Model. Some difference was observed for the data in the E-W direction where the values of the recorded data were bigger than the ones obtained from the model.

Base Shear calculations indicated that the building responded primarily linear elastic to the earthquake recorded data, at no point it exceeded the ultimate calculated Base Shear Value of UBC 97, even though UBC 97 regulations are stricter than the ones it was designed with, UBC 88. This was expected because the epicenter of the earthquake was quite far from the building, approximately 31.33 km.

The instrumentation of the building was placed and performed satisfactorily. If the data from the intermediate floors were available, it could be possible to identify the third mode as well. Furthermore if more sensors were placed in the building, recording data in the N-S direction, then it would be possible to verify the existing results and check if any inconsistencies exist comparing with the existing data in that direction; that way more accurate conclusions could be obtained.

All engineering publications that analyzed buildings damaged by the 1994 Northridge Earthquake concluded that the most important lesson learned was the seismic vulnerability of modern steel buildings (Bertero, 1994).[6] Damages were caused because of column base plate failure, welded connection failure, or because of

[6] 1. Bertero, V.V., Anderson, J.C. and Krawinker, H. (August 1994), "Performance of Steel Building Structures During the Northridge Earthquake", Report No. UCB/EERC-94/09, EERC, University of California, Berkeley

buckling of main members (Bertero, 1994). The HEDCO Neurosciences Building behaved satisfactorily during the 1994 Northridge Earthquake without undergoing any permanent deformation. This can be concluded by the present condition of the building and verified by the results of the model when subjected to the recorded data.

REFERENCES - BIBLIOGRAPHY

1. **Bertero, V.V.,** Anderson, J.C. and Krawinker, H. (August 1994), "Performance of Steel Building Structures During the Northridge Earthquake", Report No. UCB/EERC-94/09, EERC, University of California, Berkeley

2. **Goel, R.K.,** Chopra A.K., (December 1997), "Vibration Properties of Buildings Determined From Recorded Earthquakes Motions", Report No. UCB/EERC-97/14, EERC, University of California, Berkeley

3. **Hao, T-Y.,** Trifunac, M.D., Todorovska M.I. (April 1994), "Instrumented Buildings of University of Southern California-Strong Motion Data, Metadata and Soil-Structure System Frequencies, Report CE 04-01, University of Southern California, Los Angeles, California

4. **LeRoy Crandall Association**, LCA (1986), Report of Foundation Investigation, Proposed Hedco Neurosciences Building, Hoover Street and Downey Way (36th Place), Los Angeles, California, Job No. A-86258.

5. **Stewart, J.P.** and Stewart, A.F. (1997), "Analysis of Soil-Structure Interaction Effects on Building Response from Earthquake Strong Motion Recordings at 58 Sites, Report No. UCB/EERC-97/01, Earthquake Engineering Research Center, University of California, Berkeley, California.

6. **Strong Motion Instrumentation Program (SMIP),** <URL: http://www.consrv.ca.gov/CGS/smip/index.htm>, last edited on 30 March 2005.

7. **Trifunac M.D.,** Ivanovic S.S., Todorovska M.I. (May 2001), "Apparent Periods of a Building. I: Fourier Analysis", Journal of Structural Engineering, 127 (5), 517-526

8. **Trifunac M.D.,** Ivanovic S.S., Todorovska M.I. (May 2001), "Apparent Periods of a Building. II: Time-Frequency Analysis", Journal of Structural Engineering,127 (5), 527-537

9. **U.S. Geological Survey for the Federal Emergency Management Agency (FEMA)**, 'USGS Response to an Urban Earthquake: Northridge '94', Open-File Report 96-263, <URL:http://pubs.usgs.gov/of/1996/ofr-96-0263/>,(Last Modified: Fri Jun 15 13:57 EST 2001) (Accessed: 30 March 2005)

APPENDIX I

Matlab Program

```
File = ('acc.txt');
acc = fopen(File,'r');
S = fscanf(acc,'%g',inf);
FT_S = fft(S,8192);
Amp_FT_S = FT_S.*conj(FT_S)/8192;
File = ('Spectra-acc.txt');
Spectra_acc = fopen(File,'w');
fprintf(Spectra_acc,'%12.8f\n',Amp_FT_S);
fclose(acc);
fclose(Spectra_acc);

File = ('vel.txt');
vel = fopen(File,'r');
S = fscanf(vel,'%g',inf);
FT_S = fft(S,8192);
Amp_FT_S = FT_S.*conj(FT_S)/8192;

File = ('Spectra-vel.txt');
Spectra_vel = fopen(File,'w');
fprintf(Spectra_vel,'%12.8f\n',Amp_FT_S);
fclose(vel);
fclose(Spectra_vel);

File = ('disp.txt');
disp = fopen(File,'r');
S = fscanf(disp,'%g',inf);
FT_S = fft(S,8192);
Amp_FT_S = FT_S.*conj(FT_S)/8192;
File = ('Spectra-disp.txt');
Spectra_disp = fopen(File,'w');
fprintf(Spectra_disp,'%12.8f\n',Amp_FT_S);
fclose(disp);
fclose(Spectra_disp);
```

APPENDIX II

E T A B S (R)

Nonlinear Version 7.10

This copy of ETABS is for the exclusive use of

THE LICENSEE

Unauthorized use is in violation of Federal copyright laws

It is the responsibility of the user to verify all
results produced by this program

10 Apr 2005 22:47:45

Program ETABS Nonlinear Version 7.10 File:projectwall.OUT
Page
1

C O N S T R A I N T   C O O R D I N A T E S   A N D   M A S S E S

CONS 1 ================= TYPE = DIAPH, NORMAL DIRECTION = U3

LOCAL COORDINATE SYSTEM FOR CONSTRAINT MASTER

GLOBAL	U1	U2	U3	R1	R2	R3
X	1.000000	.000000	.000000	1.000000	.000000	.000000
Y	.000000	1.000000	.000000	.000000	1.000000	.000000
Z	.000000	.000000	1.000000	.000000	.000000	1.000000

TRANSLATIONAL MASS AND MASS MOMENTS OF INERTIA

U1	U2	U3	R1	R2	R3
2.817558	2.817558	.000000	.000000	.000000	600937.697

CENTER OF MASS

GLOBAL	U1	U2	U3
X	398.095037	398.095037	376.243082
Y	549.174310	549.174310	493.027980
Z	858.000000	858.000000	858.000000

CONS 2 ================= TYPE = DIAPH, NORMAL DIRECTION = U3

LOCAL COORDINATE SYSTEM FOR CONSTRAINT MASTER

GLOBAL	U1	U2	U3	R1	R2	R3
X	1.000000	.000000	.000000	1.000000	.000000	.000000
Y	.000000	1.000000	.000000	.000000	1.000000	.000000
Z	.000000	.000000	1.000000	.000000	.000000	1.000000

TRANSLATIONAL MASS AND MASS MOMENTS OF INERTIA

U1	U2	U3	R1	R2	R3
2.626310	2.626310	.000000	.000000	.000000	599537.233

CENTER OF MASS

GLOBAL	U1	U2	U3
X	393.043621	393.043621	385.267940
Y	559.885205	559.885205	596.577982
Z	690.000000	690.000000	690.000000

CONS 3 ================= TYPE = DIAPH, NORMAL DIRECTION = U3

LOCAL COORDINATE SYSTEM FOR CONSTRAINT MASTER

GLOBAL	U1	U2	U3	R1	R2	R3
X	1.000000	.000000	.000000	1.000000	.000000	.000000
Y	.000000	1.000000	.000000	.000000	1.000000	.000000
Z	.000000	.000000	1.000000	.000000	.000000	1.000000

TRANSLATIONAL MASS AND MASS MOMENTS OF INERTIA

U1	U2	U3	R1	R2	R3
2.667838	2.667838	.000000	.000000	.000000	614739.544

C O N S T R A I N T   C O O R D I N A T E S   A N D   M A S S E S

CENTER OF MASS

GLOBAL	U1	U2	U3
X	391.767633	391.767633	409.835142
Y	561.148966	561.148966	571.874545
Z	522.000000	522.000000	522.000000

CONS 4 ================= TYPE = DIAPH, NORMAL DIRECTION = U3

LOCAL COORDINATE SYSTEM FOR CONSTRAINT MASTER

GLOBAL	U1	U2	U3	R1	R2	R3
X	1.000000	.000000	.000000	1.000000	.000000	.000000
Y	.000000	1.000000	.000000	.000000	1.000000	.000000
Z	.000000	.000000	1.000000	.000000	.000000	1.000000

TRANSLATIONAL MASS AND MASS MOMENTS OF INERTIA

U1	U2	U3	R1	R2	R3
2.689702	2.689702	.000000	.000000	.000000	625237.744

CENTER OF MASS

GLOBAL	U1	U2	U3
X	392.238871	392.238871	424.054436
Y	562.031640	562.031640	589.295389
Z	354.000000	354.000000	354.000000

CONS 5 ================= TYPE = DIAPH, NORMAL DIRECTION = U3

LOCAL COORDINATE SYSTEM FOR CONSTRAINT MASTER

GLOBAL	U1	U2	U3	R1	R2	R3
X	1.000000	.000000	.000000	1.000000	.000000	.000000
Y	.000000	1.000000	.000000	.000000	1.000000	.000000
Z	.000000	.000000	1.000000	.000000	.000000	1.000000

TRANSLATIONAL MASS AND MASS MOMENTS OF INERTIA

U1	U2	U3	R1	R2	R3
2.718726	2.718726	.000000	.000000	.000000	652352.891

CENTER OF MASS

GLOBAL	U1	U2	U3
X	392.325297	392.325297	417.363099
Y	561.959125	561.959125	584.017581
Z	186.000000	186.000000	186.000000

CONS 6 ================= TYPE = DIAPH, NORMAL DIRECTION = U3

LOCAL COORDINATE SYSTEM FOR CONSTRAINT MASTER

GLOBAL	U1	U2	U3	R1	R2	R3
X	1.000000	.000000	.000000	1.000000	.000000	.000000
Y	.000000	1.000000	.000000	.000000	1.000000	.000000
Z	.000000	.000000	1.000000	.000000	.000000	1.000000

```
C O N S T R A I N T   C O O R D I N A T E S   A N D   M A S S E S

                          TRANSLATIONAL MASS AND MASS MOMENTS OF INERTIA
                      U1          U2          U3          R1          R2          R3
                2.533514    2.533514     .000000     .000000     .000000  667730.787

                          CENTER OF MASS
 GLOBAL               U1          U2          U3
    X         322.962335  322.962335  262.534586
    Y         560.059330  560.059330  555.870670
    Z            .000000     .000000     .000000

CONS          7 ================= TYPE = DIAPH, NORMAL DIRECTION = U3

                          LOCAL COORDINATE SYSTEM FOR CONSTRAINT MASTER
 GLOBAL               U1          U2          U3          R1          R2          R3
    X           1.000000     .000000     .000000    1.000000     .000000     .000000
    Y            .000000    1.000000     .000000     .000000    1.000000     .000000
    Z            .000000     .000000    1.000000     .000000     .000000    1.000000

                          TRANSLATIONAL MASS AND MASS MOMENTS OF INERTIA
                      U1          U2          U3          R1          R2          R3
                 .000000     .000000     .000000     .000000     .000000     .000000

                          CENTER OF MASS
 GLOBAL               U1          U2          U3
    X            .000000     .000000     .000000
    Y            .000000     .000000     .000000
    Z            .000000     .000000     .000000

CONS          8 ================= TYPE = DIAPH, NORMAL DIRECTION = U3

                          LOCAL COORDINATE SYSTEM FOR CONSTRAINT MASTER
 GLOBAL               U1          U2          U3          R1          R2          R3
    X           1.000000     .000000     .000000    1.000000     .000000     .000000
    Y            .000000    1.000000     .000000     .000000    1.000000     .000000
    Z            .000000     .000000    1.000000     .000000     .000000    1.000000

                          TRANSLATIONAL MASS AND MASS MOMENTS OF INERTIA
                      U1          U2          U3          R1          R2          R3
                 .000000     .000000     .000000     .000000     .000000     .000000

                          CENTER OF MASS
 GLOBAL               U1          U2          U3
    X            .000000     .000000     .000000
    Y            .000000     .000000     .000000
    Z            .000000     .000000     .000000
```

C O N S T R A I N T   C O O R D I N A T E S   A N D   M A S S E S

CONS 9 ================= TYPE = DIAPH, NORMAL DIRECTION = U3

LOCAL COORDINATE SYSTEM FOR CONSTRAINT MASTER

GLOBAL	U1	U2	U3	R1	R2	R3
X	1.000000	.000000	.000000	1.000000	.000000	.000000
Y	.000000	1.000000	.000000	.000000	1.000000	.000000
Z	.000000	.000000	1.000000	.000000	.000000	1.000000

TRANSLATIONAL MASS AND MASS MOMENTS OF INERTIA

U1	U2	U3	R1	R2	R3
.000000	.000000	.000000	.000000	.000000	.000000

CENTER OF MASS

GLOBAL	U1	U2	U3
X	.000000	.000000	.000000
Y	.000000	.000000	.000000
Z	.000000	.000000	.000000

CONS 10 ================= TYPE = DIAPH, NORMAL DIRECTION = U3

LOCAL COORDINATE SYSTEM FOR CONSTRAINT MASTER

GLOBAL	U1	U2	U3	R1	R2	R3
X	1.000000	.000000	.000000	1.000000	.000000	.000000
Y	.000000	1.000000	.000000	.000000	1.000000	.000000
Z	.000000	.000000	1.000000	.000000	.000000	1.000000

TRANSLATIONAL MASS AND MASS MOMENTS OF INERTIA

U1	U2	U3	R1	R2	R3
.000000	.000000	.000000	.000000	.000000	.000000

CENTER OF MASS

GLOBAL	U1	U2	U3
X	.000000	.000000	.000000
Y	.000000	.000000	.000000
Z	.000000	.000000	.000000

CONS 11 ================= TYPE = DIAPH, NORMAL DIRECTION = U3

LOCAL COORDINATE SYSTEM FOR CONSTRAINT MASTER

GLOBAL	U1	U2	U3	R1	R2	R3
X	1.000000	.000000	.000000	1.000000	.000000	.000000
Y	.000000	1.000000	.000000	.000000	1.000000	.000000
Z	.000000	.000000	1.000000	.000000	.000000	1.000000

TRANSLATIONAL MASS AND MASS MOMENTS OF INERTIA

U1	U2	U3	R1	R2	R3
.000000	.000000	.000000	.000000	.000000	.000000

C O N S T R A I N T   C O O R D I N A T E S   A N D   M A S S E S

CENTER OF MASS

GLOBAL	U1	U2	U3
X	.000000	.000000	.000000
Y	.000000	.000000	.000000
Z	.000000	.000000	.000000

CONS 12 ================= TYPE = DIAPH, NORMAL DIRECTION = U3

LOCAL COORDINATE SYSTEM FOR CONSTRAINT MASTER

GLOBAL	U1	U2	U3	R1	R2	R3
X	1.000000	.000000	.000000	1.000000	.000000	.000000
Y	.000000	1.000000	.000000	.000000	1.000000	.000000
Z	.000000	.000000	1.000000	.000000	.000000	1.000000

TRANSLATIONAL MASS AND MASS MOMENTS OF INERTIA

U1	U2	U3	R1	R2	R3
.000000	.000000	.000000	.000000	.000000	.000000

CENTER OF MASS

GLOBAL	U1	U2	U3
X	.000000	.000000	.000000
Y	.000000	.000000	.000000
Z	.000000	.000000	.000000

CONS 13 ================= TYPE = DIAPH, NORMAL DIRECTION = U3

LOCAL COORDINATE SYSTEM FOR CONSTRAINT MASTER

GLOBAL	U1	U2	U3	R1	R2	R3
X	1.000000	.000000	.000000	1.000000	.000000	.000000
Y	.000000	1.000000	.000000	.000000	1.000000	.000000
Z	.000000	.000000	1.000000	.000000	.000000	1.000000

TRANSLATIONAL MASS AND MASS MOMENTS OF INERTIA

U1	U2	U3	R1	R2	R3
.000000	.000000	.000000	.000000	.000000	.000000

CENTER OF MASS

GLOBAL	U1	U2	U3
X	.000000	.000000	.000000
Y	.000000	.000000	.000000
Z	.000000	.000000	.000000

CONS 14 ================= TYPE = DIAPH, NORMAL DIRECTION = U3

LOCAL COORDINATE SYSTEM FOR CONSTRAINT MASTER

GLOBAL	U1	U2	U3	R1	R2	R3
X	1.000000	.000000	.000000	1.000000	.000000	.000000
Y	.000000	1.000000	.000000	.000000	1.000000	.000000
Z	.000000	.000000	1.000000	.000000	.000000	1.000000

C O N S T R A I N T   C O O R D I N A T E S   A N D   M A S S E S

TRANSLATIONAL MASS AND MASS MOMENTS OF INERTIA

U1	U2	U3	R1	R2	R3
.000000	.000000	.000000	.000000	.000000	.000000

CENTER OF MASS

GLOBAL	U1	U2	U3
X	.000000	.000000	.000000
Y	.000000	.000000	.000000
Z	.000000	.000000	.000000

CONS 15 ================= TYPE = DIAPH, NORMAL DIRECTION = U3

LOCAL COORDINATE SYSTEM FOR CONSTRAINT MASTER

GLOBAL	U1	U2	U3	R1	R2	R3
X	1.000000	.000000	.000000	1.000000	.000000	.000000
Y	.000000	1.000000	.000000	.000000	1.000000	.000000
Z	.000000	.000000	1.000000	.000000	.000000	1.000000

TRANSLATIONAL MASS AND MASS MOMENTS OF INERTIA

U1	U2	U3	R1	R2	R3
.000000	.000000	.000000	.000000	.000000	.000000

CENTER OF MASS

GLOBAL	U1	U2	U3
X	.000000	.000000	.000000
Y	.000000	.000000	.000000
Z	.000000	.000000	.000000

CONS 16 ================= TYPE = DIAPH, NORMAL DIRECTION = U3

LOCAL COORDINATE SYSTEM FOR CONSTRAINT MASTER

GLOBAL	U1	U2	U3	R1	R2	R3
X	1.000000	.000000	.000000	1.000000	.000000	.000000
Y	.000000	1.000000	.000000	.000000	1.000000	.000000
Z	.000000	.000000	1.000000	.000000	.000000	1.000000

TRANSLATIONAL MASS AND MASS MOMENTS OF INERTIA

U1	U2	U3	R1	R2	R3
.000000	.000000	.000000	.000000	.000000	.000000

CENTER OF MASS

GLOBAL	U1	U2	U3
X	.000000	.000000	.000000
Y	.000000	.000000	.000000
Z	.000000	.000000	.000000

C O N S T R A I N T   C O O R D I N A T E S   A N D   M A S S E S

CONS 17 ================= TYPE = DIAPH, NORMAL DIRECTION = U3

LOCAL COORDINATE SYSTEM FOR CONSTRAINT MASTER

GLOBAL	U1	U2	U3	R1	R2	R3
X	1.000000	.000000	.000000	1.000000	.000000	.000000
Y	.000000	1.000000	.000000	.000000	1.000000	.000000
Z	.000000	.000000	1.000000	.000000	.000000	1.000000

TRANSLATIONAL MASS AND MASS MOMENTS OF INERTIA

U1	U2	U3	R1	R2	R3
.000000	.000000	.000000	.000000	.000000	.000000

CENTER OF MASS

GLOBAL	U1	U2	U3
X	.000000	.000000	.000000
Y	.000000	.000000	.000000
Z	.000000	.000000	.000000

CONS 18 ================= TYPE = DIAPH, NORMAL DIRECTION = U3

LOCAL COORDINATE SYSTEM FOR CONSTRAINT MASTER

GLOBAL	U1	U2	U3	R1	R2	R3
X	1.000000	.000000	.000000	1.000000	.000000	.000000
Y	.000000	1.000000	.000000	.000000	1.000000	.000000
Z	.000000	.000000	1.000000	.000000	.000000	1.000000

TRANSLATIONAL MASS AND MASS MOMENTS OF INERTIA

U1	U2	U3	R1	R2	R3
.000000	.000000	.000000	.000000	.000000	.000000

CENTER OF MASS

GLOBAL	U1	U2	U3
X	.000000	.000000	.000000
Y	.000000	.000000	.000000
Z	.000000	.000000	.000000

CONS 19 ================= TYPE = DIAPH, NORMAL DIRECTION = U3

LOCAL COORDINATE SYSTEM FOR CONSTRAINT MASTER

GLOBAL	U1	U2	U3	R1	R2	R3
X	1.000000	.000000	.000000	1.000000	.000000	.000000
Y	.000000	1.000000	.000000	.000000	1.000000	.000000
Z	.000000	.000000	1.000000	.000000	.000000	1.000000

TRANSLATIONAL MASS AND MASS MOMENTS OF INERTIA

U1	U2	U3	R1	R2	R3
.000000	.000000	.000000	.000000	.000000	.000000

C O N S T R A I N T   C O O R D I N A T E S   A N D   M A S S E S

CENTER OF MASS

GLOBAL	U1	U2	U3
X	.000000	.000000	.000000
Y	.000000	.000000	.000000
Z	.000000	.000000	.000000

CONS 20 ================= TYPE = DIAPH, NORMAL DIRECTION = U3

LOCAL COORDINATE SYSTEM FOR CONSTRAINT MASTER

GLOBAL	U1	U2	U3	R1	R2	R3
X	1.000000	.000000	.000000	1.000000	.000000	.000000
Y	.000000	1.000000	.000000	.000000	1.000000	.000000
Z	.000000	.000000	1.000000	.000000	.000000	1.000000

TRANSLATIONAL MASS AND MASS MOMENTS OF INERTIA

U1	U2	U3	R1	R2	R3
.000000	.000000	.000000	.000000	.000000	.000000

CENTER OF MASS

GLOBAL	U1	U2	U3
X	.000000	.000000	.000000
Y	.000000	.000000	.000000
Z	.000000	.000000	.000000

CONS 21 ================= TYPE = DIAPH, NORMAL DIRECTION = U3

LOCAL COORDINATE SYSTEM FOR CONSTRAINT MASTER

GLOBAL	U1	U2	U3	R1	R2	R3
X	1.000000	.000000	.000000	1.000000	.000000	.000000
Y	.000000	1.000000	.000000	.000000	1.000000	.000000
Z	.000000	.000000	1.000000	.000000	.000000	1.000000

TRANSLATIONAL MASS AND MASS MOMENTS OF INERTIA

U1	U2	U3	R1	R2	R3
.000000	.000000	.000000	.000000	.000000	.000000

CENTER OF MASS

GLOBAL	U1	U2	U3
X	.000000	.000000	.000000
Y	.000000	.000000	.000000
Z	.000000	.000000	.000000

CONS 22 ================= TYPE = DIAPH, NORMAL DIRECTION = U3

LOCAL COORDINATE SYSTEM FOR CONSTRAINT MASTER

GLOBAL	U1	U2	U3	R1	R2	R3
X	1.000000	.000000	.000000	1.000000	.000000	.000000
Y	.000000	1.000000	.000000	.000000	1.000000	.000000
Z	.000000	.000000	1.000000	.000000	.000000	1.000000

C O N S T R A I N T   C O O R D I N A T E S   A N D   M A S S E S

TRANSLATIONAL MASS AND MASS MOMENTS OF INERTIA

U1	U2	U3	R1	R2	R3
.000000	.000000	.000000	.000000	.000000	.000000

CENTER OF MASS

GLOBAL	U1	U2	U3
X	.000000	.000000	.000000
Y	.000000	.000000	.000000
Z	.000000	.000000	.000000

CONS 23 ================== TYPE = DIAPH, NORMAL DIRECTION = U3

LOCAL COORDINATE SYSTEM FOR CONSTRAINT MASTER

GLOBAL	U1	U2	U3	R1	R2	R3
X	1.000000	.000000	.000000	1.000000	.000000	.000000
Y	.000000	1.000000	.000000	.000000	1.000000	.000000
Z	.000000	.000000	1.000000	.000000	.000000	1.000000

TRANSLATIONAL MASS AND MASS MOMENTS OF INERTIA

U1	U2	U3	R1	R2	R3
.000000	.000000	.000000	.000000	.000000	.000000

CENTER OF MASS

GLOBAL	U1	U2	U3
X	.000000	.000000	.000000
Y	.000000	.000000	.000000
Z	.000000	.000000	.000000

CONS 24 ================== TYPE = DIAPH, NORMAL DIRECTION = U3

LOCAL COORDINATE SYSTEM FOR CONSTRAINT MASTER

GLOBAL	U1	U2	U3	R1	R2	R3
X	1.000000	.000000	.000000	1.000000	.000000	.000000
Y	.000000	1.000000	.000000	.000000	1.000000	.000000
Z	.000000	.000000	1.000000	.000000	.000000	1.000000

TRANSLATIONAL MASS AND MASS MOMENTS OF INERTIA

U1	U2	U3	R1	R2	R3
.000000	.000000	.000000	.000000	.000000	.000000

CENTER OF MASS

GLOBAL	U1	U2	U3
X	.000000	.000000	.000000
Y	.000000	.000000	.000000
Z	.000000	.000000	.000000

C O N S T R A I N T   C O O R D I N A T E S   A N D   M A S S E S

CONS 25 ================= TYPE = DIAPH, NORMAL DIRECTION = U3

LOCAL COORDINATE SYSTEM FOR CONSTRAINT MASTER

GLOBAL	U1	U2	U3	R1	R2	R3
X	1.000000	.000000	.000000	1.000000	.000000	.000000
Y	.000000	1.000000	.000000	.000000	1.000000	.000000
Z	.000000	.000000	1.000000	.000000	.000000	1.000000

TRANSLATIONAL MASS AND MASS MOMENTS OF INERTIA

U1	U2	U3	R1	R2	R3
.000000	.000000	.000000	.000000	.000000	.000000

CENTER OF MASS

GLOBAL	U1	U2	U3
X	.000000	.000000	.000000
Y	.000000	.000000	.000000
Z	.000000	.000000	.000000

CONS 26 ================= TYPE = DIAPH, NORMAL DIRECTION = U3

LOCAL COORDINATE SYSTEM FOR CONSTRAINT MASTER

GLOBAL	U1	U2	U3	R1	R2	R3
X	1.000000	.000000	.000000	1.000000	.000000	.000000
Y	.000000	1.000000	.000000	.000000	1.000000	.000000
Z	.000000	.000000	1.000000	.000000	.000000	1.000000

TRANSLATIONAL MASS AND MASS MOMENTS OF INERTIA

U1	U2	U3	R1	R2	R3
.000000	.000000	.000000	.000000	.000000	.000000

CENTER OF MASS

GLOBAL	U1	U2	U3
X	.000000	.000000	.000000
Y	.000000	.000000	.000000
Z	.000000	.000000	.000000

CONS 27 ================= TYPE = DIAPH, NORMAL DIRECTION = U3

LOCAL COORDINATE SYSTEM FOR CONSTRAINT MASTER

GLOBAL	U1	U2	U3	R1	R2	R3
X	1.000000	.000000	.000000	1.000000	.000000	.000000
Y	.000000	1.000000	.000000	.000000	1.000000	.000000
Z	.000000	.000000	1.000000	.000000	.000000	1.000000

TRANSLATIONAL MASS AND MASS MOMENTS OF INERTIA

U1	U2	U3	R1	R2	R3
.000000	.000000	.000000	.000000	.000000	.000000

C O N S T R A I N T   C O O R D I N A T E S   A N D   M A S S E S

CENTER OF MASS

GLOBAL	U1	U2	U3
X	.000000	.000000	.000000
Y	.000000	.000000	.000000
Z	.000000	.000000	.000000

CONS 28 ================== TYPE = DIAPH, NORMAL DIRECTION = U3

LOCAL COORDINATE SYSTEM FOR CONSTRAINT MASTER

GLOBAL	U1	U2	U3	R1	R2	R3
X	1.000000	.000000	.000000	1.000000	.000000	.000000
Y	.000000	1.000000	.000000	.000000	1.000000	.000000
Z	.000000	.000000	1.000000	.000000	.000000	1.000000

TRANSLATIONAL MASS AND MASS MOMENTS OF INERTIA

U1	U2	U3	R1	R2	R3
.000000	.000000	.000000	.000000	.000000	.000000

CENTER OF MASS

GLOBAL	U1	U2	U3
X	.000000	.000000	.000000
Y	.000000	.000000	.000000
Z	.000000	.000000	.000000

CONS 29 ================== TYPE = DIAPH, NORMAL DIRECTION = U3

LOCAL COORDINATE SYSTEM FOR CONSTRAINT MASTER

GLOBAL	U1	U2	U3	R1	R2	R3
X	1.000000	.000000	.000000	1.000000	.000000	.000000
Y	.000000	1.000000	.000000	.000000	1.000000	.000000
Z	.000000	.000000	1.000000	.000000	.000000	1.000000

TRANSLATIONAL MASS AND MASS MOMENTS OF INERTIA

U1	U2	U3	R1	R2	R3
.000000	.000000	.000000	.000000	.000000	.000000

CENTER OF MASS

GLOBAL	U1	U2	U3
X	.000000	.000000	.000000
Y	.000000	.000000	.000000
Z	.000000	.000000	.000000

CONS 30 ================== TYPE = DIAPH, NORMAL DIRECTION = U3

LOCAL COORDINATE SYSTEM FOR CONSTRAINT MASTER

GLOBAL	U1	U2	U3	R1	R2	R3
X	1.000000	.000000	.000000	1.000000	.000000	.000000
Y	.000000	1.000000	.000000	.000000	1.000000	.000000
Z	.000000	.000000	1.000000	.000000	.000000	1.000000

Program ETABS Nonlinear Version 7.10 File:projectwall.OUT
Page
12

C O N S T R A I N T   C O O R D I N A T E S   A N D   M A S S E S

TRANSLATIONAL MASS AND MASS MOMENTS OF INERTIA

U1	U2	U3	R1	R2	R3
.000000	.000000	.000000	.000000	.000000	.000000

CENTER OF MASS

GLOBAL	U1	U2	U3
X	.000000	.000000	.000000
Y	.000000	.000000	.000000
Z	.000000	.000000	.000000

CONS 31 ================= TYPE = DIAPH, NORMAL DIRECTION = U3

LOCAL COORDINATE SYSTEM FOR CONSTRAINT MASTER

GLOBAL	U1	U2	U3	R1	R2	R3
X	1.000000	.000000	.000000	1.000000	.000000	.000000
Y	.000000	1.000000	.000000	.000000	1.000000	.000000
Z	.000000	.000000	1.000000	.000000	.000000	1.000000

TRANSLATIONAL MASS AND MASS MOMENTS OF INERTIA

U1	U2	U3	R1	R2	R3
.000000	.000000	.000000	.000000	.000000	.000000

CENTER OF MASS

GLOBAL	U1	U2	U3
X	.000000	.000000	.000000
Y	.000000	.000000	.000000
Z	.000000	.000000	.000000

CONS 32 ================= TYPE = DIAPH, NORMAL DIRECTION = U3

LOCAL COORDINATE SYSTEM FOR CONSTRAINT MASTER

GLOBAL	U1	U2	U3	R1	R2	R3
X	1.000000	.000000	.000000	1.000000	.000000	.000000
Y	.000000	1.000000	.000000	.000000	1.000000	.000000
Z	.000000	.000000	1.000000	.000000	.000000	1.000000

TRANSLATIONAL MASS AND MASS MOMENTS OF INERTIA

U1	U2	U3	R1	R2	R3
.000000	.000000	.000000	.000000	.000000	.000000

CENTER OF MASS

GLOBAL	U1	U2	U3
X	.000000	.000000	.000000
Y	.000000	.000000	.000000
Z	.000000	.000000	.000000

C O N S T R A I N T   C O O R D I N A T E S   A N D   M A S S E S

CONS 33 ================= TYPE = DIAPH, NORMAL DIRECTION = U3

LOCAL COORDINATE SYSTEM FOR CONSTRAINT MASTER

GLOBAL	U1	U2	U3	R1	R2	R3
X	1.000000	.000000	.000000	1.000000	.000000	.000000
Y	.000000	1.000000	.000000	.000000	1.000000	.000000
Z	.000000	.000000	1.000000	.000000	.000000	1.000000

TRANSLATIONAL MASS AND MASS MOMENTS OF INERTIA

U1	U2	U3	R1	R2	R3
.000000	.000000	.000000	.000000	.000000	.000000

CENTER OF MASS

GLOBAL	U1	U2	U3
X	.000000	.000000	.000000
Y	.000000	.000000	.000000
Z	.000000	.000000	.000000

CONS 34 ================= TYPE = DIAPH, NORMAL DIRECTION = U3

LOCAL COORDINATE SYSTEM FOR CONSTRAINT MASTER

GLOBAL	U1	U2	U3	R1	R2	R3
X	1.000000	.000000	.000000	1.000000	.000000	.000000
Y	.000000	1.000000	.000000	.000000	1.000000	.000000
Z	.000000	.000000	1.000000	.000000	.000000	1.000000

TRANSLATIONAL MASS AND MASS MOMENTS OF INERTIA

U1	U2	U3	R1	R2	R3
.000000	.000000	.000000	.000000	.000000	.000000

CENTER OF MASS

GLOBAL	U1	U2	U3
X	.000000	.000000	.000000
Y	.000000	.000000	.000000
Z	.000000	.000000	.000000

CONS 35 ================= TYPE = DIAPH, NORMAL DIRECTION = U3

LOCAL COORDINATE SYSTEM FOR CONSTRAINT MASTER

GLOBAL	U1	U2	U3	R1	R2	R3
X	1.000000	.000000	.000000	1.000000	.000000	.000000
Y	.000000	1.000000	.000000	.000000	1.000000	.000000
Z	.000000	.000000	1.000000	.000000	.000000	1.000000

TRANSLATIONAL MASS AND MASS MOMENTS OF INERTIA

U1	U2	U3	R1	R2	R3
.000000	.000000	.000000	.000000	.000000	.000000

C O N S T R A I N T   C O O R D I N A T E S   A N D   M A S S E S

CENTER OF MASS

GLOBAL	U1	U2	U3
X	.000000	.000000	.000000
Y	.000000	.000000	.000000
Z	.000000	.000000	.000000

CONS 36 ================= TYPE = DIAPH, NORMAL DIRECTION = U3

LOCAL COORDINATE SYSTEM FOR CONSTRAINT MASTER

GLOBAL	U1	U2	U3	R1	R2	R3
X	1.000000	.000000	.000000	1.000000	.000000	.000000
Y	.000000	1.000000	.000000	.000000	1.000000	.000000
Z	.000000	.000000	1.000000	.000000	.000000	1.000000

TRANSLATIONAL MASS AND MASS MOMENTS OF INERTIA

U1	U2	U3	R1	R2	R3
.000000	.000000	.000000	.000000	.000000	.000000

CENTER OF MASS

GLOBAL	U1	U2	U3
X	.000000	.000000	.000000
Y	.000000	.000000	.000000
Z	.000000	.000000	.000000

CONS 37 ================= TYPE = DIAPH, NORMAL DIRECTION = U3

LOCAL COORDINATE SYSTEM FOR CONSTRAINT MASTER

GLOBAL	U1	U2	U3	R1	R2	R3
X	1.000000	.000000	.000000	1.000000	.000000	.000000
Y	.000000	1.000000	.000000	.000000	1.000000	.000000
Z	.000000	.000000	1.000000	.000000	.000000	1.000000

TRANSLATIONAL MASS AND MASS MOMENTS OF INERTIA

U1	U2	U3	R1	R2	R3
.000000	.000000	.000000	.000000	.000000	.000000

CENTER OF MASS

GLOBAL	U1	U2	U3
X	.000000	.000000	.000000
Y	.000000	.000000	.000000
Z	.000000	.000000	.000000

CONS 38 ================= TYPE = DIAPH, NORMAL DIRECTION = U3

LOCAL COORDINATE SYSTEM FOR CONSTRAINT MASTER

GLOBAL	U1	U2	U3	R1	R2	R3
X	1.000000	.000000	.000000	1.000000	.000000	.000000
Y	.000000	1.000000	.000000	.000000	1.000000	.000000
Z	.000000	.000000	1.000000	.000000	.000000	1.000000

C O N S T R A I N T   C O O R D I N A T E S   A N D   M A S S E S

TRANSLATIONAL MASS AND MASS MOMENTS OF INERTIA

U1	U2	U3	R1	R2	R3
.000000	.000000	.000000	.000000	.000000	.000000

CENTER OF MASS

GLOBAL	U1	U2	U3
X	.000000	.000000	.000000
Y	.000000	.000000	.000000
Z	.000000	.000000	.000000

CONS 39 ================= TYPE = DIAPH, NORMAL DIRECTION = U3

LOCAL COORDINATE SYSTEM FOR CONSTRAINT MASTER

GLOBAL	U1	U2	U3	R1	R2	R3
X	1.000000	.000000	.000000	1.000000	.000000	.000000
Y	.000000	1.000000	.000000	.000000	1.000000	.000000
Z	.000000	.000000	1.000000	.000000	.000000	1.000000

TRANSLATIONAL MASS AND MASS MOMENTS OF INERTIA

U1	U2	U3	R1	R2	R3
.000000	.000000	.000000	.000000	.000000	.000000

CENTER OF MASS

GLOBAL	U1	U2	U3
X	.000000	.000000	.000000
Y	.000000	.000000	.000000
Z	.000000	.000000	.000000

CONS 40 ================= TYPE = DIAPH, NORMAL DIRECTION = U3

LOCAL COORDINATE SYSTEM FOR CONSTRAINT MASTER

GLOBAL	U1	U2	U3	R1	R2	R3
X	1.000000	.000000	.000000	1.000000	.000000	.000000
Y	.000000	1.000000	.000000	.000000	1.000000	.000000
Z	.000000	.000000	1.000000	.000000	.000000	1.000000

TRANSLATIONAL MASS AND MASS MOMENTS OF INERTIA

U1	U2	U3	R1	R2	R3
.000000	.000000	.000000	.000000	.000000	.000000

CENTER OF MASS

GLOBAL	U1	U2	U3
X	.000000	.000000	.000000
Y	.000000	.000000	.000000
Z	.000000	.000000	.000000

C O N S T R A I N T   C O O R D I N A T E S   A N D   M A S S E S

CONS 41 ================== TYPE = DIAPH, NORMAL DIRECTION = U3

LOCAL COORDINATE SYSTEM FOR CONSTRAINT MASTER

GLOBAL	U1	U2	U3	R1	R2	R3
X	1.000000	.000000	.000000	1.000000	.000000	.000000
Y	.000000	1.000000	.000000	.000000	1.000000	.000000
Z	.000000	.000000	1.000000	.000000	.000000	1.000000

TRANSLATIONAL MASS AND MASS MOMENTS OF INERTIA

U1	U2	U3	R1	R2	R3
.000000	.000000	.000000	.000000	.000000	.000000

CENTER OF MASS

GLOBAL	U1	U2	U3
X	.000000	.000000	.000000
Y	.000000	.000000	.000000
Z	.000000	.000000	.000000

CONS 42 ================== TYPE = DIAPH, NORMAL DIRECTION = U3

LOCAL COORDINATE SYSTEM FOR CONSTRAINT MASTER

GLOBAL	U1	U2	U3	R1	R2	R3
X	1.000000	.000000	.000000	1.000000	.000000	.000000
Y	.000000	1.000000	.000000	.000000	1.000000	.000000
Z	.000000	.000000	1.000000	.000000	.000000	1.000000

TRANSLATIONAL MASS AND MASS MOMENTS OF INERTIA

U1	U2	U3	R1	R2	R3
.000000	.000000	.000000	.000000	.000000	.000000

CENTER OF MASS

GLOBAL	U1	U2	U3
X	.000000	.000000	.000000
Y	.000000	.000000	.000000
Z	.000000	.000000	.000000

D I S P L A C E M E N T   D E G R E E S   O F   F R E E D O M

(A) = Active DOF, equilibrium equation
(-) = Restrained DOF, reaction computed
(+) = Constrained DOF
(>) = External substructure DOF
( ) = Null DOF

JOINTS			UX	UY	UZ	RX	RY	RZ
1			-	-	-	A	A	A
2	TO	3	+	+	A	A	A	+
4			-	-	-	A	A	A
5	TO	24	+	+	A	A	A	+
25			-	-	-	A	A	A
26			+	+	A	A	A	+
27			-	-	-	A	A	A
28			+	+	A	A	A	+
29			-	-	-	A	A	A
30	TO	31	+	+	A	A	A	+
32			-	-	-	A	A	A
33	TO	52	+	+	A	A	A	+
53			-	-	-	A	A	A
54			+	+	A	A	A	+
55			-	-	-	A	A	A
56			+	+	A	A	A	+
57			-	-	-	A	A	A
58	TO	59	+	+	A	A	A	+
60			-	-	-	A	A	A
61	TO	80	+	+	A	A	A	+
81			-	-	-	A	A	A
82			+	+	A	A	A	+
83			-	-	-	A	A	A
84			+	+	A	A	A	+
85			-	-	-	A	A	A
86	TO	87	+	+	A	A	A	+
88			-	-	-	A	A	A
89	TO	108	+	+	A	A	A	+
109			-	-	-	A	A	A
110			+	+	A	A	A	+
111			-	-	-	A	A	A
112			+	+	A	A	A	+
113			-	-	-	A	A	A
114	TO	115	+	+	A	A	A	+
116			-	-	-	A	A	A
117	TO	126	+	+	A	A	A	+
127			-	-	-	A	A	A
128	TO	129	+	+	A	A	A	+
130			-	-	-	A	A	A
131	TO	140	+	+	A	A	A	+
141			-	-	-	A	A	A
142			+	+	A	A	A	+
143			-	-	-	A	A	A
144			+	+	A	A	A	+
145			-	-	-	A	A	A

D I S P L A C E M E N T   D E G R E E S   O F   F R E E D O M

(A) = Active DOF, equilibrium equation
(-) = Restrained DOF, reaction computed
(+) = Constrained DOF
(>) = External substructure DOF
( ) = Null DOF

JOINTS			UX	UY	UZ	RX	RY	RZ
146			+	+	A	A	A	+
147			-	-	-	A	A	A
148			+	+	A	A	A	+
149			-	-	-	A	A	A
150			+	+	A	A	A	+
151			-	-	-	A	A	A
152			+	+	A	A	A	+
153			-	-	-	A	A	A
154			+	+	A	A	A	+
155			-	-	-	A	A	A
156			+	+	A	A	A	+
157			-	-	-	A	A	A
158			+	+	A	A	A	+
159			-	-	-	A	A	A
160			+	+	A	A	A	+
161			-	-	-	A	A	A
162			+	+	A	A	A	+
163			-	-	-	A	A	A
164			+	+	A	A	A	+
165			-	-	-	A	A	A
166			+	+	A	A	A	+
167			-	-	-	A	A	A
168			+	+	A	A	A	+
169			-	-	-	A	A	A
170			+	+	A	A	A	+
171			-	-	-	A	A	A
172			+	+	A	A	A	+
173			-	-	-	A	A	A
174			+	+	A	A	A	+
175			-	-	-	A	A	A
176	TO	224	+	+	A	A	A	+
225			-	-	-	A	A	A
226			+	+	A	A	A	+
227			-	-	-	A	A	A
228	TO	1060	+	+	A	A	A	+
1061	TO	1066	+	+				+

CONSTRAINTS			U1	U2	U3	R1	R2	R3
1	TO	6	A	A				A
7	TO	42						

M O D A L P E R I O D S A N D F R E Q U E N C I E S

MODE	PERIOD (TIME)	FREQUENCY (CYC/TIME)	FREQUENCY (RAD/TIME)	EIGENVALUE (RAD/TIME)**2
1	1.105866	0.904269	5.681689	32.281585
2	0.796164	1.256023	7.891822	62.280858
3	0.786476	1.271495	7.989040	63.824765
4	0.350671	2.851678	17.917622	321.041163
5	0.250676	3.989208	25.064933	628.250874
6	0.244875	4.083709	25.658701	658.368960
7	0.182491	5.479719	34.430090	1185.431
8	0.138953	7.196693	45.218154	2044.681
9	0.137481	7.273732	45.702205	2088.692
10	0.116628	8.574299	53.873912	2902.398
11	0.100397	9.960412	62.583114	3916.646
12	0.099171	10.083636	63.357354	4014.154
13	0.084913	11.776780	73.995691	5475.362
14	0.079906	12.514726	78.632340	6183.045
15	0.078782	12.693270	79.754166	6360.727
16	0.066522	15.032566	94.452395	8921.255
17	0.065535	15.258948	95.874800	9191.977
18	0.018232	54.847733	344.618468	118761.888

M O D A L   P A R T I C I P A T I O N   F A C T O R S

FOR UNIT ACCELERATION LOADS IN GLOBAL COORDINATES

MODE	PERIOD	UX	UY	UZ
1	1.105866	0.150352	0.431701	.000000
2	0.796164	3.001908	-1.440775	.000000
3	0.786476	1.444998	2.960077	.000000
4	0.350671	0.079899	0.263517	.000000
5	0.250676	1.725276	-0.530583	.000000
6	0.244875	0.552661	1.613808	.000000
7	0.182491	-0.051545	0.120426	.000000
8	0.138953	-0.868232	0.309373	.000000
9	0.137481	-0.357378	-0.756618	.000000
10	0.116628	0.033627	-0.180293	.000000
11	0.100397	-0.611178	0.084426	.000000
12	0.099171	0.098944	0.507631	.000000
13	0.084913	0.024233	-0.072859	.000000
14	0.079906	0.454280	-0.049960	.000000
15	0.078782	0.065791	0.341087	.000000
16	0.066522	-0.037012	-0.120953	.000000
17	0.065535	-0.402315	0.013828	.000000
18	0.018232	-0.000285	-0.977286	.000000

M O D A L   P A R T I C I P A T I N G   M A S S   R A T I O S

MODE	PERIOD	INDIVIDUAL MODE (PERCENT)			CUMULATIVE SUM (PERCENT)		
		UX	UY	UZ	UX	UY	UZ
1	1.105866	0.1408	1.1609	0.0000	0.1408	1.1609	0.0000
2	0.796164	56.1334	12.9306	0.0000	56.2742	14.0915	0.0000
3	0.786476	13.0065	54.5798	0.0000	69.2807	68.6713	0.0000
4	0.350671	0.0398	0.4326	0.0000	69.3204	69.1039	0.0000
5	0.250676	18.5414	1.7536	0.0000	87.8619	70.8575	0.0000
6	0.244875	1.9026	16.2229	0.0000	89.7645	87.0804	0.0000
7	0.182491	0.0166	0.0903	0.0000	89.7810	87.1708	0.0000
8	0.138953	4.6957	0.5962	0.0000	94.4767	87.7670	0.0000
9	0.137481	0.7956	3.5660	0.0000	95.2723	91.3330	0.0000
10	0.116628	0.0070	0.2025	0.0000	95.2793	91.5354	0.0000
11	0.100397	2.3268	0.0444	0.0000	97.6061	91.5798	0.0000
12	0.099171	0.0610	1.6052	0.0000	97.6671	93.1850	0.0000
13	0.084913	0.0037	0.0331	0.0000	97.6708	93.2181	0.0000
14	0.079906	1.2855	0.0155	0.0000	98.9563	93.2336	0.0000
15	0.078782	0.0270	0.7247	0.0000	98.9832	93.9583	0.0000
16	0.066522	0.0085	0.0911	0.0000	98.9918	94.0495	0.0000
17	0.065535	1.0082	0.0012	0.0000	100.0000	94.0506	0.0000
18	0.018232	0.0000	5.9494	0.0000	100.0000	100.0000	0.0000

M O D A L   L O A D   P A R T I C I P A T I O N   R A T I O S

LOAD, ACC, OR LINK/DEF (TYPE)	(NAME)	STATIC (PERCENT)	DYNAMIC (PERCENT)		EFFECTIVE PERIOD
LOAD	DEAD	0.0062	->100.0000<-	(*) SEE NOTE	0.005490
LOAD	LIVE	0.0000	0.0000		-INFINITY-
LOAD	EQUAKE	100.0000	100.0000		0.796203
LOAD	DUMMY	0.0051	-> 0.0000<-	(*) SEE NOTE	0.004813
ACC	UX	100.0000	100.0000		0.784362
ACC	UY	100.0000	100.0000		0.790564
ACC	UZ	0.0000	0.0000		-INFINITY-
ACC	RX	126.6244	100.0000		0.709909
ACC	RY	73.7316	100.0000		0.928905
ACC	RZ	94.0469	100.0000		1.364305

(*) NOTE: DYNAMIC LOAD PARTICIPATION RATIO EXCLUDES LOAD APPLIED
TO NON-MASS DEGREES OF FREEDOM

Program ETABS Nonlinear Version 7.10 File:projectwall.OUT
Page
23

G L O B A L   F O R C E   B A L A N C E

TOTAL FORCE AND MOMENT AT THE ORIGIN, IN GLOBAL COORDINATES

LOADDEAD ------------------

	FX	FY	FZ	MX	MY	MZ
APPLIED	-1.50E-15	1.32E-15	-6655.168	-3.7225E+06	2.4820E+06	1.67E-12
INERTIA	.000000	.000000	.000000	.000000	.000000	.000000
REACTNS	7.06E-14	1.21E-12	6655.168	3.7225E+06	-2.4820E+06	-6.68E-10
CONSTRS	1.16E-12	-8.19E-13	.000000	5.75E-10	9.67E-10	-7.32E-10
TOTAL	1.23E-12	3.94E-13	-5.18E-11	-2.13E-08	2.52E-08	-1.40E-09

LOADLIVE ------------------

	FX	FY	FZ	MX	MY	MZ
APPLIED	.000000	.000000	.000000	.000000	.000000	.000000
INERTIA	.000000	.000000	.000000	.000000	.000000	.000000
REACTNS	.000000	.000000	.000000	.000000	.000000	.000000
CONSTRS	.000000	.000000	.000000	.000000	.000000	.000000
TOTAL	.000000	.000000	.000000	.000000	.000000	.000000

LOADEQUAKE ------------------

	FX	FY	FZ	MX	MY	MZ
APPLIED	502.993608	.000000	.000000	.000000	324890.152	-279902.649
INERTIA	.000000	.000000	.000000	.000000	.000000	.000000
REACTNS	-502.993608	1.57E-11	-6.85E-13	-8.44E-09	-324890.152	279902.649
CONSTRS	3.64E-11	-1.84E-11	.000000	1.32E-08	2.80E-08	-2.45E-08
TOTAL	4.50E-11	-2.66E-12	-6.85E-13	4.76E-09	3.58E-08	-2.29E-08

LOADDUMMY ------------------

	FX	FY	FZ	MX	MY	MZ
APPLIED	.000000	.000000	-6.4487E+06	-3.6144E+09	2.5474E+09	.000000
INERTIA	.000000	.000000	.000000	.000000	.000000	.000000
REACTNS	1.35E-10	1.19E-09	6.4487E+06	3.6144E+09	-2.5474E+09	-8.28E-07
CONSTRS	7.00E-10	-6.85E-10	.000000	5.46E-07	5.34E-07	-1.13E-07
TOTAL	8.34E-10	5.00E-10	-6.33E-08	-2.76E-05	3.06E-05	-9.41E-07

G L O B A L   F O R C E   B A L A N C E

TOTAL FORCE AND MOMENT AT THE ORIGIN, IN GLOBAL COORDINATES

MODE 1 ------------------

	FX	FY	FZ	MX	MY	MZ
APPLIED	.000000	.000000	.000000	.000000	.000000	.000000
INERTIA	4.853614	13.935977	.000000	-7996.427	3389.911	53318.779
REACTNS	-4.853614	-13.935977	-1.43E-13	7996.427	-3389.911	-53318.779
CONSTRS	3.66E-12	1.52E-11	.000000	1.27E-09	2.56E-09	-3.72E-09
TOTAL	6.23E-12	7.38E-12	-1.43E-13	-7.95E-09	3.08E-09	-1.79E-08

MODE 2 ------------------

	FX	FY	FZ	MX	MY	MZ
APPLIED	.000000	.000000	.000000	.000000	.000000	.000000
INERTIA	186.961394	-89.732692	.000000	57109.819	118531.425	-140460.892
REACTNS	-186.961394	89.732692	6.15E-13	-57109.819	-118531.425	140460.892
CONSTRS	-1.09E-11	-1.04E-11	.000000	2.43E-09	-5.74E-09	9.63E-09
TOTAL	-9.58E-12	1.46E-11	6.15E-13	-5.52E-09	-4.52E-09	1.29E-08

MODE 3 ------------------

	FX	FY	FZ	MX	MY	MZ
APPLIED	.000000	.000000	.000000	.000000	.000000	.000000
INERTIA	92.226636	188.926193	.000000	-120375.299	58242.007	12781.902
REACTNS	-92.226636	-188.926193	7.48E-14	120375.299	-58242.007	-12781.902
CONSTRS	-8.56E-12	-2.42E-11	.000000	5.13E-09	-6.25E-09	1.49E-09
TOTAL	-2.68E-12	-3.19E-11	7.48E-14	1.72E-08	-2.18E-09	-9.24E-09

MODE 4 ------------------

	FX	FY	FZ	MX	MY	MZ
APPLIED	.000000	.000000	.000000	.000000	.000000	.000000
INERTIA	25.650902	84.599952	.000000	18110.146	6679.771	243596.541
REACTNS	-25.650902	-84.599952	-2.51E-16	-18110.146	-6679.771	-243596.541
CONSTRS	-1.61E-11	7.84E-11	.000000	-9.68E-10	-7.64E-09	-1.19E-08
TOTAL	-4.21E-12	-1.19E-11	-2.51E-16	7.57E-09	-3.26E-09	-1.70E-08

G L O B A L   F O R C E   B A L A N C E

TOTAL FORCE AND MOMENT AT THE ORIGIN, IN GLOBAL COORDINATES

MODE 5 ------------------

	FX	FY	FZ	MX	MY	MZ
APPLIED	.000000	.000000	.000000	.000000	.000000	.000000
INERTIA	1083.906	-333.338920	.000000	16604.715	47568.991	-755031.371
REACTNS	-1083.906	333.338920	1.08E-13	-16604.715	-47568.991	755031.371
CONSTRS	-9.38E-13	3.52E-12	.000000	-3.15E-09	-8.47E-10	-1.67E-08
TOTAL	-1.09E-11	1.81E-11	1.08E-13	-5.49E-09	-5.85E-10	1.41E-08

MODE 6 ------------------

	FX	FY	FZ	MX	MY	MZ
APPLIED	.000000	.000000	.000000	.000000	.000000	.000000
INERTIA	363.854695	1062.481	.000000	-49392.344	11914.336	220479.344
REACTNS	-363.854695	-1062.481	1.81E-13	49392.344	-11914.336	-220479.344
CONSTRS	-4.29E-12	5.71E-12	.000000	1.80E-09	3.95E-10	1.79E-08
TOTAL	-1.68E-12	-3.95E-11	1.81E-13	1.50E-08	8.65E-10	-1.53E-08

MODE 7 ------------------

	FX	FY	FZ	MX	MY	MZ
APPLIED	.000000	.000000	.000000	.000000	.000000	.000000
INERTIA	-61.103357	142.757269	.000000	-74478.514	801.683396	-392519.810
REACTNS	61.103357	-142.757269	3.83E-12	74478.514	-801.683396	392519.810
CONSTRS	1.48E-11	1.76E-09	.000000	2.41E-09	-3.53E-09	-6.13E-07
TOTAL	-4.12E-12	-1.99E-11	3.83E-12	1.45E-08	-3.39E-09	-3.95E-09

MODE 8 ------------------

	FX	FY	FZ	MX	MY	MZ
APPLIED	.000000	.000000	.000000	.000000	.000000	.000000
INERTIA	-1775.258	632.568360	.000000	22016.472	52389.156	1.3445E+06
REACTNS	1775.258	-632.568360	-3.52E-12	-22016.472	-52389.156	-1.3445E+06
CONSTRS	-1.13E-10	1.19E-09	.000000	7.81E-09	3.77E-09	-2.88E-07
TOTAL	2.39E-11	-6.88E-12	-3.52E-12	8.19E-11	-2.70E-09	-1.65E-08

G L O B A L   F O R C E   B A L A N C E

TOTAL FORCE AND MOMENT AT THE ORIGIN, IN GLOBAL COORDINATES

MODE 9 ------------------

	FX	FY	FZ	MX	MY	MZ
APPLIED	.000000	.000000	.000000	.000000	.000000	.000000
INERTIA	-746.452032	-1580.341	.000000	-40872.393	20185.738	-378962.401
REACTNS	746.452032	1580.341	-1.21E-12	40872.393	-20185.738	378962.401
CONSTRS	-2.37E-11	-2.24E-09	.000000	-4.52E-09	-5.59E-09	7.20E-07
TOTAL	-4.26E-12	.000000	-1.21E-12	7.66E-09	-3.08E-09	8.07E-09

MODE 10 ------------------

	FX	FY	FZ	MX	MY	MZ
APPLIED	.000000	.000000	.000000	.000000	.000000	.000000
INERTIA	97.599110	-523.282893	.000000	124566.259	-828.573153	479961.416
REACTNS	-97.599110	523.282893	-4.15E-12	-124566.259	828.573153	-479961.416
CONSTRS	2.28E-11	5.05E-10	.000000	-4.53E-09	-2.69E-09	-2.48E-07
TOTAL	-3.10E-12	-6.65E-12	-4.15E-12	8.13E-09	-1.54E-09	-6.60E-09

MODE 11 ------------------

	FX	FY	FZ	MX	MY	MZ
APPLIED	.000000	.000000	.000000	.000000	.000000	.000000
INERTIA	-2393.769	330.666187	.000000	37428.232	226914.242	1.5483E+06
REACTNS	2393.769	-330.666187	4.64E-12	-37428.232	-226914.242	-1.5483E+06
CONSTRS	-1.72E-10	-2.22E-09	.000000	-1.91E-08	1.97E-08	7.42E-07
TOTAL	2.23E-11	-6.25E-12	4.64E-12	-1.71E-09	-6.27E-09	-1.45E-08

MODE 12 ------------------

	FX	FY	FZ	MX	MY	MZ
APPLIED	.000000	.000000	.000000	.000000	.000000	.000000
INERTIA	397.177378	2037.711	.000000	197242.662	-39252.078	917911.856
REACTNS	-397.177378	-2037.711	-5.86E-12	-197242.662	39252.078	-917911.856
CONSTRS	2.72E-10	-8.97E-10	.000000	-1.54E-08	-4.66E-08	1.33E-07
TOTAL	-3.52E-12	9.78E-12	-5.86E-12	7.56E-09	3.77E-09	-4.47E-09

G L O B A L   F O R C E   B A L A N C E

TOTAL FORCE AND MOMENT AT THE ORIGIN, IN GLOBAL COORDINATES

MODE 13 ------------------

	FX	FY	FZ	MX	MY	MZ
APPLIED	.000000	.000000	.000000	.000000	.000000	.000000
INERTIA	132.686803	-398.926991	.000000	165597.619	-17509.937	775521.645
REACTNS	-132.686803	398.926991	-7.94E-12	-165597.619	17509.937	-775521.645
CONSTRS	-3.21E-10	-7.05E-09	.000000	1.67E-08	3.77E-08	2.55E-06
TOTAL	-7.67E-12	-2.79E-12	-7.94E-12	-7.08E-09	-6.21E-10	3.64E-09

MODE 14 ------------------

	FX	FY	FZ	MX	MY	MZ
APPLIED	.000000	.000000	.000000	.000000	.000000	.000000
INERTIA	2808.837	-308.904156	.000000	-52521.970	-327096.333	-1.8349E+06
REACTNS	-2808.837	308.904156	8.39E-12	52521.970	327096.333	1.8349E+06
CONSTRS	-1.07E-10	1.03E-08	.000000	7.30E-08	3.15E-08	-3.04E-06
TOTAL	-3.27E-11	1.02E-11	8.39E-12	1.36E-08	-1.88E-08	1.91E-08

MODE 15 ------------------

	FX	FY	FZ	MX	MY	MZ
APPLIED	.000000	.000000	.000000	.000000	.000000	.000000
INERTIA	418.479490	2169.563	.000000	267732.148	-48526.321	1.0989E+06
REACTNS	-418.479490	-2169.563	-1.26E-11	-267732.148	48526.321	-1.0989E+06
CONSTRS	-5.28E-11	6.39E-09	.000000	3.38E-08	4.61E-09	-1.94E-06
TOTAL	5.40E-12	4.55E-12	-1.26E-11	-1.18E-08	1.67E-08	-6.09E-09

MODE 16 ------------------

	FX	FY	FZ	MX	MY	MZ
APPLIED	.000000	.000000	.000000	.000000	.000000	.000000
INERTIA	-330.193541	-1079.051	.000000	-422306.196	48363.334	-1.8200E+06
REACTNS	330.193541	1079.051	-9.32E-12	422306.196	-48363.334	1.8200E+06
CONSTRS	-5.15E-10	-5.11E-09	.000000	-1.08E-07	4.47E-08	1.47E-06
TOTAL	-5.12E-13	-1.21E-11	-9.32E-12	-8.00E-09	6.86E-09	5.10E-10

G L O B A L F O R C E B A L A N C E

TOTAL FORCE AND MOMENT AT THE ORIGIN, IN GLOBAL COORDINATES

MODE 17 ------------------

	FX	FY	FZ	MX	MY	MZ
APPLIED	.000000	.000000	.000000	.000000	.000000	.000000
INERTIA	-3698.069	127.104005	.000000	34382.557	521977.000	2.2413E+06
REACTNS	3698.069	-127.104005	-1.58E-11	-34382.557	-521977.000	-2.2413E+06
CONSTRS	1.24E-10	-1.55E-08	.000000	-7.00E-08	-6.95E-09	4.76E-06
TOTAL	5.50E-11	-1.35E-11	-1.58E-11	-1.65E-08	2.48E-08	-4.37E-08

MODE 18 ------------------

	FX	FY	FZ	MX	MY	MZ
APPLIED	.000000	.000000	.000000	.000000	.000000	.000000
INERTIA	-33.897441	-116064.371	.000000	-498053.472	4339.788	3.7215E+07
REACTNS	33.897441	116064.371	2.10E-10	498053.472	-4339.788	-3.7215E+07
CONSTRS	-1.35E-08	-3.84E-06	.000000	-1.66E-05	1.74E-06	0.001237
TOTAL	-1.24E-11	-1.46E-11	2.10E-10	1.13E-07	-2.47E-07	-4.96E-09

APPENDIX III

SHAPE MODES

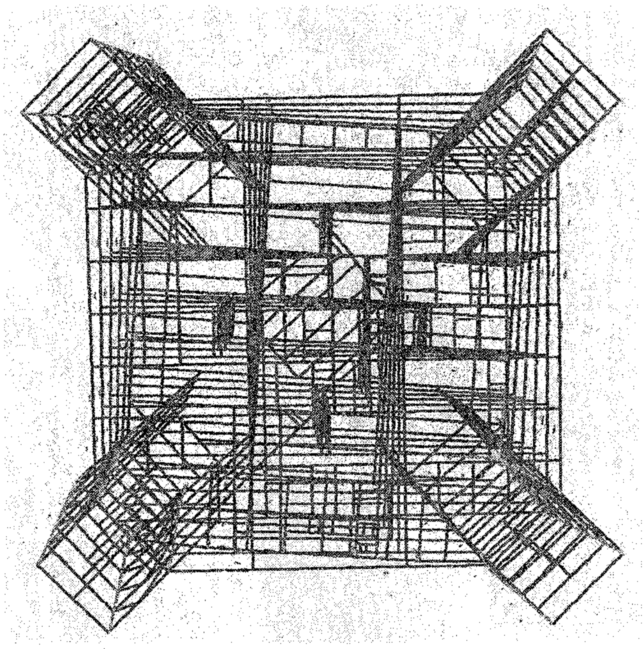

Mode 1 – Period 1.1059 seconds

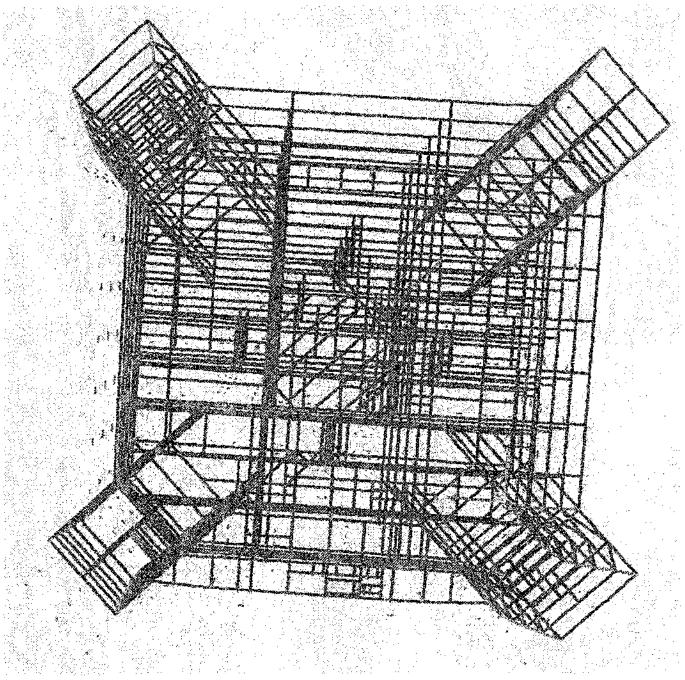

Mode 2 – Period 0.7962 seconds

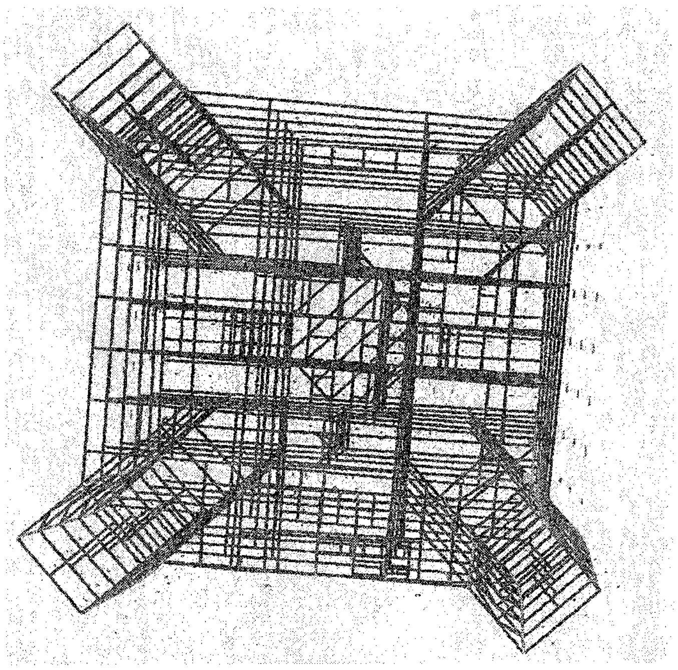

Mode 3 – Period 0.7865 seconds

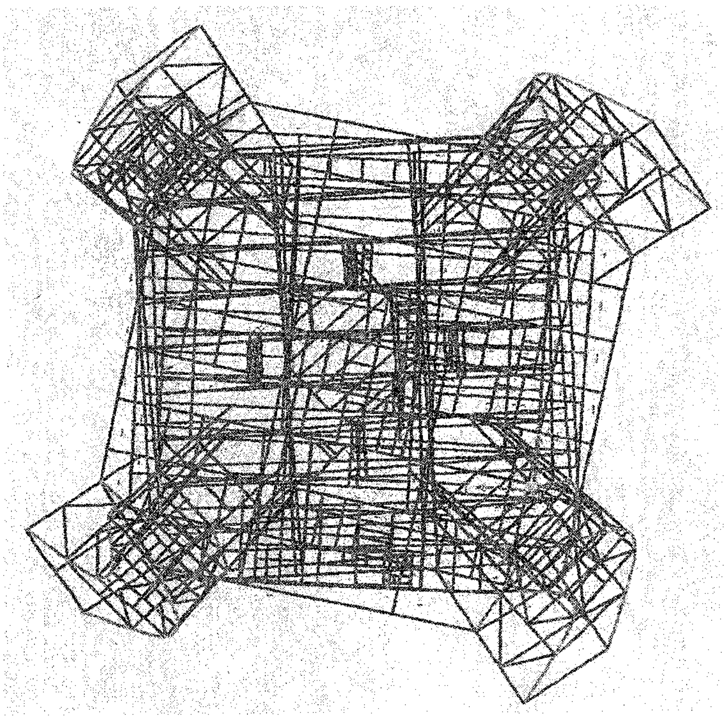

Mode 4 – Period 0.3507 seconds

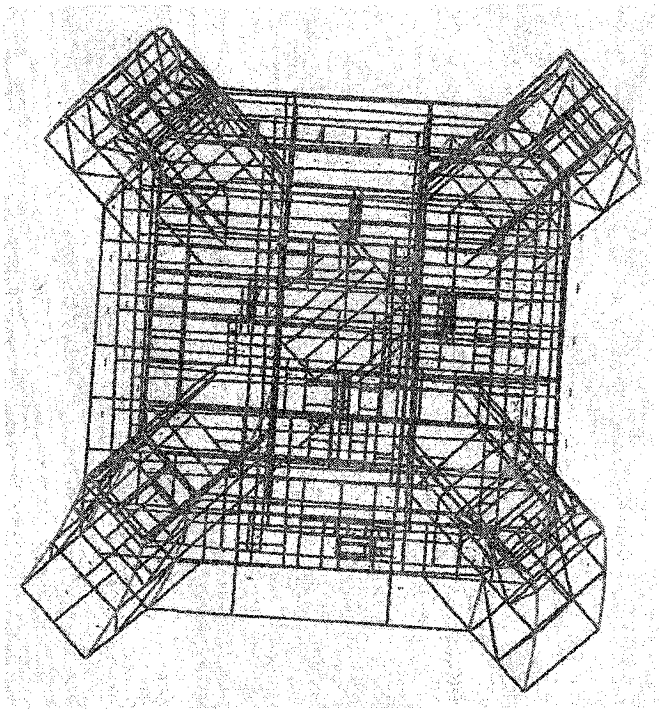

Mode 5 – Period 0.2507 seconds

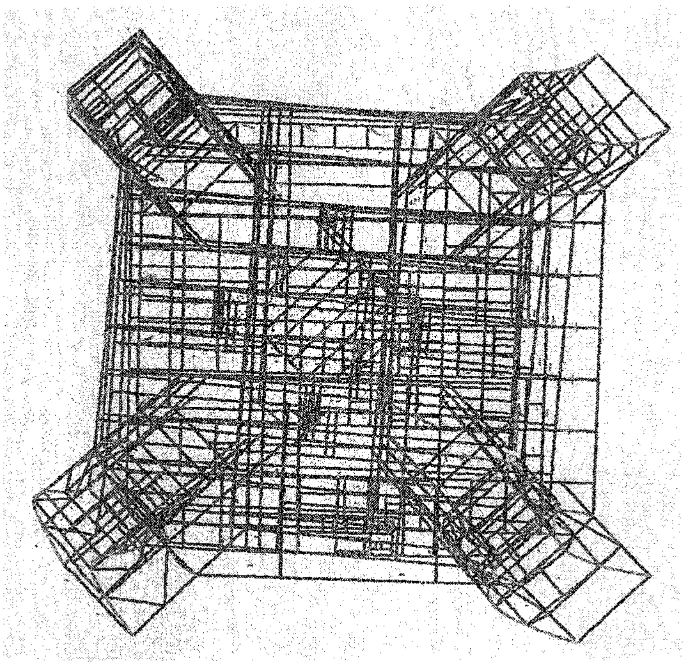

Mode 6 – Period 0.2449 seconds

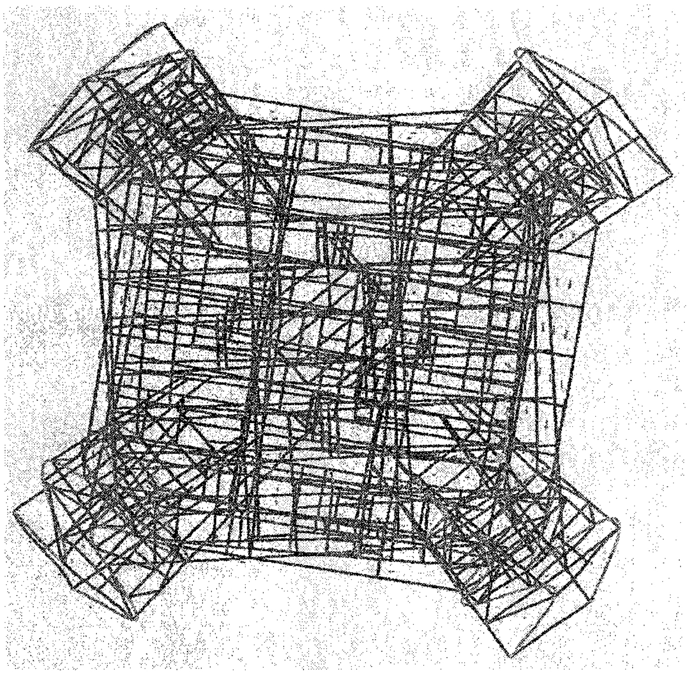

Mode 7 – Period 0.1825 seconds

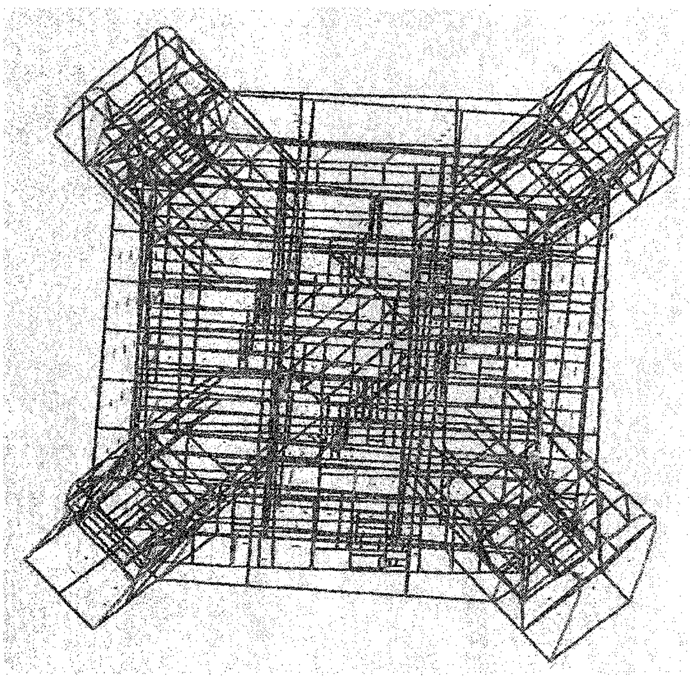

Mode 8 – Period 0.1390 seconds

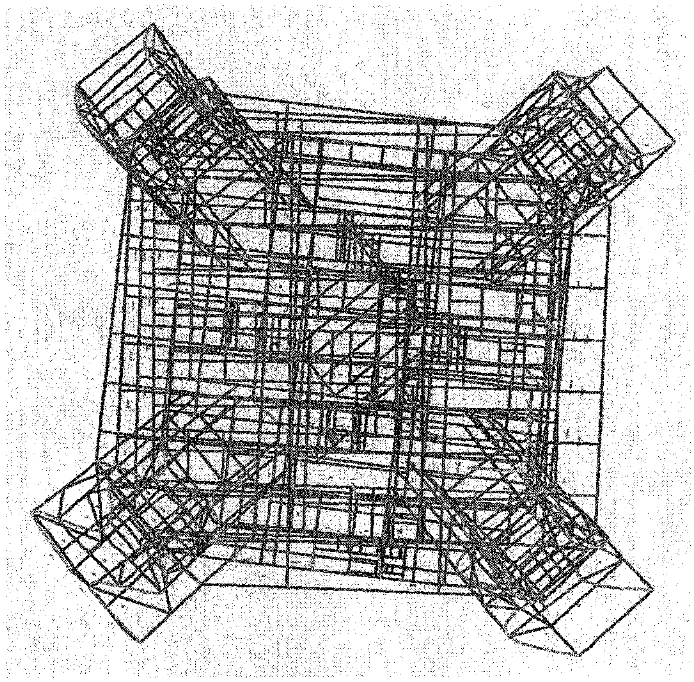

Mode 9 – Period 0.1375 seconds